FHI-aims
The ab initio materials simulation package

NOMAD
NOVEL MATERIALS DISCOVERY

FRITZ-HABER-INSTITUT
MAX-PLANCK-GESELLSCHAFT

上海大学材料基因组工程研究院
MGI
Materials Genome Institute of Shanghai University

Introduction to electron and phonon transport

--from computational science perspective

Jiong Yang

jiongy@t.shu.edu.cn

Materials Genome Institute, Shanghai University

2025/11/06

Overview

Background

Electrical transport

Lattice thermal conductivity

Electron and phonon transport

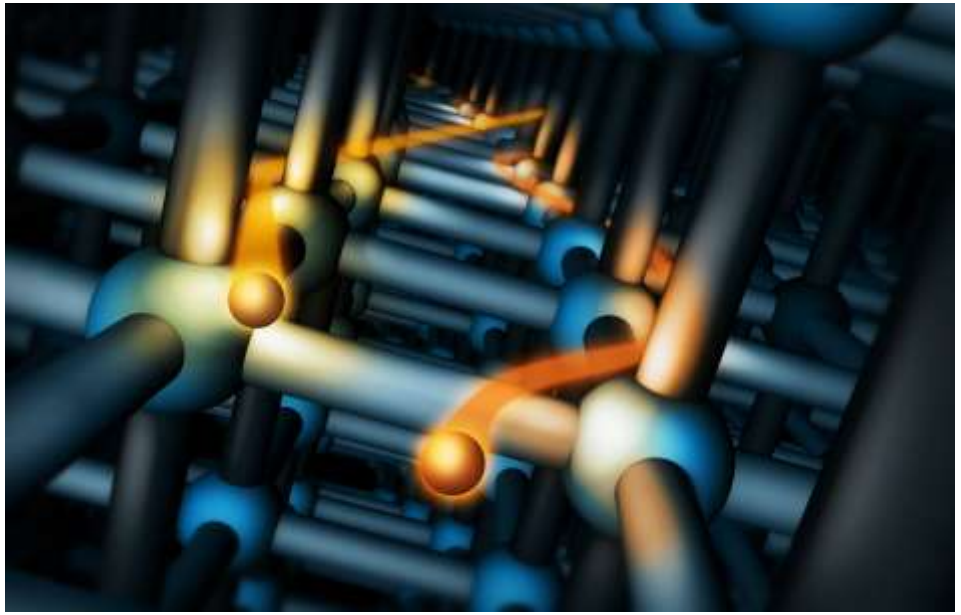

$J=\sigma E$

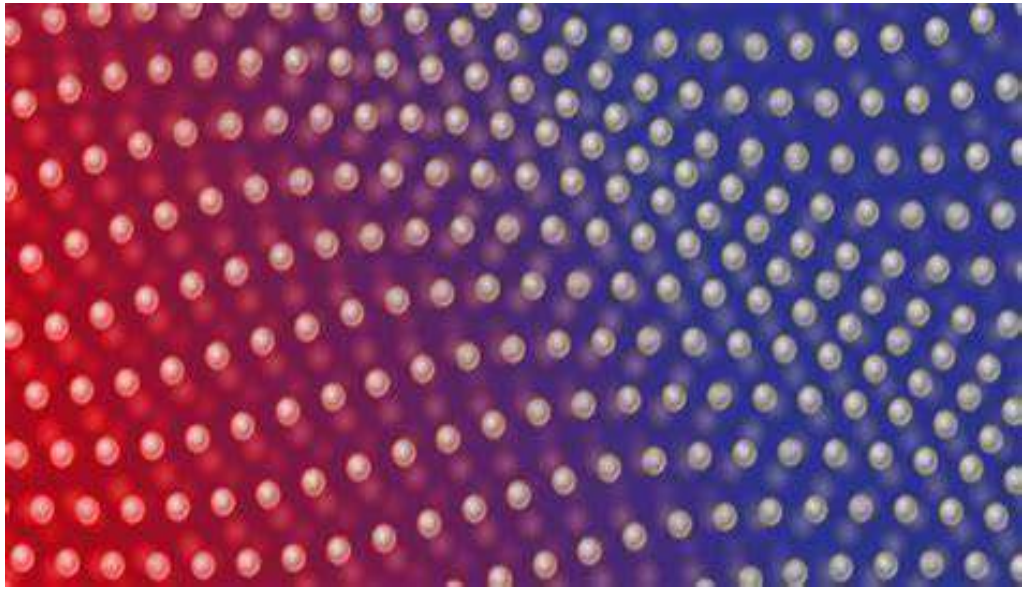

$J=\kappa dT/dx$

1. Background **Dimensions of electrical and thermal conductivities**

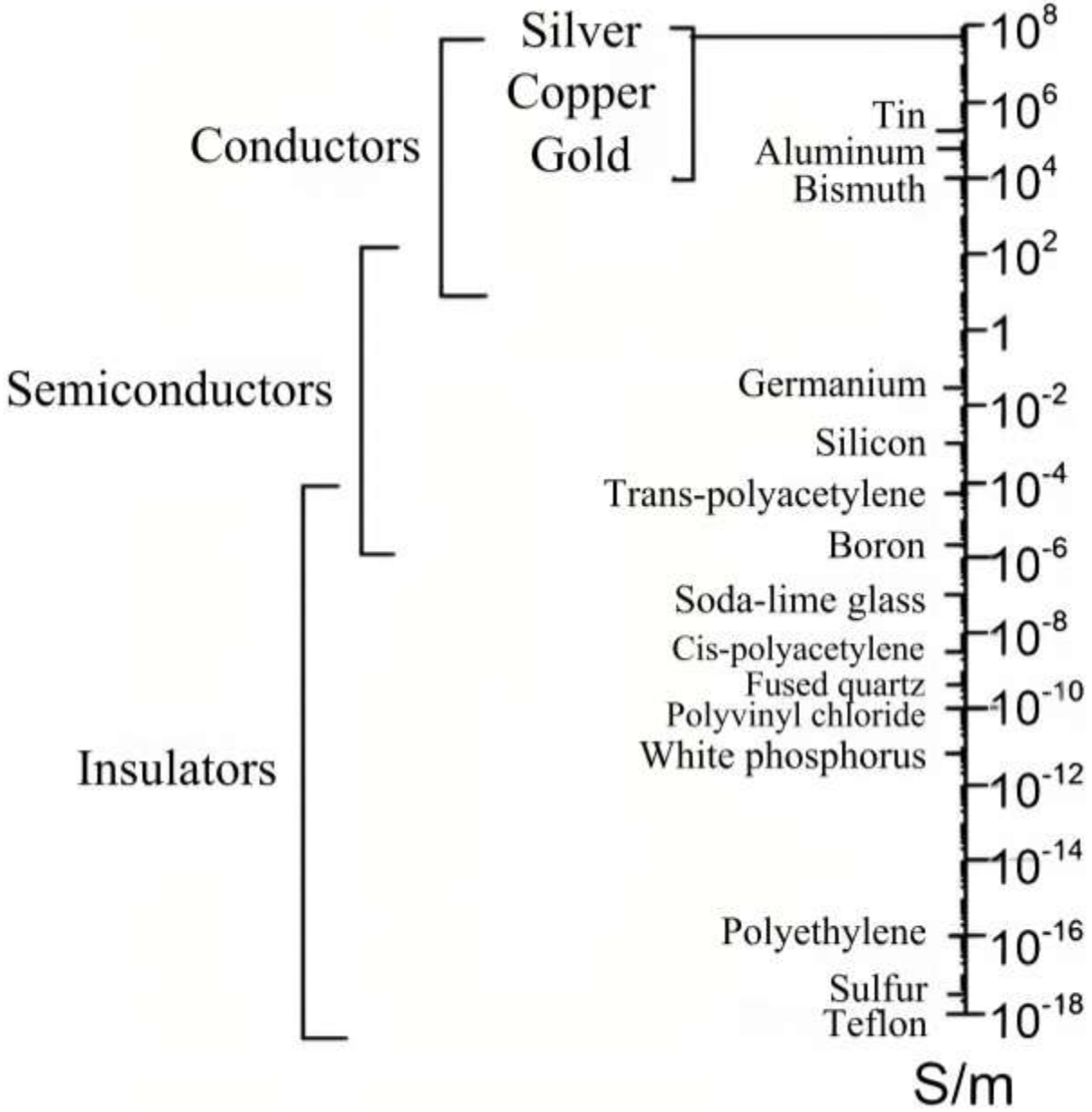

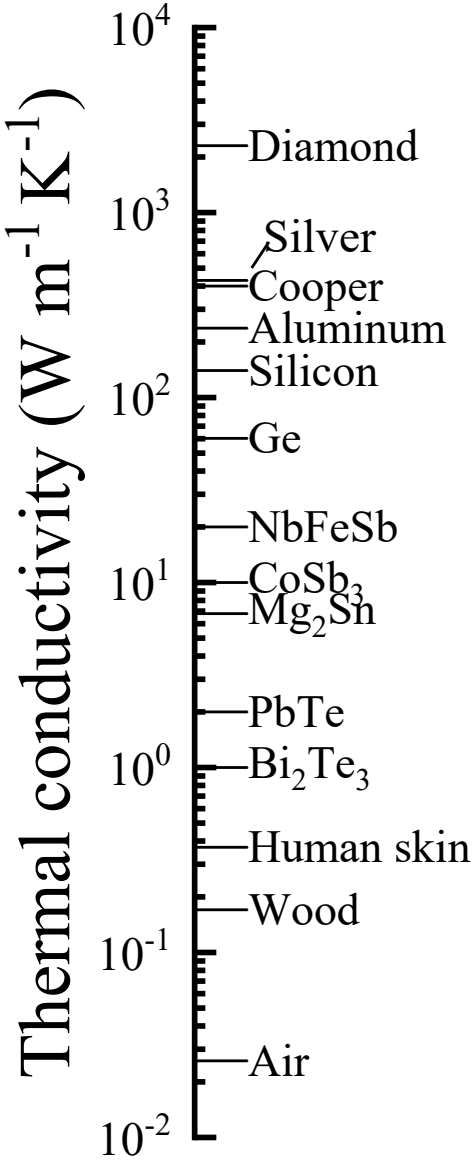

1. Background **Thermoelectric Effect**

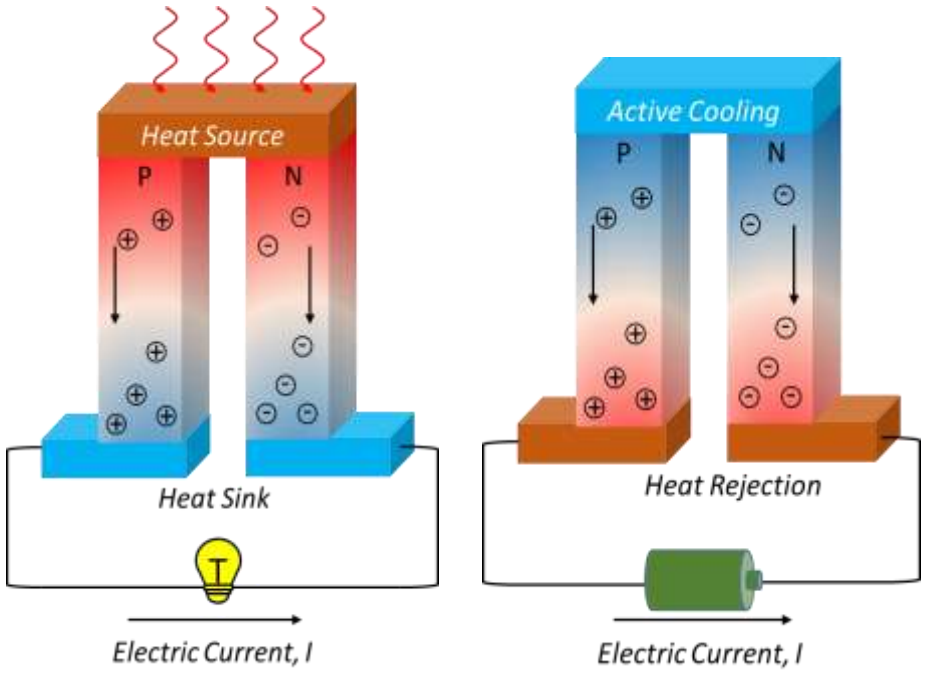

$$ZT = \frac{S^2\sigma T}{\kappa_E + \kappa_L}$$

Electrical transport

σ: electrical conductivity

S: Seebeck coefficient

Thermal transport

κ_L: lattice thermal conductivity

κ_E: electronic thermal conductivity

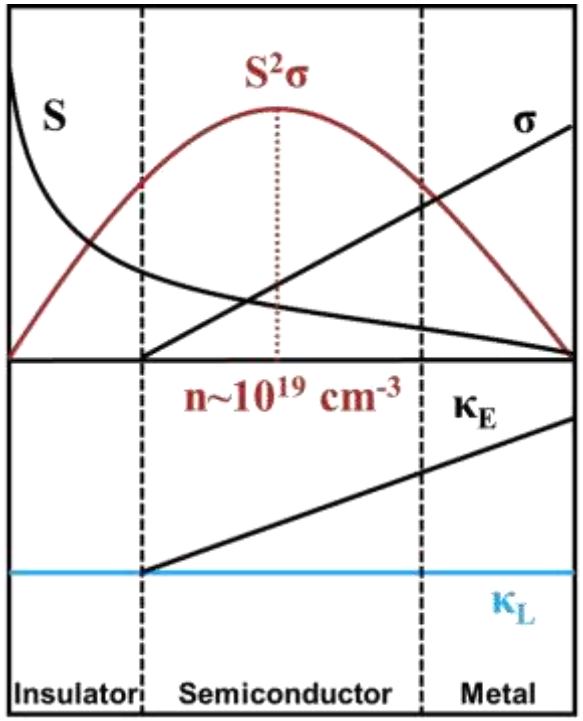

- Adjusting the optimal carrier concentration to reach the peak power factor.
- Reducing the lattice thermal conductivity.

J. Phys. Chem. Solids, 342, 321-335 (1973)
ROWE D M.,USA, Boca Raton: CRC Press, 2018

Dimensions of electrical and thermal conductivities

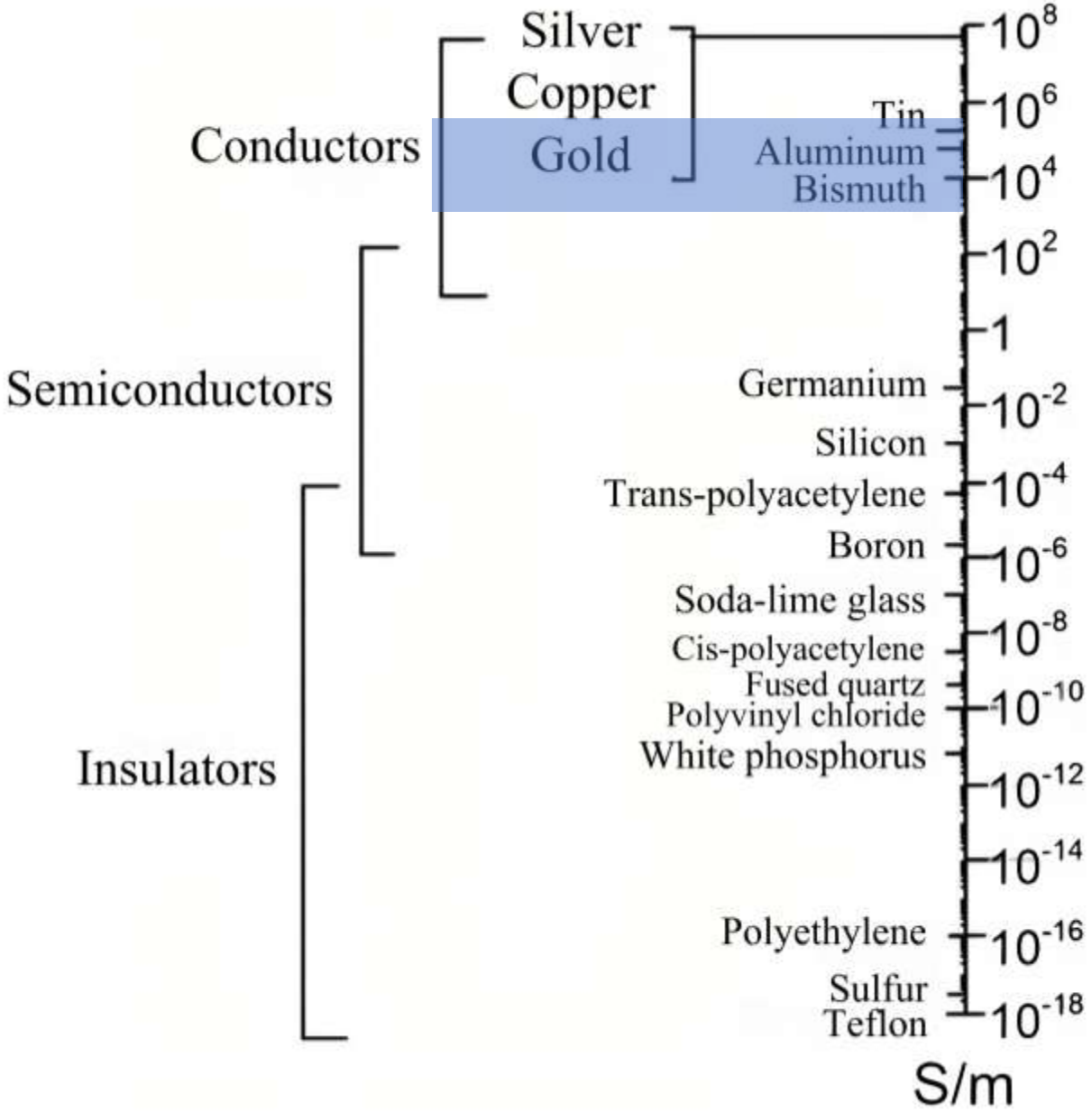

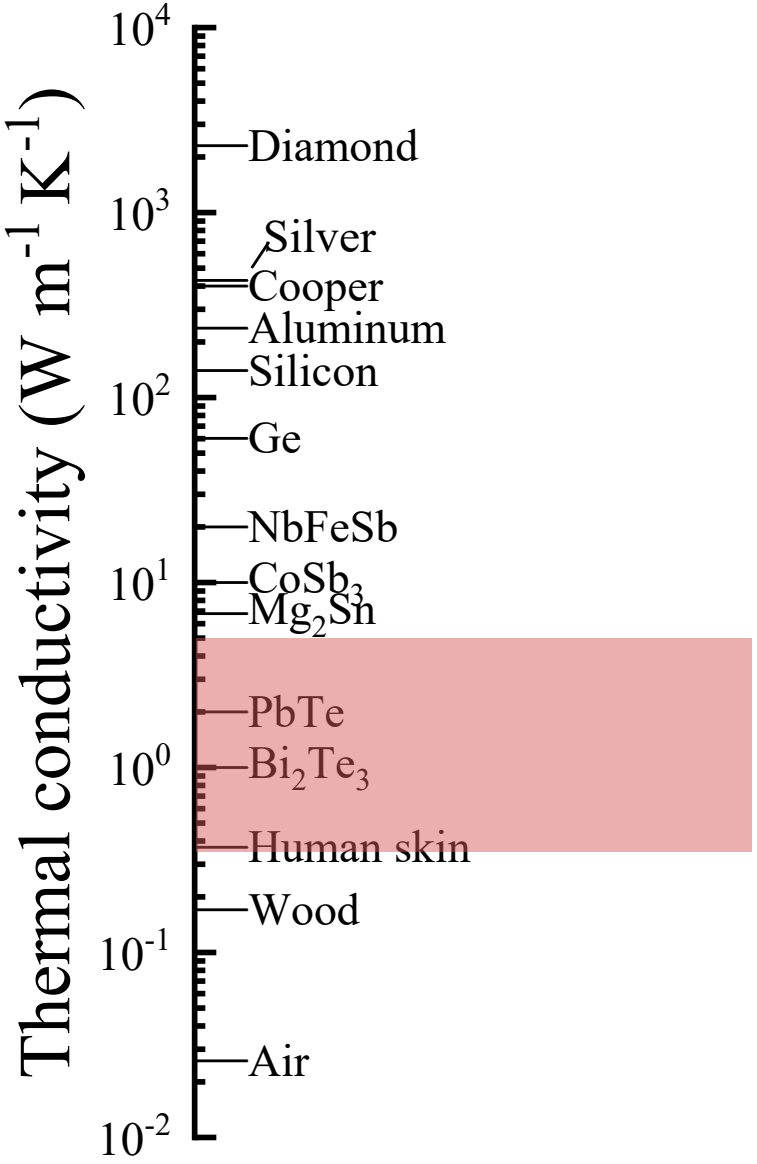

Electron and phonon transport

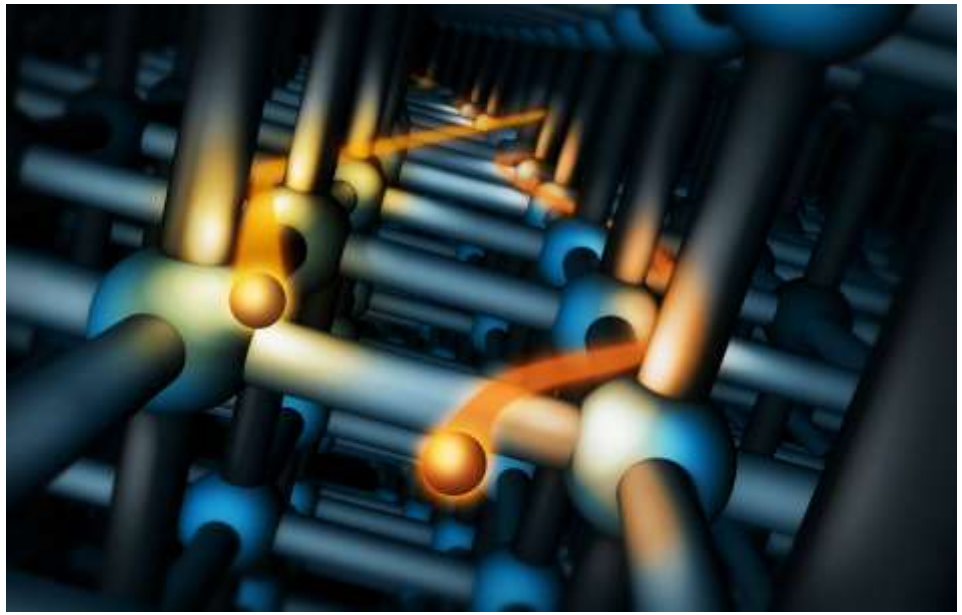

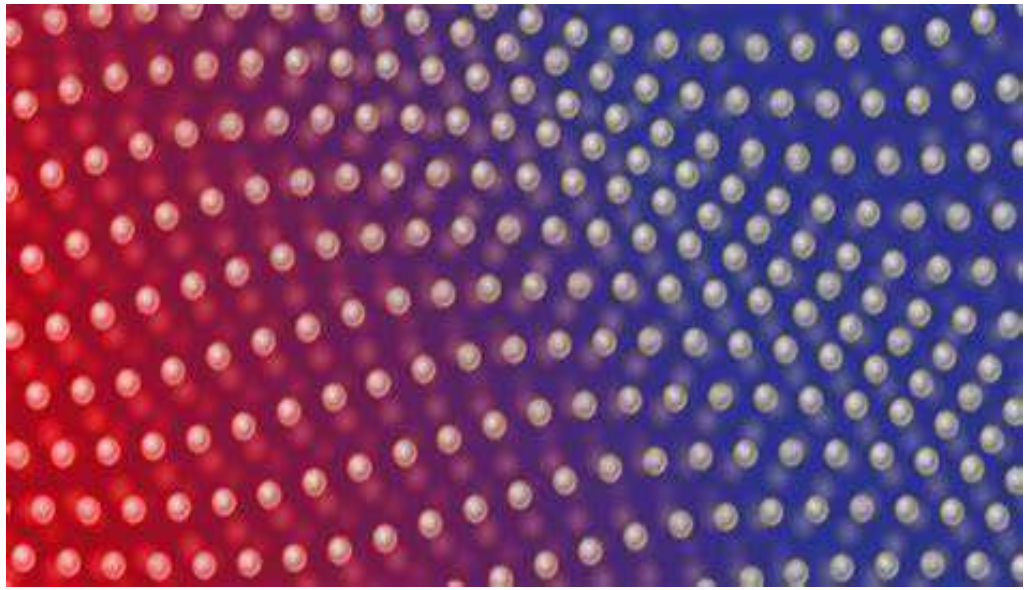

$$\sigma = \frac{1}{\Omega}\int N(\varepsilon)\mathbf{v_e^2}\tau_\mathbf{e}\left[-\frac{\partial f_0(T,\varepsilon)}{\partial \varepsilon}\right]d\varepsilon$$

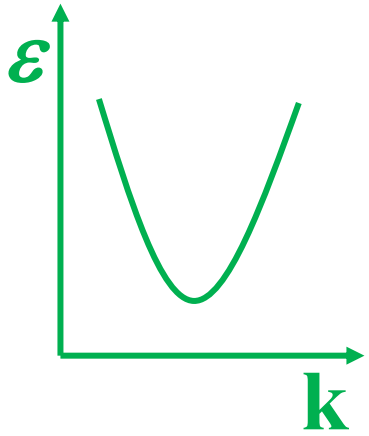

$\mathbf{k \rightarrow k'}$

$$\kappa_L = \frac{1}{3}\sum_{\mathbf{q}} \hbar\omega_\mathbf{q}\mathbf{v_q^2}\tau_\mathbf{q}\frac{\partial N_\mathbf{q}^0}{\partial T}$$

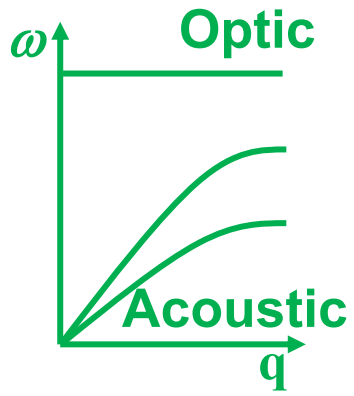

$\mathbf{q \rightarrow q'}$

Classical electron transport model

$$F_i = \int_0^\infty \frac{\epsilon^i d\epsilon}{1+Exp[\epsilon-\eta]} \qquad \eta = \frac{E_F}{k_B T}$$

$$n = 4\pi\left(\frac{2m_D^* k_b T}{h^2}\right)^{1.5} F_{\frac{1}{2}}(\eta) \qquad m_D^* = N_v^{2/3} m_b^*$$

$$S = \pm\frac{k_B}{e}\left(\frac{2F_1(\eta)}{F_0(\eta)} - \eta\right) \qquad \sigma = en\mu$$

- Effective mass
- Degeneracy

Acoustic phonon $\mu_{H,AP} = \frac{F_{-0.5}}{2F_0}\frac{e\pi\hbar^4}{\sqrt{2}(kT)^{1.5}}\frac{C_l}{E_{def}^2(m_I)(m_b^*)^{1.5}}$

Scattering by optical modes: polar crystals $\mu = \frac{\gamma(\hbar\omega)^{\frac{3}{2}}}{\pi 2^{\frac{5}{2}} e m^{*\frac{3}{2}}}(e^{\hbar\omega/kT}-1).$

Scattering by impurities and imperfections $\mu_i = \frac{2^{\frac{7}{2}}}{\pi^{\frac{3}{2}}}\frac{\epsilon^2}{Z^2 e^3 m^{*\frac{1}{2}}}\frac{(kT)^{\frac{3}{2}}}{N_i}F(3kT).$ $\quad F(\mathscr{E}) \equiv \ln\left(1+\frac{8m^*\mathscr{E}}{q^2\hbar^2}\right)-\left(1+\frac{q^2\hbar^2}{8m^*\mathscr{E}}\right)^{-1}$

J. Materiomics, 7, 603e611 (2021)
Ziman, J.M., *Electrons and Phonons: The Theory of Transport Phenomena in Solids* (Oxford University Press, 1960)

Classical phonon transport model

- **Phonon Gas Model :**

$$\kappa_L = \frac{1}{3}\sum C_V \mathbf{v}_\mathbf{q}^2 \tau_\mathbf{q}$$

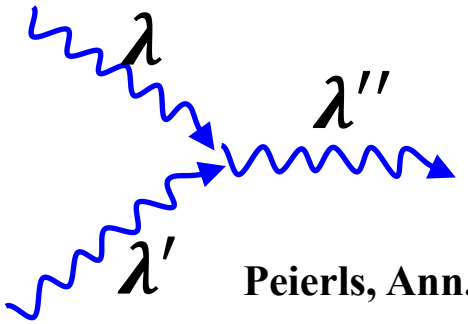

Peierls, Ann. Phys. 3, 1055 (1929)

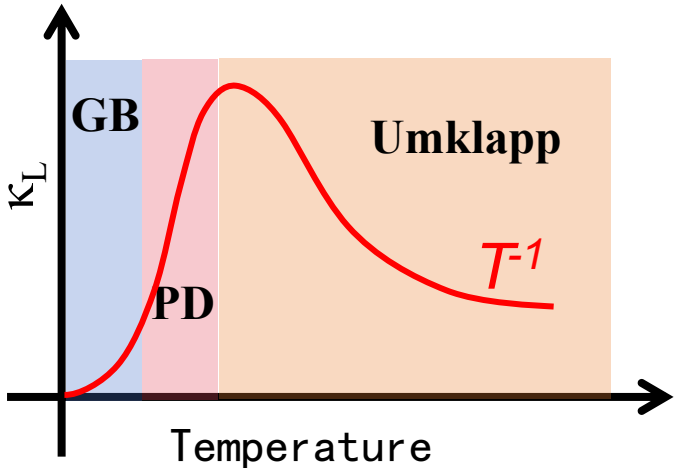

Matthiessen's rule :

$$\frac{1}{\tau_\mathbf{q}} = \frac{1}{\tau_U} + \frac{1}{\tau_{e-p}} + \frac{1}{\tau_{PD}} + \frac{1}{\tau_B} + \cdots$$

Phonon-phonon	Electron-phonon	Point defect	Grain boundary

Slack model for Umklapp process under Debye phonon

in the high-temperature limit

$$\kappa_L = A \cdot \frac{\bar{M}\theta^3\delta}{\gamma^2 n^{2/3}} T^{-1}$$

Tritt T M. *Thermal Conductivity. Theory, Properties, and Applications*, 2004
Slack, *J. Phys. Chem. Solids,* 34, 321 (1973)

Debye-Callaway Model

- **Based on the linear phonon dispersion and independent scattering approximations**

$$\kappa_L = \frac{k_B}{2\pi^2 v_s}\left(\frac{k_B}{\hbar}\right)^3 T^3 \int_0^{\theta_D/T} \tau \frac{x^4 e^x}{(e^x-1)^2} dx$$

$$\tau^{-1} = A\omega^2 + B\omega^2 + C\omega^4 + \frac{v}{L}$$

Other scattering mechanisms

Umklapp phonon scattering

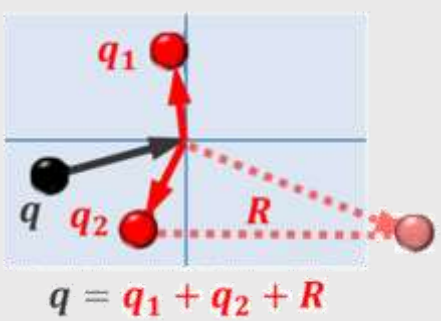

$$\frac{1}{\tau_U} = \frac{\hbar\gamma^2\omega^2 T}{\bar{M}v^2\theta_D}\exp\left(-\frac{\theta_D}{3T}\right)$$

Electron-phonon scattering

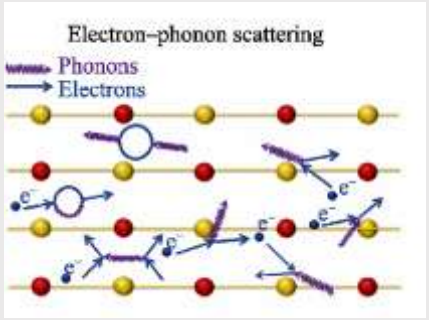

$$\frac{1}{\tau_{EP}} = \frac{E_{def}^2 m^* \omega^2}{2\pi\hbar^3 \rho v_L}$$

Point defect scattering

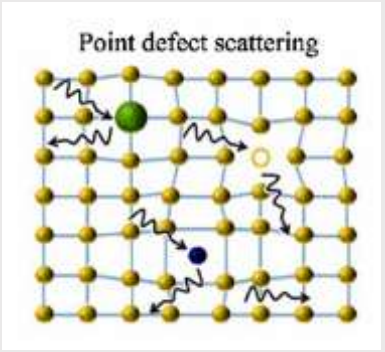

$$\frac{1}{\tau_{PD}} = \frac{\bar{V}\omega^4}{4\pi v^3}\Gamma$$

Grain boundary scattering

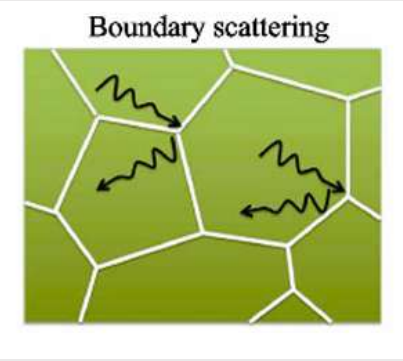

$$\frac{1}{\tau_B} = \frac{v}{L}$$

Phys. Rev., 113, 1046-1051 (1959); *Adv. Energy Mater.*, 8, 1702333 (2018)

Timeline for the electrical and thermal transport

Time

1900 Drude model

1912 Debye model

1928 Bloch theorem Tight-binding model

1929 Boltzmann theory for κ_L

1930 Boltzmann theory in solid

1959 Debye-Callaway model

195? Empirical forms for τ

1960 Ziman

1973 Slack model

198?-9? Band calculation

199? Phonon calculation

2006 BoltzTrap

2007 3rd IFC calculation

This talk

Overview

Background

Electrical transport

Lattice thermal conductivity

2.1 BTE in Electrical Transport

☐ Boltzmann transport equation within the relaxation time approximation

$$\sigma_{\alpha\beta}(\mu,T) = \frac{1}{V}\sum_{n\mathbf{k}} v_{n\mathbf{k}\alpha}\, v_{n\mathbf{k}\beta}\tau_{n\mathbf{k}}\left[-\frac{\partial f_\mu(\varepsilon_{n\mathbf{k}},T)}{\partial \varepsilon_{n\mathbf{k}}}\right]$$

$$S_{\alpha\beta}(\mu,T) = \frac{1}{eTV}\sigma_{\alpha\beta}(\mu,T)^{-1}\sum_{n\mathbf{k}} v_{n\mathbf{k}\alpha} v_{n\mathbf{k}\beta}\tau_{n\mathbf{k}}(\mu-\varepsilon_{n\mathbf{k}})\left[-\frac{\partial f_\mu(\varepsilon_{n\mathbf{k}},T)}{\partial \varepsilon_{n\mathbf{k}}}\right]$$

$$f_\mu = \frac{1}{\exp(\varepsilon_{n\mathbf{k}}-\mu)+1}$$ Fermi-Dirac Distribution

μ Fermi level $\varepsilon_{n\mathbf{k}}$ band energy

$\mathbf{v}_{n\mathbf{k}}$ Group velocity

$\tau_{n\mathbf{k}}$ Relaxation time

Effective Range of Electronic States

$$\sigma_{\alpha\beta}(\mu,T)=\frac{1}{V}\sum_{n\mathbf{k}} v_{n\mathbf{k}\alpha}\, v_{n\mathbf{k}\beta}\tau_{n\mathbf{k}}\left[-\frac{\partial f_{\mu}(\varepsilon_{n\mathbf{k}},T)}{\partial \varepsilon_{n\mathbf{k}}}\right]$$

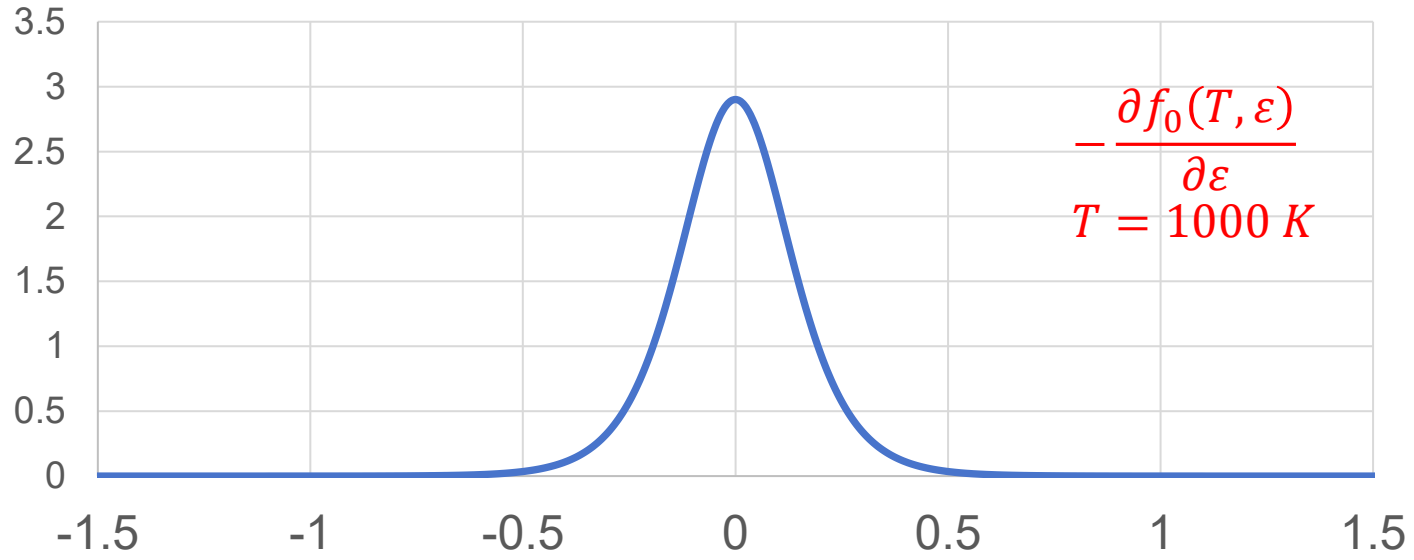

- **Only electronic states within a few $k_B T$ around E_F contribute significantly to transport**
- **The importance of electronic states far from E_F decreases exponentially**
- **The effective energy range expands with increasing temperature**

2.1 BTE in Electrical Transport

- **Fermi surface at the Fermi level: the origin of electrical conductivity in metals and heavily-doped semiconductors**

$$\sigma_{\alpha\beta}(\mu,T)=\frac{1}{V}\sum_{n\mathbf{k}} v_{n\mathbf{k}\alpha}\, v_{n\mathbf{k}\beta}\tau_{n\mathbf{k}}\left[-\frac{\partial f_{\mu}(\varepsilon_{n\mathbf{k}},T)}{\partial \varepsilon_{n\mathbf{k}}}\right]$$

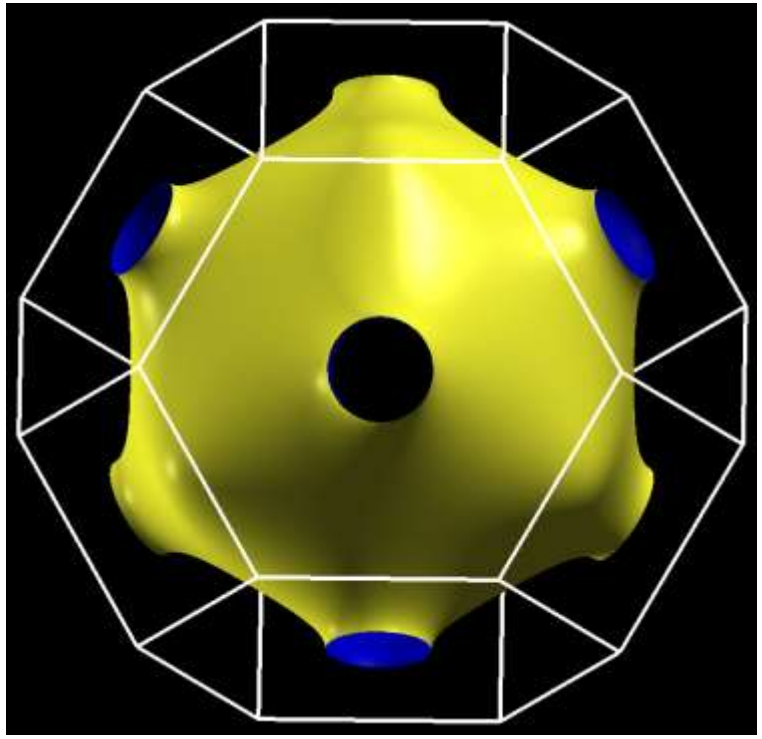

Fermi Surface at E_F in Metal Cu

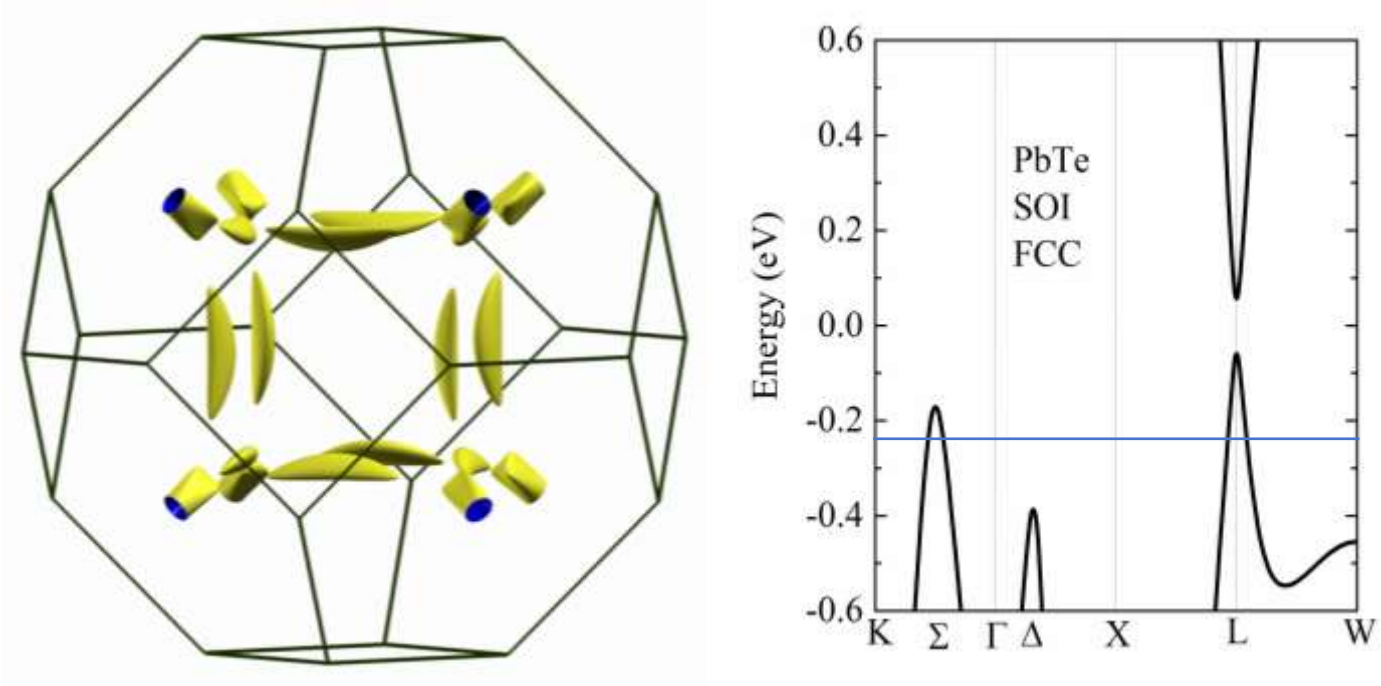

Fermi surface in heavily doped semiconductors reflects the band degeneracy.

ACS appl. Mater. Interface, 9, 8729 (2017)

2.1 BTE in Electrical Transport

$$\sigma_{\alpha\beta}(\mu,T)=\frac{1}{V}\sum_{n\mathbf{k}} v_{n\mathbf{k}\alpha}\, v_{n\mathbf{k}\beta}\tau_{n\mathbf{k}}\left[-\frac{\partial f_{\mu}(\varepsilon_{n\mathbf{k}},T)}{\partial \varepsilon_{n\mathbf{k}}}\right]$$

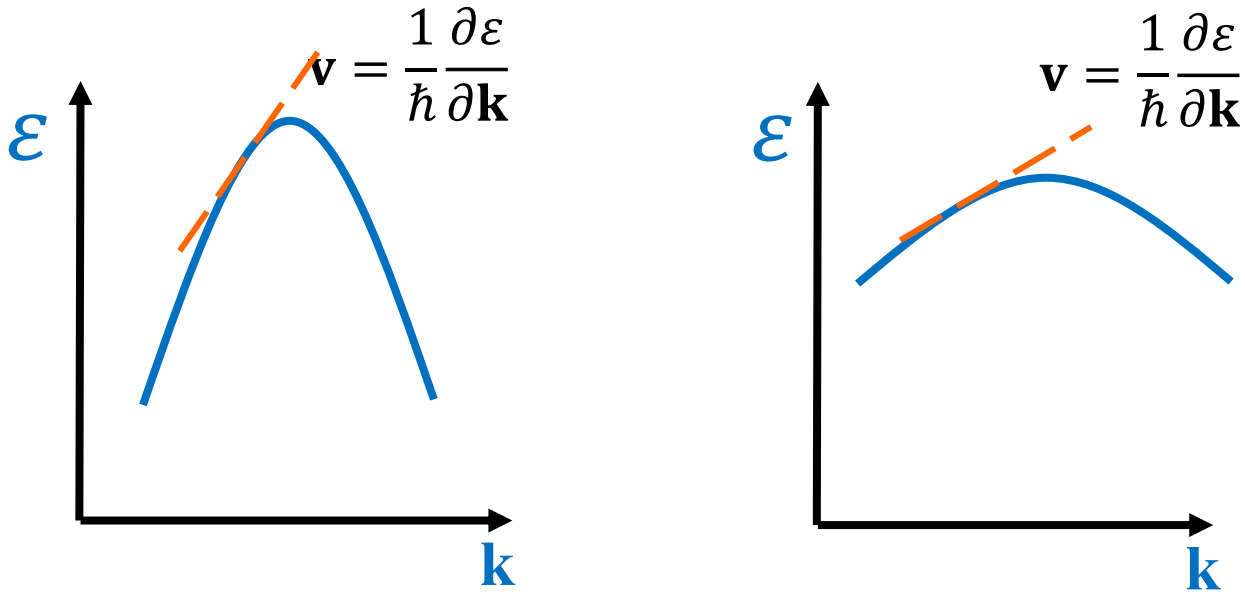

The average electron group velocity lies within the range of 10^4-10^5 m/s

2.1 BTE in Electrical Transport

$$\sigma_{\alpha\beta}(\mu,T)=\frac{1}{V}\sum_{n\mathbf{k}} v_{n\mathbf{k}\alpha}\, v_{n\mathbf{k}\beta}\tau_{n\mathbf{k}}\left[-\frac{\partial f_{\mu}(\varepsilon_{n\mathbf{k}},T)}{\partial \varepsilon_{n\mathbf{k}}}\right]$$

$$\tau:\ 10^{-15}\sim 10^{-14}\ s$$

Matthiessen's Rule

$$\frac{1}{\tau_{n\mathbf{k}}}=\frac{1}{\tau_{\mathrm{e-ph}}}+\frac{1}{\tau_{\mathrm{IMP}}}\ldots$$

The mobility is determined by the integral of group velocity and relaxation time.

2.1 BTE in Electrical Transport

Relaxation time under full electron-phonon interaction (FEPI)

$$\frac{1}{\tau_{\mathbf{k}}} = \frac{2\pi}{\hbar}\sum_{\mathbf{k}'}\left|\langle \mathbf{k}'|\partial_{\mathbf{q}}V|\mathbf{k}\rangle\right|^2\left[\left(f_{\mathbf{k}'}+n_{\mathbf{q}}\right)\delta\left(\varepsilon_{\mathbf{k}}-\varepsilon_{\mathbf{k}'}+\hbar\omega_{\mathbf{q}}\right)\delta_{\mathbf{k}+\mathbf{q},\mathbf{k}'+\mathbf{G}}\right.$$

$$\left.+\left(1-f_{\mathbf{k}'}+n_{\mathbf{q}}\right)\delta\left(\varepsilon_{\mathbf{k}}-\varepsilon_{\mathbf{k}'}-\hbar\omega_{\mathbf{q}}\right)\delta_{\mathbf{k}-\mathbf{q},\mathbf{k}'+\mathbf{G}}\right]\left(1-\frac{\mathbf{v}_{\mathbf{k}'}\cdot\mathbf{v}_{\mathbf{k}}}{|\mathbf{v}_{\mathbf{k}'}||\mathbf{v}_{\mathbf{k}}|}\right) \quad .$$

Relaxation time under constant values of EPI matrix

acoustic deformation potential (ADP) short range

$$\frac{1}{\tau_{\mathrm{ADP},n\mathbf{k}}} = \frac{2\pi k_{\mathrm{B}}E_{\mathrm{def}}^2 T}{\hbar G V}\sum_{m\mathbf{k}'}\delta(\varepsilon_{n\mathbf{k}}-\varepsilon_{m\mathbf{k}'})$$

Bardeen-Shockley

polar optical phonon (POP) long range

$$\frac{1}{\tau_{\mathrm{POP},n\mathbf{k}}} = \sum_{m\mathbf{k}'}\frac{\pi\omega_{\mathrm{po}}e^2}{V|\mathbf{k}'-\mathbf{k}|^2\kappa_0}\left(\frac{1}{\varepsilon_\infty}-\frac{1}{\varepsilon_{\mathrm{s}}}\right)(2N_\omega+1)\,\delta\left(\varepsilon_{n\mathbf{k}}-\varepsilon_{m\mathbf{k}'}\right)$$

Frölich

2.2 Softwares for Electrical Transport

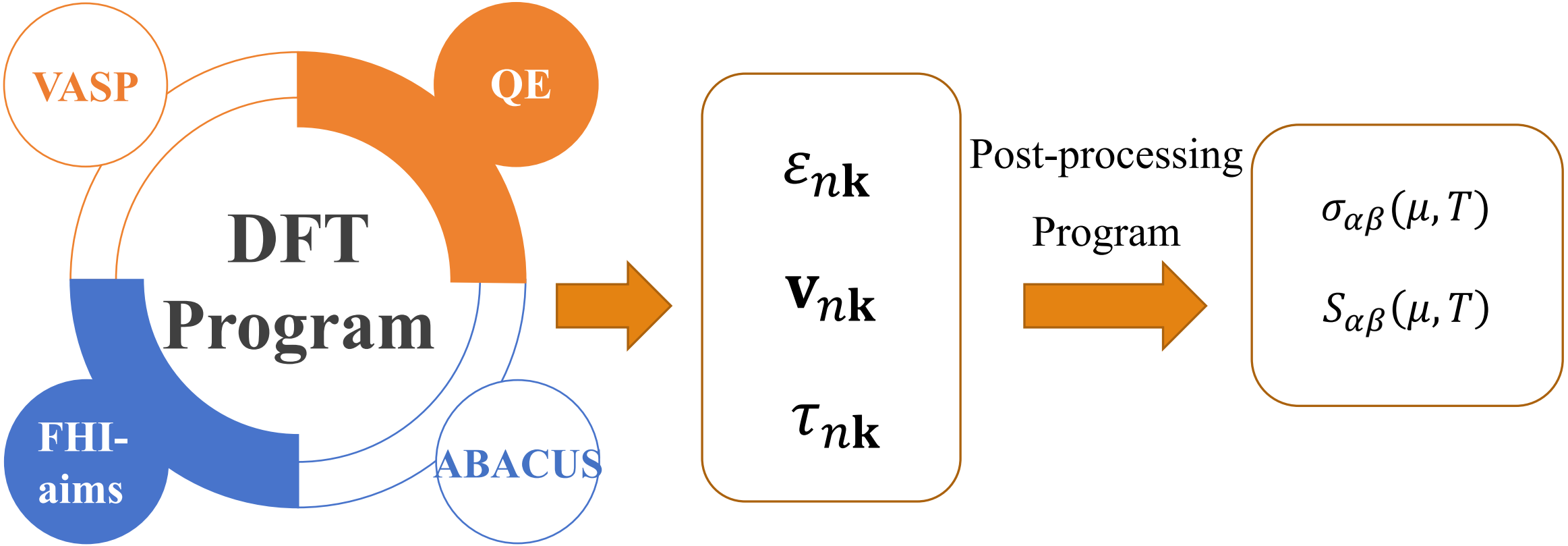

2.2 Softwares for Electrical Transport

Constant Scattering Time	Leading Order Approximation	Energy-Dependent EPI matrix	Fourier-Wannier Interpolation	Direct DFPT Sampling
BoltzTraP	TransOpt	EPA	EPW	Quantum Espresso
BoltzWann	AMSET	EPIC STAR	Abinit	Abinit
	ElecTra		Perturbo	
			EPIq	

Complexity, Cost, Completeness

Acknowledgement to Prof. Tianqi Deng
Zhejiang University

2.2 Softwares for Electrical Transport **BoltzTrap**

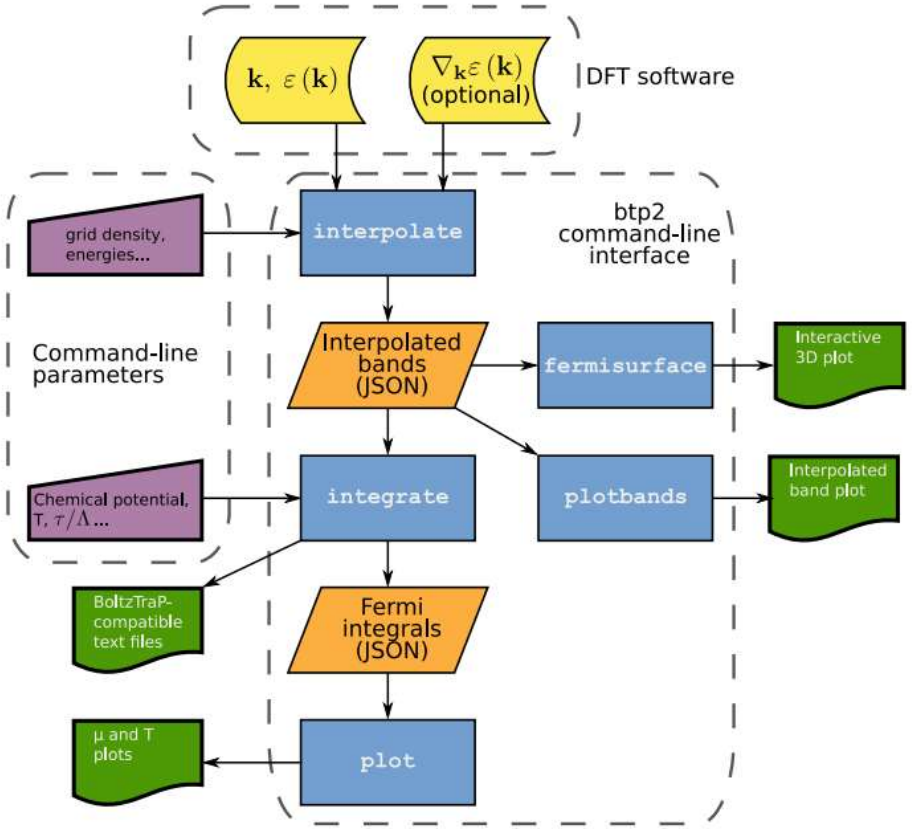

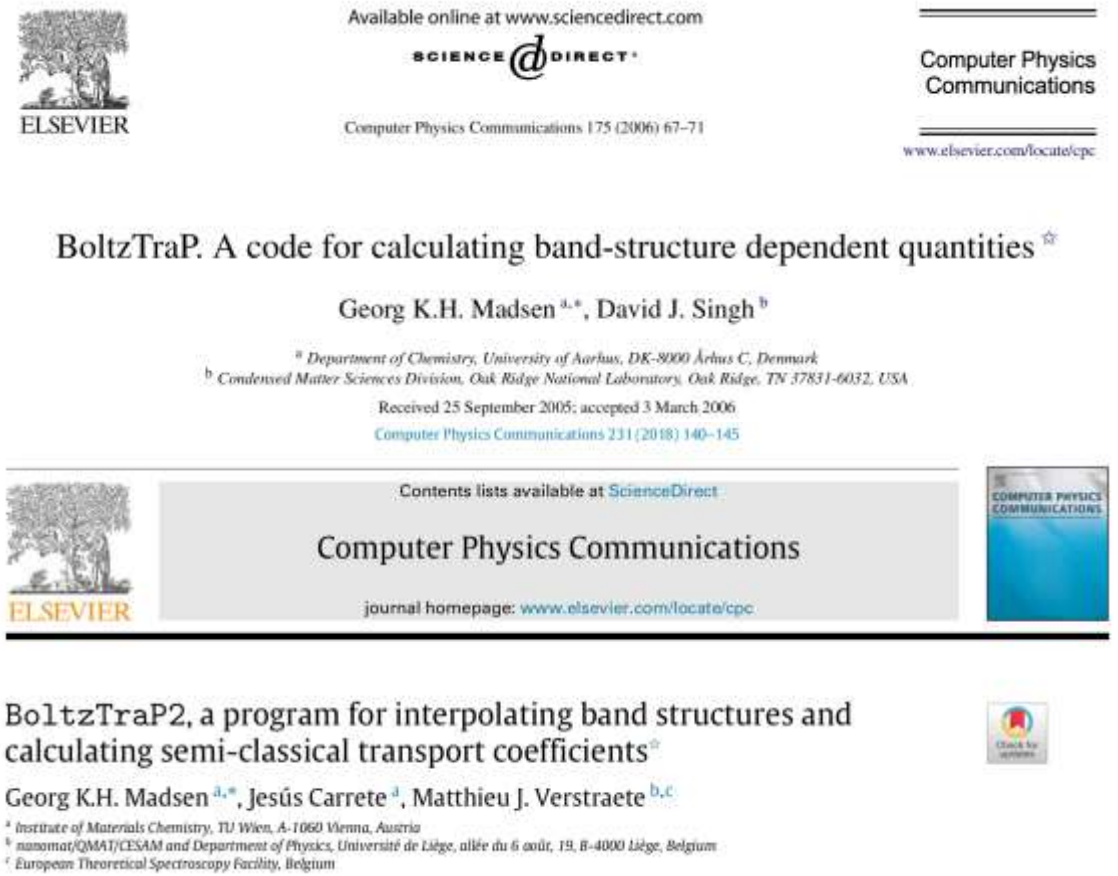

ELSEVIER

Available online at www.sciencedirect.com

SCIENCE DIRECT

Computer Physics Communications 175 (2006) 67–71

Computer Physics Communications

www.elsevier.com/locate/cpc

BoltzTraP. A code for calculating band-structure dependent quantities ☆

Georg K.H. Madsen [a,*], David J. Singh [b]

[a] Department of Chemistry, University of Aarhus, DK-8000 Århus C, Denmark
[b] Condensed Matter Sciences Division, Oak Ridge National Laboratory, Oak Ridge, TN 37831-6032, USA

Received 25 September 2005; accepted 3 March 2006

Computer Physics Communications 231 (2018) 140–145

ELSEVIER

Contents lists available at ScienceDirect

Computer Physics Communications

journal homepage: www.elsevier.com/locate/cpc

BoltzTraP2, a program for interpolating band structures and calculating semi-classical transport coefficients ☆

Georg K.H. Madsen [a,*], Jesús Carrete [a], Matthieu J. Verstraete [b,c]

[a] Institute of Materials Chemistry, TU Wien, A-1060 Vienna, Austria
[b] nanomat/QMAT/CESAM and Department of Physics, Université de Liège, allée du 6 août, 19, B-4000 Liège, Belgium
[c] European Theoretical Spectroscopy Facility, Belgium

- Early Release & Broad Application: including Seebeck coefficient and other properties under the constant relaxation time approximation (CRTA).
- High-Throughput Suitable: ideal for high-throughput computational workflows.
- Star function method for band interpolation

2.2 Softwares for Electrical Transport **Amset**

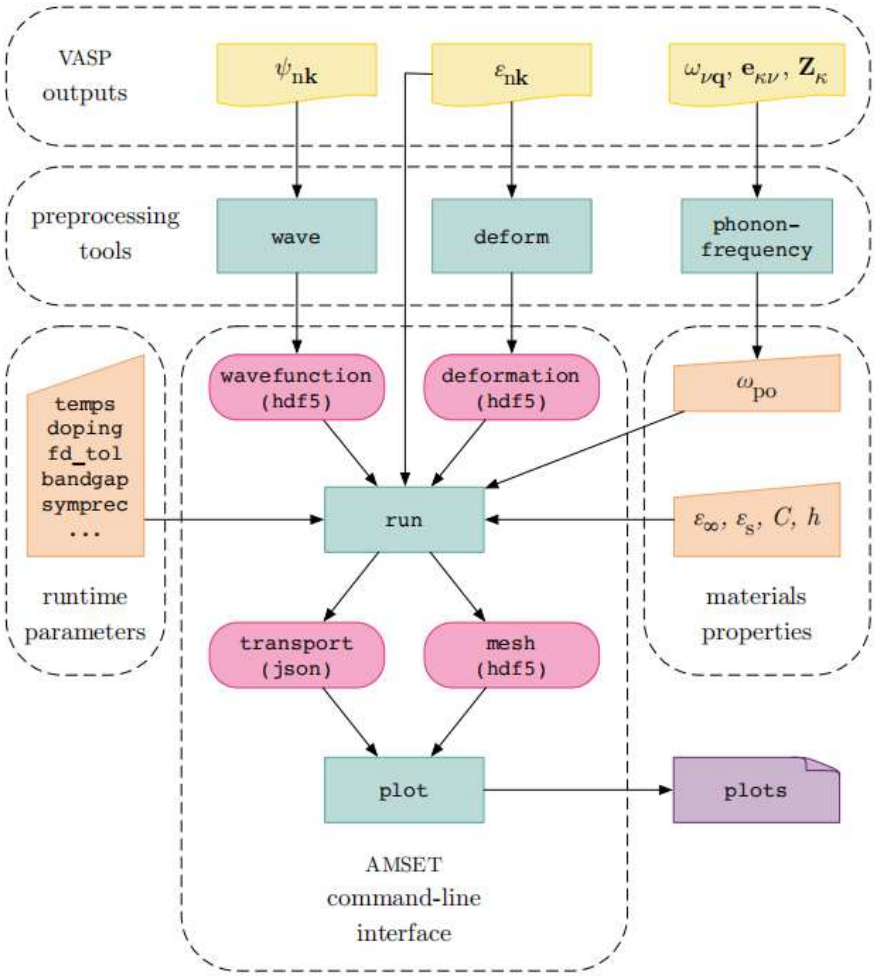

Supplementary Figure 3. Schematic of the AMSET program indicating the typical inputs and outputs, command-line tools, and program flow.

NATURE COMMUNICATIONS | 12:2222 (2021)

- Eliminates the computationally expensive DFPT matrix element calculations.
- Anisotropy models and scattering mechanisms: ADP, POP, PI, and IMP
- Utilize BoltzTraP2 for band structure interpolation

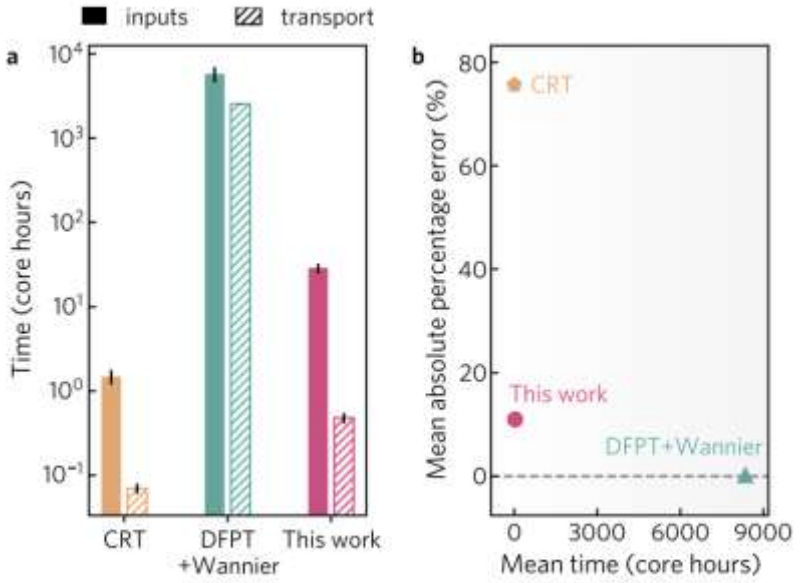

Fig. 2 Comparison of speed against accuracy for transport calculations.

2.2 Softwares for Electrical Transport

EPIC STAR

Article | Open access | Published: 07 May 2020

EPIC STAR: a reliable and efficient approach for phonon- and impurity-limited charge transport calculations

Tianqi Deng, Gang Wu ✉, Michael B. Sullivan, Zicong Marvin Wong, Kedar Hippalgaonkar, Jian-Sheng Wang & Shuo-Wang Yang ✉

npj Computational Materials **6**, Article number: 46 (2020) | Cite this article

Silicon

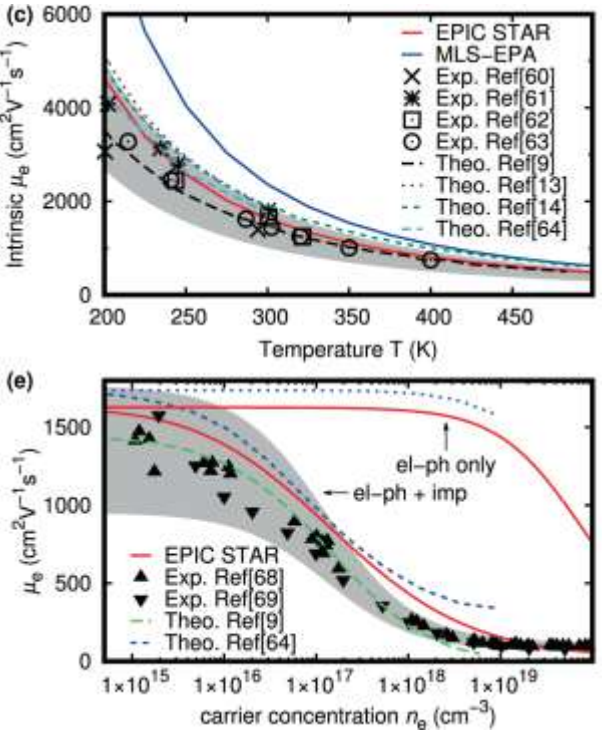

NbFeSb

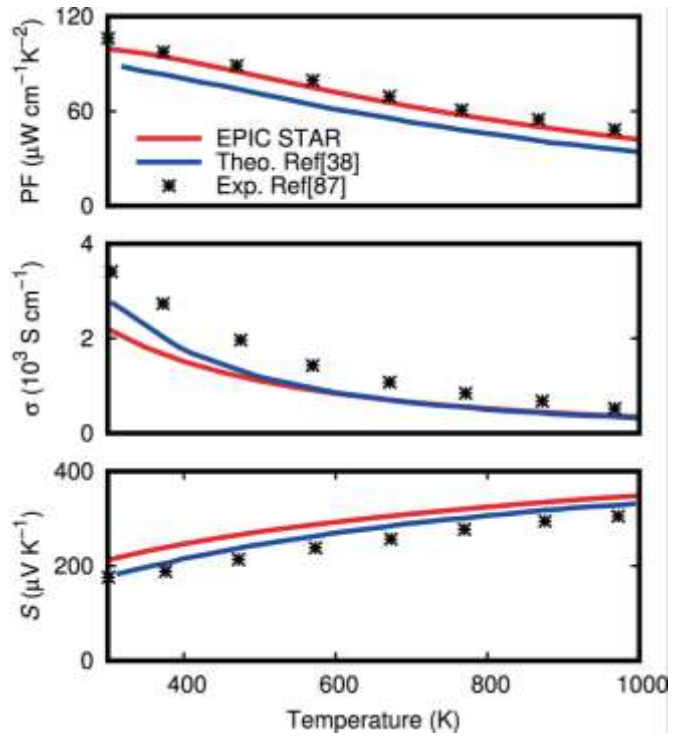

npj Comput. Mater., 6, 46 (2020)

EPIC STAR

- Generalized Eliashberg function for short-range electron-phonon scattering
- Analytical expressions for long-range electron-phonon and electron-impurity scattering

Utilize BoltzTraP2 for band interpolation

$$\alpha_l^2 F(E,\omega) = \frac{\omega}{\rho(E)} \sum_{mn} \int_{BZ} \frac{d\mathbf{k}}{\Omega_{BZ}} \frac{d\mathbf{q}}{\Omega_{BZ}} \frac{\left|g^S_{nml}(\mathbf{k},\mathbf{q})\right|^2}{\omega_{l\mathbf{q}}} \delta(E - \varepsilon_{n\mathbf{k}}) \times \delta(\hbar\omega + E - \varepsilon_{m\mathbf{k}+\mathbf{q}}) \left[\delta(\omega - \omega_{l\mathbf{q}}) + \delta(\omega + \omega_{l\mathbf{q}})\right]$$

$$\tau_l^{-1}(E,\mu,T) = 2\pi \left\{ \int_0^{+\infty} \alpha_l^2 F(E,\omega)[f(E+\hbar\omega-\mu,T) + n(\hbar\omega,T)]d\omega + \int_{-\infty}^{0} \alpha_l^2 F(E,\omega)[1 - f(E+\hbar\omega-\mu,T) + n(\hbar\omega,T)]d\omega \right\}$$

$$\tau^{-1}_{\mathrm{POP},l}(E) = C^2_{\mathrm{POP},l} \frac{\Omega}{\pi\hbar^2} \sqrt{\frac{m_b(E)}{2E}} \left\{ \sinh^{-1}\sqrt{\frac{E}{\hbar\omega_l}} [n(\hbar\omega_l, T) + f(E+\hbar\omega_l-\mu, T)] + \sinh^{-1}\sqrt{\frac{E}{\hbar\omega_l} - 1} [n(\hbar\omega_l, T) + 1 - f(E-\hbar\omega_l-\mu, T)] \right\}$$

$$\tau^{-1}_{\mathrm{imp}}(E) \approx \frac{n_{\mathrm{imp}} e^4}{16\sqrt{2m_b(E)}\pi\epsilon^2\epsilon_0^2} \frac{1}{\sqrt{E^3}} \left[\ln\left(1 + \frac{8m_b(E)EL^2}{\hbar^2}\right) - \frac{8m_b(E)EL^2}{\hbar^2 + 8m_b(E)EL^2} \right]$$

2.2 Softwares for Electrical Transport **Quantum Espresso: EPW**

QUANTUMESPRESSO

HOME PROJECT DOWNLOAD RESOURCES PSEUDOPOTENTIALS CONTACTS NEWS & EVENTS

PHYSICAL REVIEW B **92**, 075405 (2015)

Electrical transport limited by electron-phonon coupling from Boltzmann transport equation: An *ab initio* study of Si, Al, and MoS_2

Wu Li*

Scientific Computing & Modelling NV, De Boelelaan 1083, 1081 HV Amsterdam, The Netherlands

(Received 24 March 2015; published 4 August 2015)

- Relaxation times based on *ab initio* electron-phonon interaction. $g_{mn\nu}(\mathbf{k},\mathbf{q}) = \langle m\mathbf{k}+\mathbf{q}|\partial_{\nu\mathbf{q}}\hat{V}_{DFT}|n\mathbf{k}\rangle$
- Only can calculate the mobility.
- Requires third-party post-processing tools (e.g., TransOpt) to obtain the full electrical transport results (Seebeck coefficient, electrical conductivity, electrical thermal conductivity, *etc*).

2.2 Softwares for Electrical Transport **Quantum Espresso: EPW**

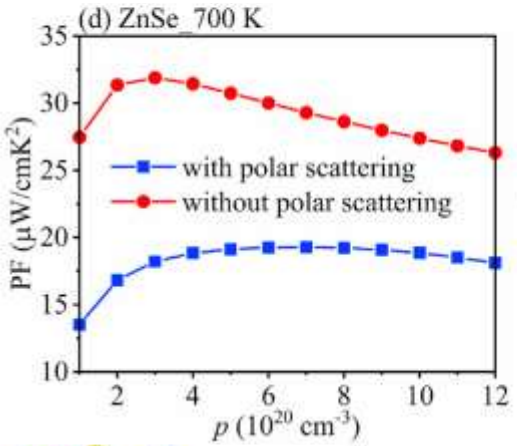

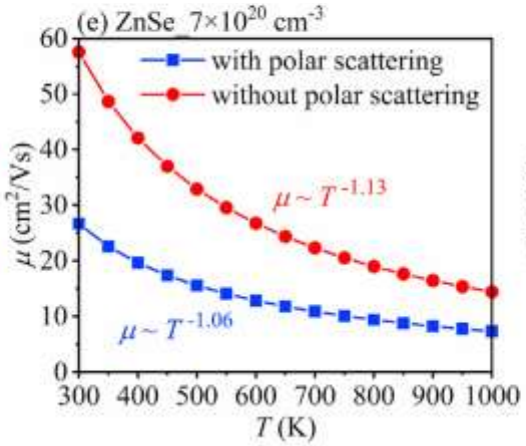

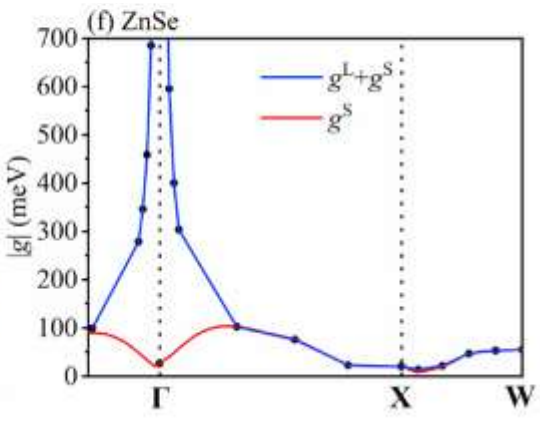

$$g^{L}_{mn\lambda}(\mathbf{k},\mathbf{q}) = i\frac{4\pi}{\Omega}\frac{e^2}{4\pi\varepsilon_0}\sum_{\kappa}\left(\frac{\hbar}{2NM_{\kappa}\omega_{\mathbf{q}\lambda}}\right)^{1/2} \times \sum_{\mathbf{G}\neq\mathbf{q}}\frac{(\mathbf{q}+\mathbf{G})\cdot Z^{*}_{\kappa}\cdot \mathbf{e}_{\kappa\lambda}(\mathbf{q})}{(\mathbf{q}+\mathbf{G})\cdot\epsilon^{\infty}\cdot(\mathbf{q}+\mathbf{G})} \times \langle\psi_{m\mathbf{k}+\mathbf{q}}|e^{i(\mathbf{q}+\mathbf{G})\cdot\mathbf{r}}|\psi_{n\mathbf{k}}\rangle$$

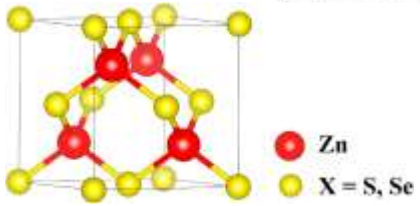

Due to the strong polarity, the polar optical phonon (POP) scattering is the dominant mechanism for the electrical transport in ZnX.

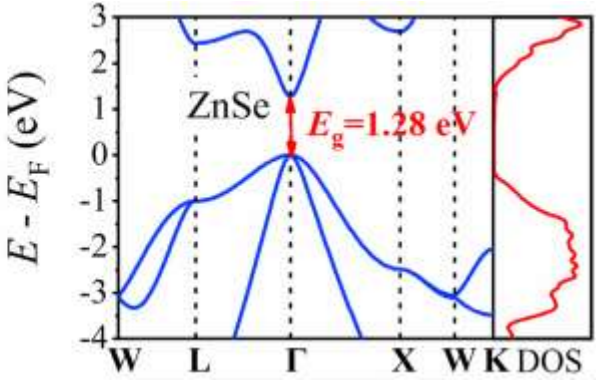

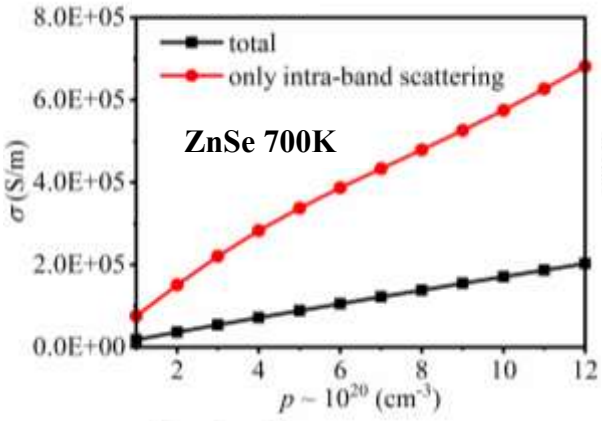

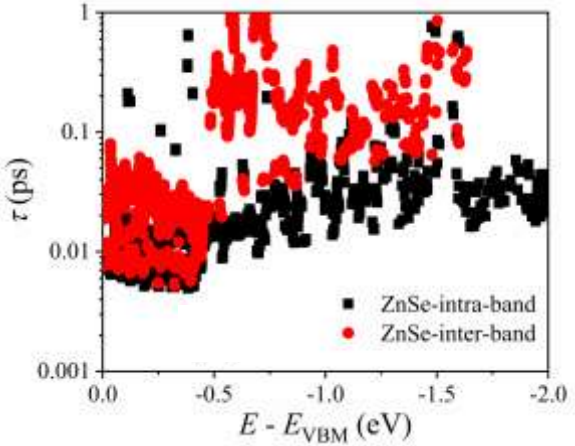

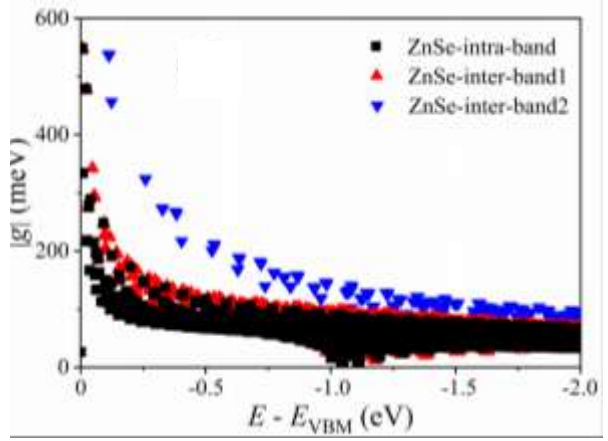

Due to the triple degeneracy near the VBM, the inter-band scattering also has detrimental contributions to the electrical conductivities.

J. Materiomics, 2021, 7, 310

☐ Origin of the strong E_{2g}- optical phonon coupling in α-graphyne

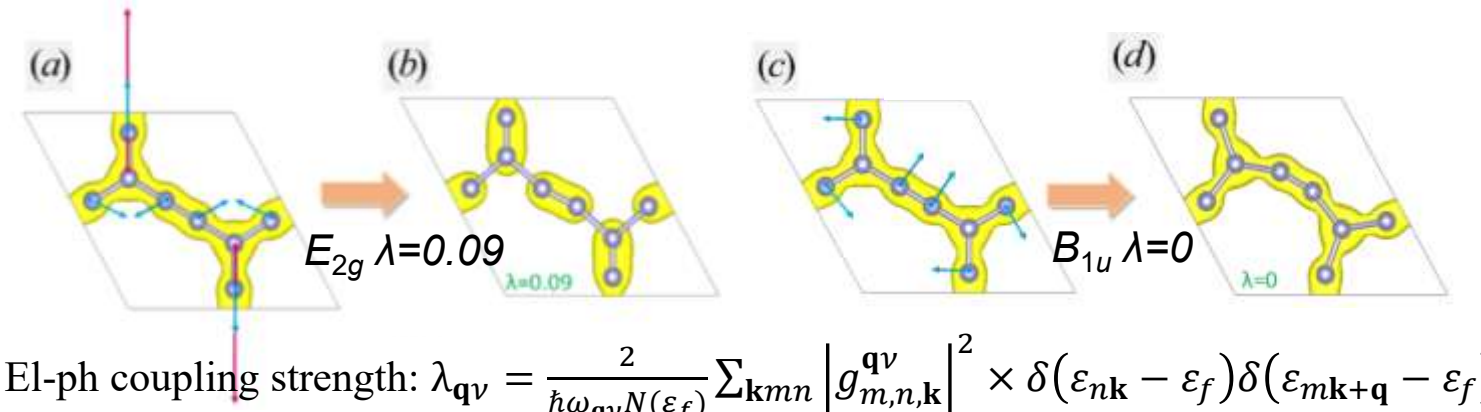

El-ph coupling strength: $\lambda_{\mathbf{q}\nu} = \frac{2}{\hbar\omega_{\mathbf{q}\nu}N(\varepsilon_f)}\sum_{\mathbf{k}mn}\left|g^{\mathbf{q}\nu}_{m,n,\mathbf{k}}\right|^2 \times \delta(\varepsilon_{n\mathbf{k}} - \varepsilon_f)\delta(\varepsilon_{m\mathbf{k}+\mathbf{q}} - \varepsilon_f)$

➢ **a larger $\lambda_{\mathbf{q}\nu}$ of E_{2g} phonon can be understandable from the group theory. In real space, E_{2g} phonon greatly disrupts electronic state.**

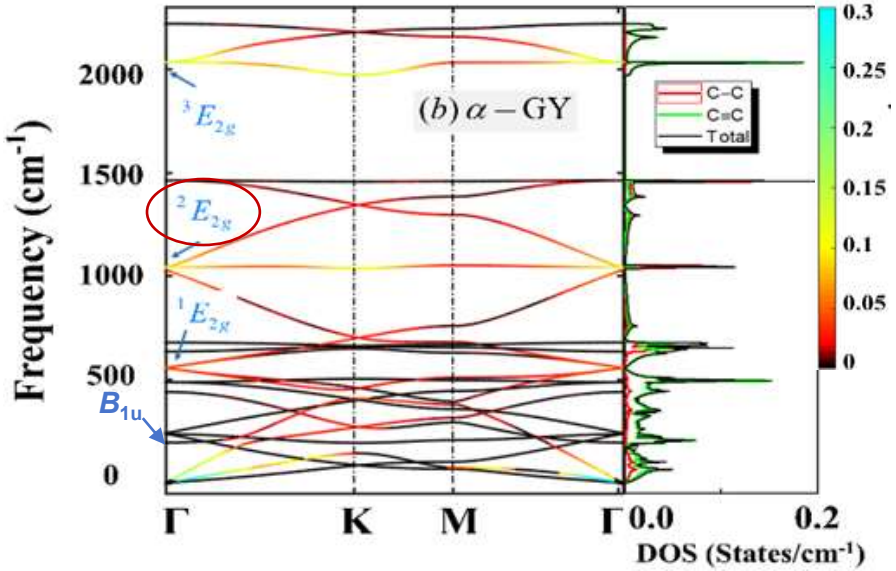

Nanoscale, 11, 10828 (2019)

☐ ZA (out-of-plane acoustic) phonon in TMD monolayers

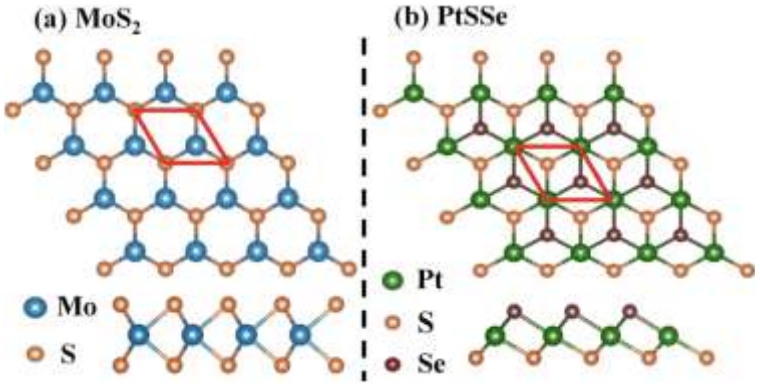

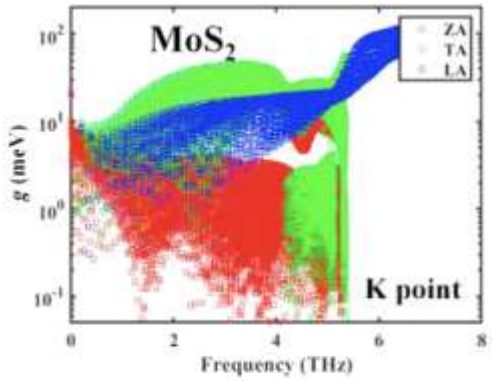

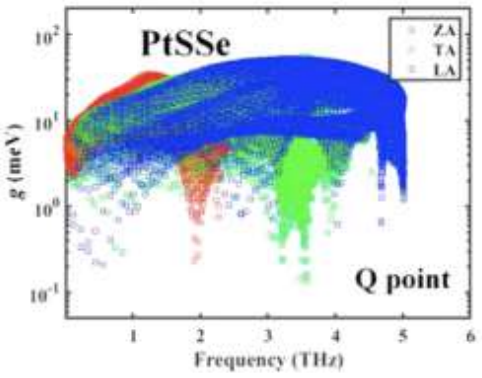

Lack of horizontal mirror symmetry in PtSSe enables a strong el-ZA ph coupling

Mater. Today Phys., 15, 100277 (2020)

2.3 TransOpt

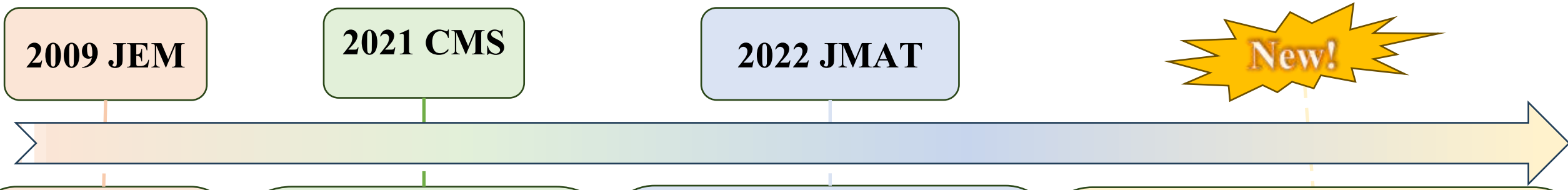

Transoptic

- CRTA
- Momentum matrix

TransOpt_1.0

- ADP
- SYMMETRY

TransOpt_1.1

Different spin deformation potentials are considered

TransOpt_2.0

- IMP
- Cuda GPU acceleration

TransOpt_3.0

- POP
- Versatile program interfaces
- OpenACC CPU/GPU acceleration

***J. Electron. Mater.*, 38, 1397 (2009)**
***Comput. Mater. Sci.*, 186, 110074 (2021)**
***npj Comput. Mater.*, 9, 190 (2023)**
***J. Materiomics*, 8, 1222-1229 (2022)**

2.3 Formulas in TransOpt

$$\frac{1}{\tau_{\mathrm{e-ph}}}$$

acoustical phonon (ADP)

$$\frac{1}{\tau_{\mathrm{ADP},n\mathbf{k}}} = \frac{2\pi k_{\mathrm{B}} E_{\mathrm{def}}^2 T}{\hbar G V} \sum_{m\mathbf{k}'} \delta(\varepsilon_{n\mathbf{k}} - \varepsilon_{m\mathbf{k}'})$$

Bardeen-Shockley

polar optical phonon (POP)

$$\frac{1}{\tau_{\mathrm{POP},n\mathbf{k}}} = \sum_{m\mathbf{k}'} \frac{\pi \omega_{\mathrm{po}} e^2}{V|\mathbf{k}' - \mathbf{k}|^2 \kappa_0} \left(\frac{1}{\varepsilon_\infty} - \frac{1}{\varepsilon_{\mathrm{s}}}\right)(2N_\omega + 1)\, \delta(\varepsilon_{n\mathbf{k}} - \varepsilon_{m\mathbf{k}'})$$

Frölich

…

$$\frac{1}{\tau_{\mathrm{IMP}}}$$

ionized impurity (IMP)

$$\frac{1}{\tau_{\mathrm{IMP},n\mathbf{k}}} = \sum_{m\mathbf{k}'} \frac{2\pi n_{\mathrm{imp}} Z_{\mathrm{imp}}^2 e^4}{V\hbar(\varepsilon_{\mathrm{s}}\kappa_0)^2 \left(L_{\mathrm{D}}^{-2} + |\mathbf{k}' - \mathbf{k}|^2\right)^2} \delta(\varepsilon_{n\mathbf{k}} - \varepsilon_{m\mathbf{k}'})$$

Brooks-Herring

$$L_{\mathrm{D}} = \sqrt{\frac{\varepsilon_{\mathrm{s}} \kappa_0 k_{\mathrm{B}} T}{e^2 n_0}}$$

E_{def} Deformation potential; G Modulus; n_{imp} Impurity concentration; Z_{imp} Impurity charge; ε_{s} Static dielectric; ε_∞ high frequency dielectric; κ_0 vacuum dielectric constant; L_{D} Debye screening length; n_0 carrier concentration; ω_{po} Effective polar phonon frequency

2.3 TransOpt **Recent works by TransOpt 1.0**

$$\frac{1}{\tau_{\mathrm{ADP},n\mathbf{k}}} = \frac{2\pi k_B E_{\mathrm{def}}^2 T}{\hbar G V} \sum_{m\mathbf{k}'} \delta(\varepsilon_{n\mathbf{k}} - \varepsilon_{m\mathbf{k}'})$$

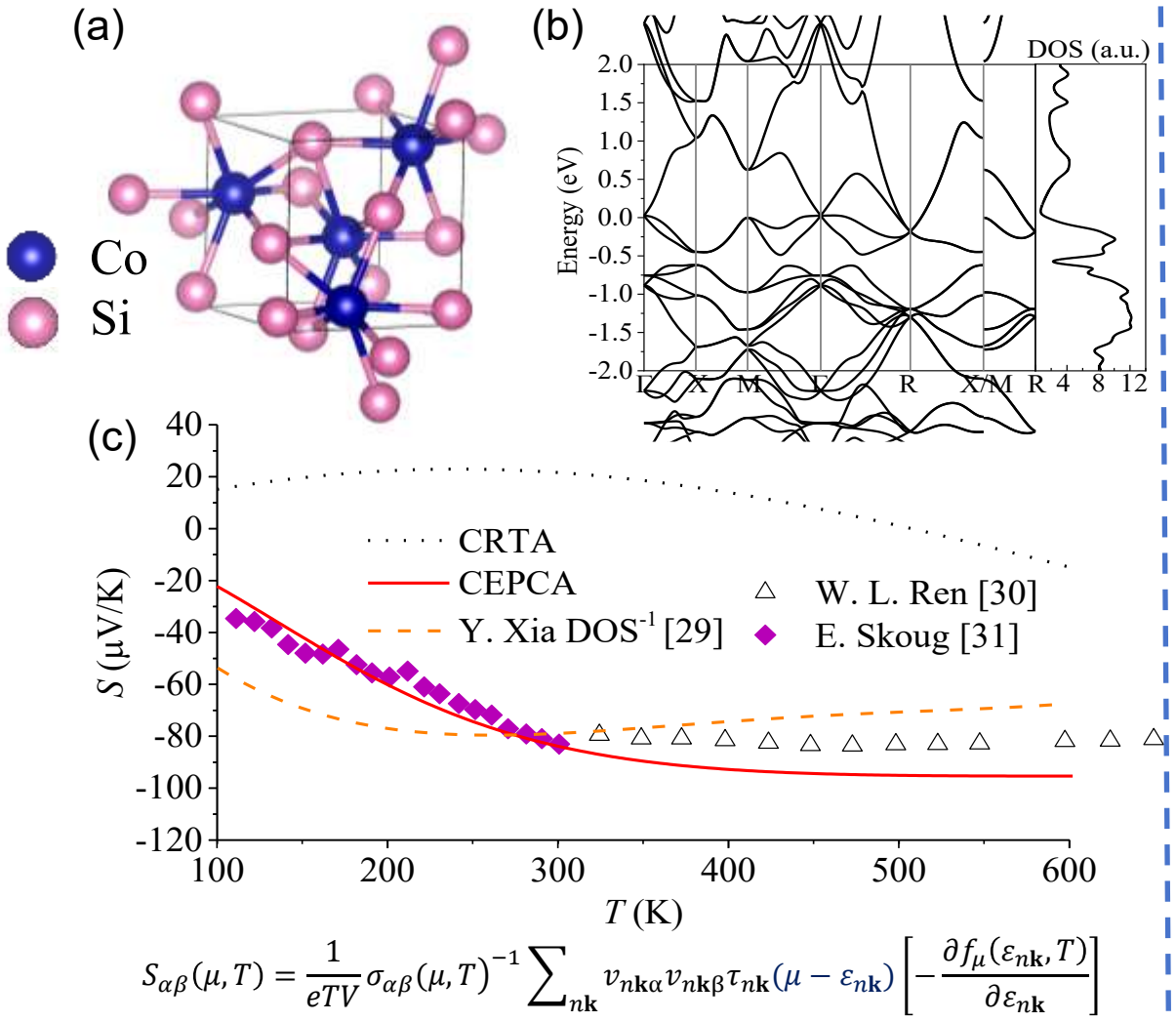

$$S_{\alpha\beta}(\mu,T) = \frac{1}{eTV}\sigma_{\alpha\beta}(\mu,T)^{-1}\sum_{n\mathbf{k}} v_{n\mathbf{k}\alpha}v_{n\mathbf{k}\beta}\tau_{n\mathbf{k}}(\mu-\varepsilon_{n\mathbf{k}})\left[-\frac{\partial f_\mu(\varepsilon_{n\mathbf{k}},T)}{\partial\varepsilon_{n\mathbf{k}}}\right]$$

- Higher accuracy for Seebeck coefficient than CRTA, due to explicit treatment of relaxation time.

***Comp. Mater. Sci.*, 186, 110074 (2021)**

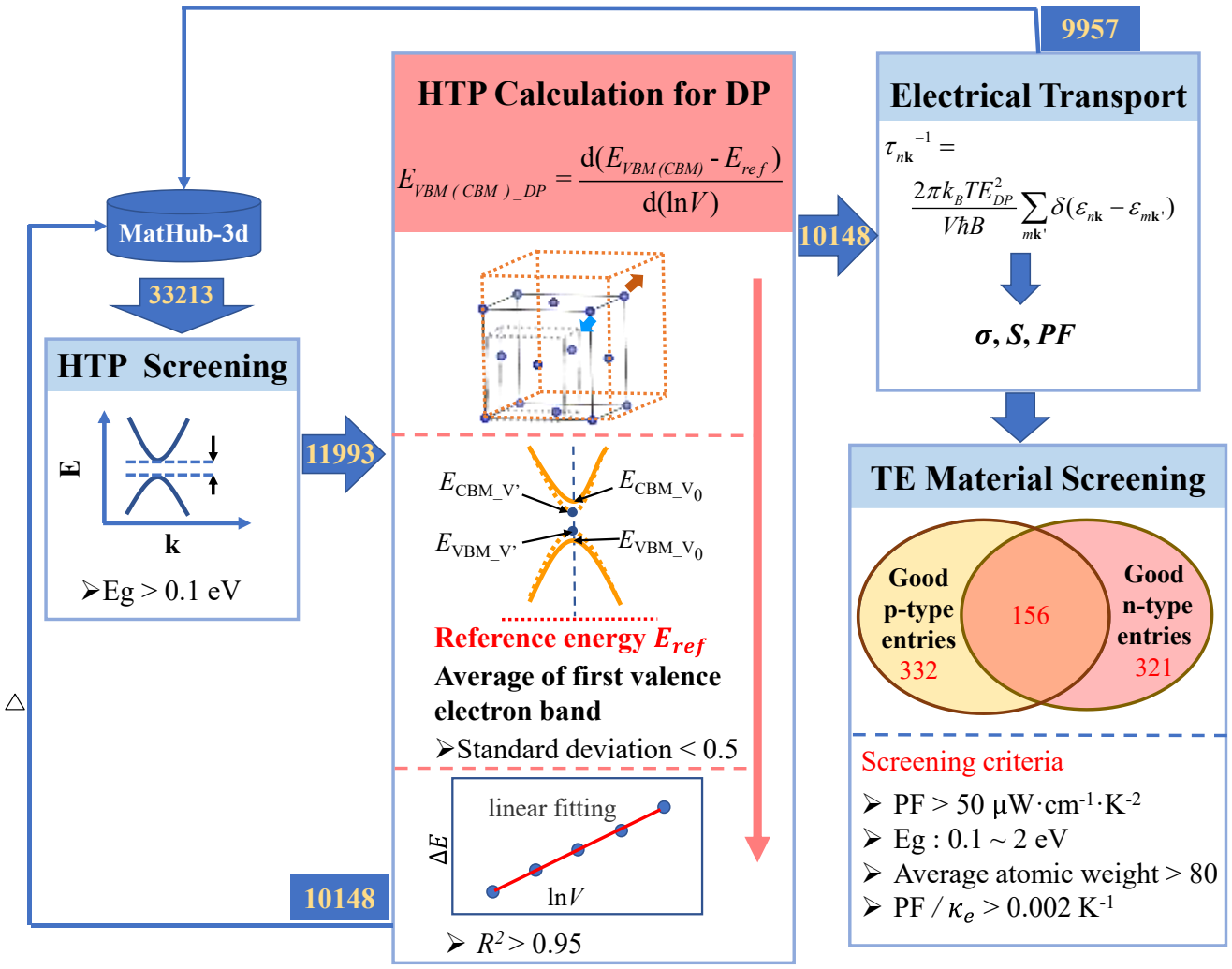

- A high-throughput screening workflow based on MatHub-3d and the deformation potential method.

***npj Comput. Mater.*, 9, 190 (2023)** www.mathub3d.net

2.3 TransOpt **Recent works by TransOpt 2.0**

$$\frac{1}{\tau_{\mathrm{IMP},n\mathbf{k}}}=\sum_{m\mathbf{k}'}\frac{2\pi n_{\mathrm{imp}}Z_{\mathrm{imp}}^{2}e^{4}}{V\hbar(\varepsilon_{\mathrm{s}}\kappa_{0})^{2}\left(L_{\mathrm{D}}^{-2}+|\mathbf{k}'-\mathbf{k}|^{2}\right)^{2}}\delta(\varepsilon_{n\mathbf{k}}-\varepsilon_{m\mathbf{k}'})$$

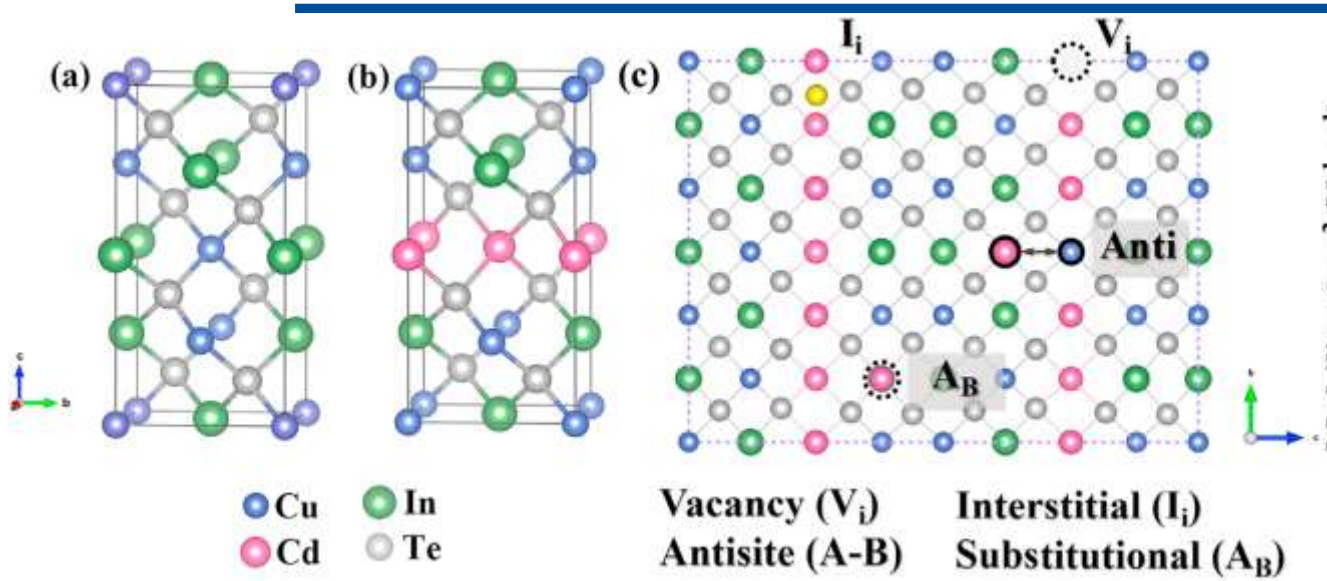

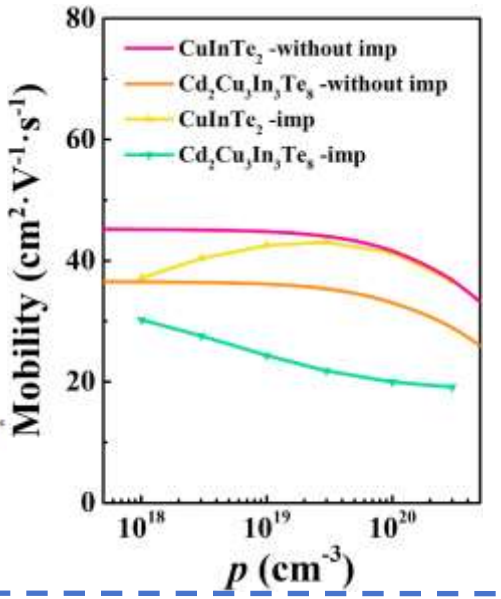

- Low formation energies of the defects in $Cd_2Cu_3In_3Te_8$ cause high defect density ($4.80\times10^{20}cm^{-3}$) and severely reduced mobility.

J. Materiomics, 8 1222 (2022)

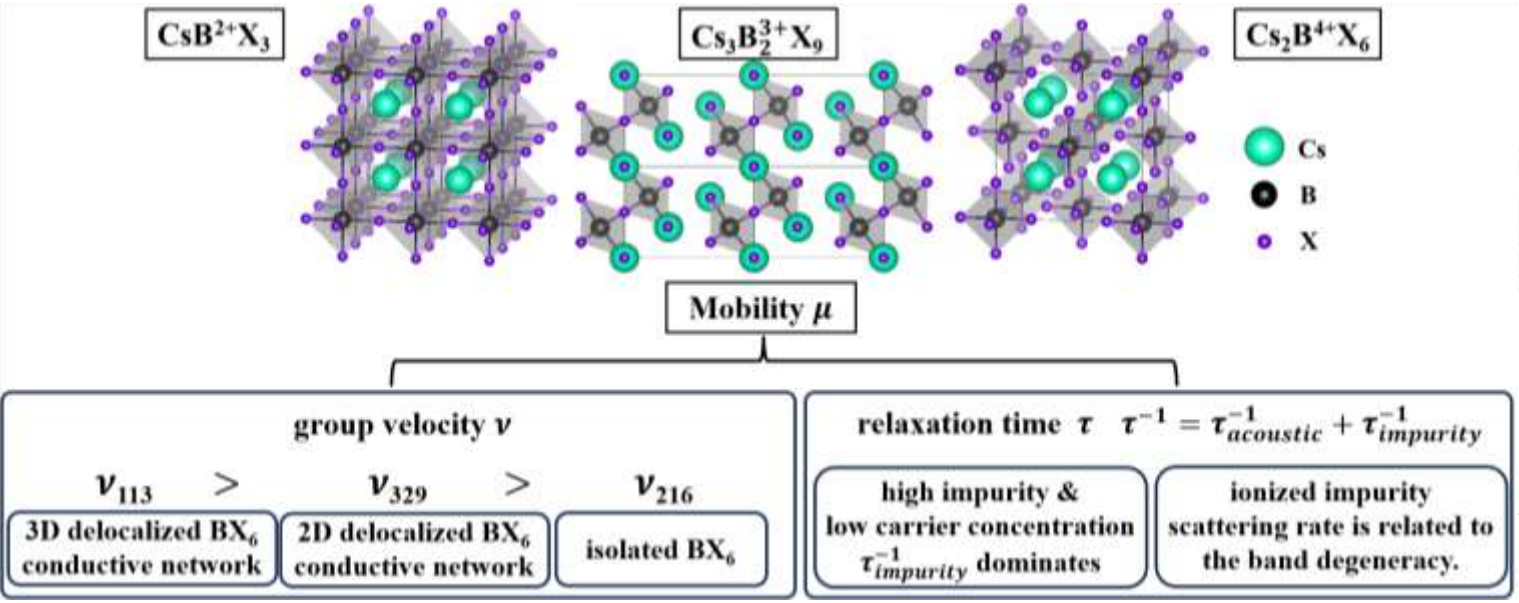

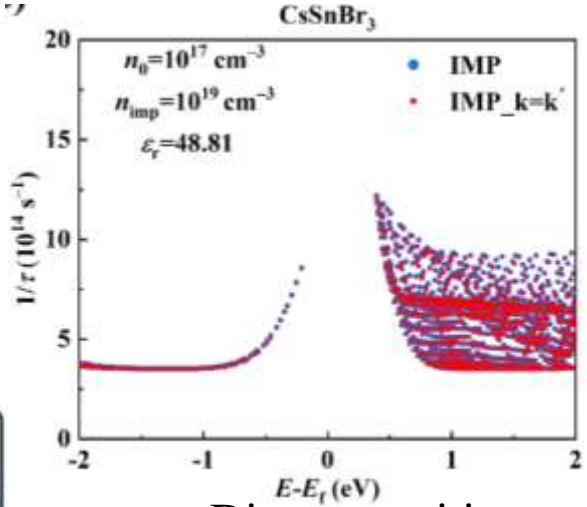

Direct transition process ($\mathbf{k}'=\mathbf{k}$) dominates IMP

J. Mater. Sci. Technol., 204, 245–254 (2025)

2.3 TransOpt 3.0

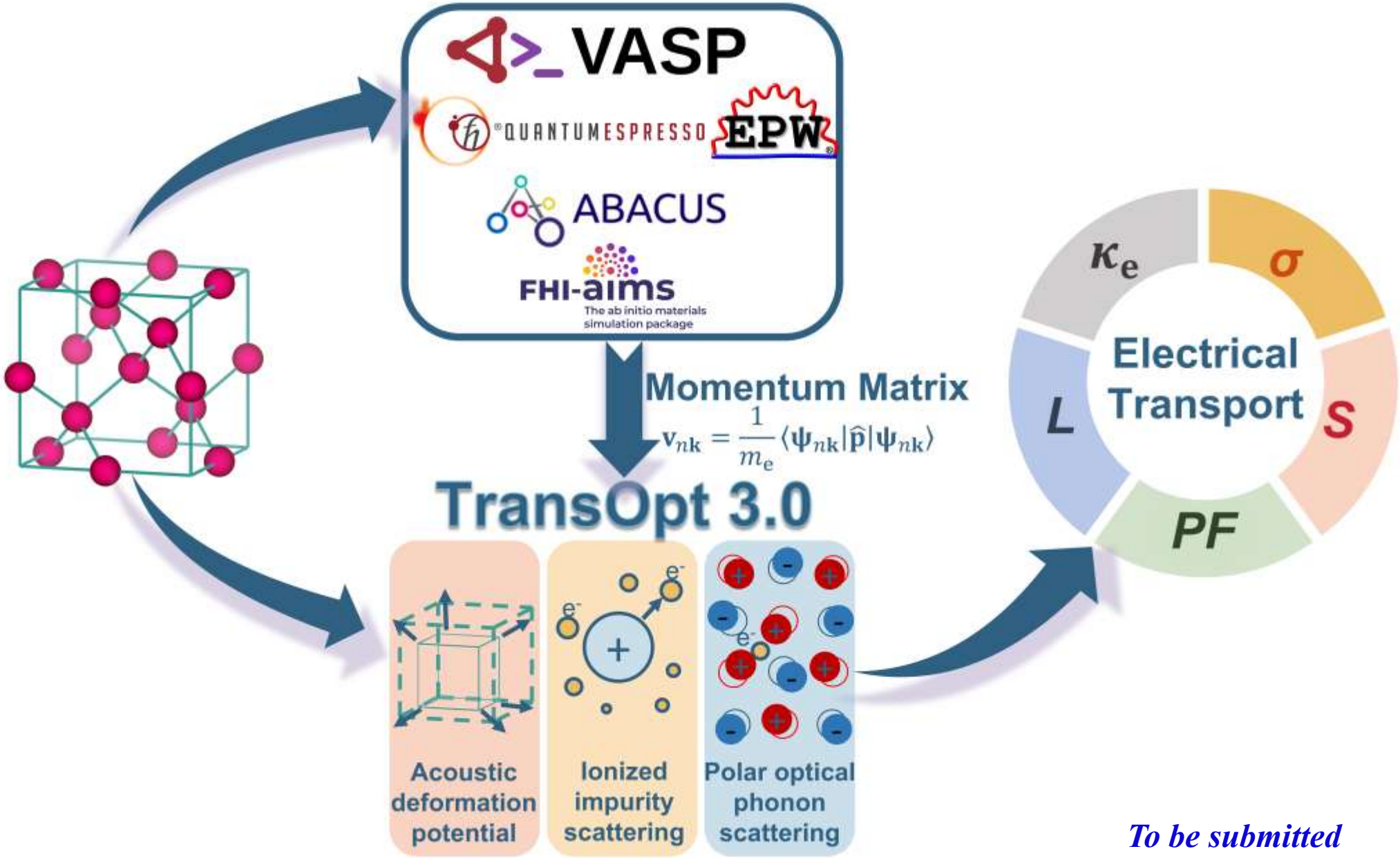

To be submitted

Group velocity

$$\mathbf{v}_{nk} = \frac{1}{m_e}\langle \psi_{nk}|\hat{\mathbf{p}}|\psi_{nk}\rangle \quad \textit{vs} \quad \mathbf{v}_{nk} = \frac{1}{\hbar}\nabla_{\mathbf{k}}\varepsilon_{nk}$$

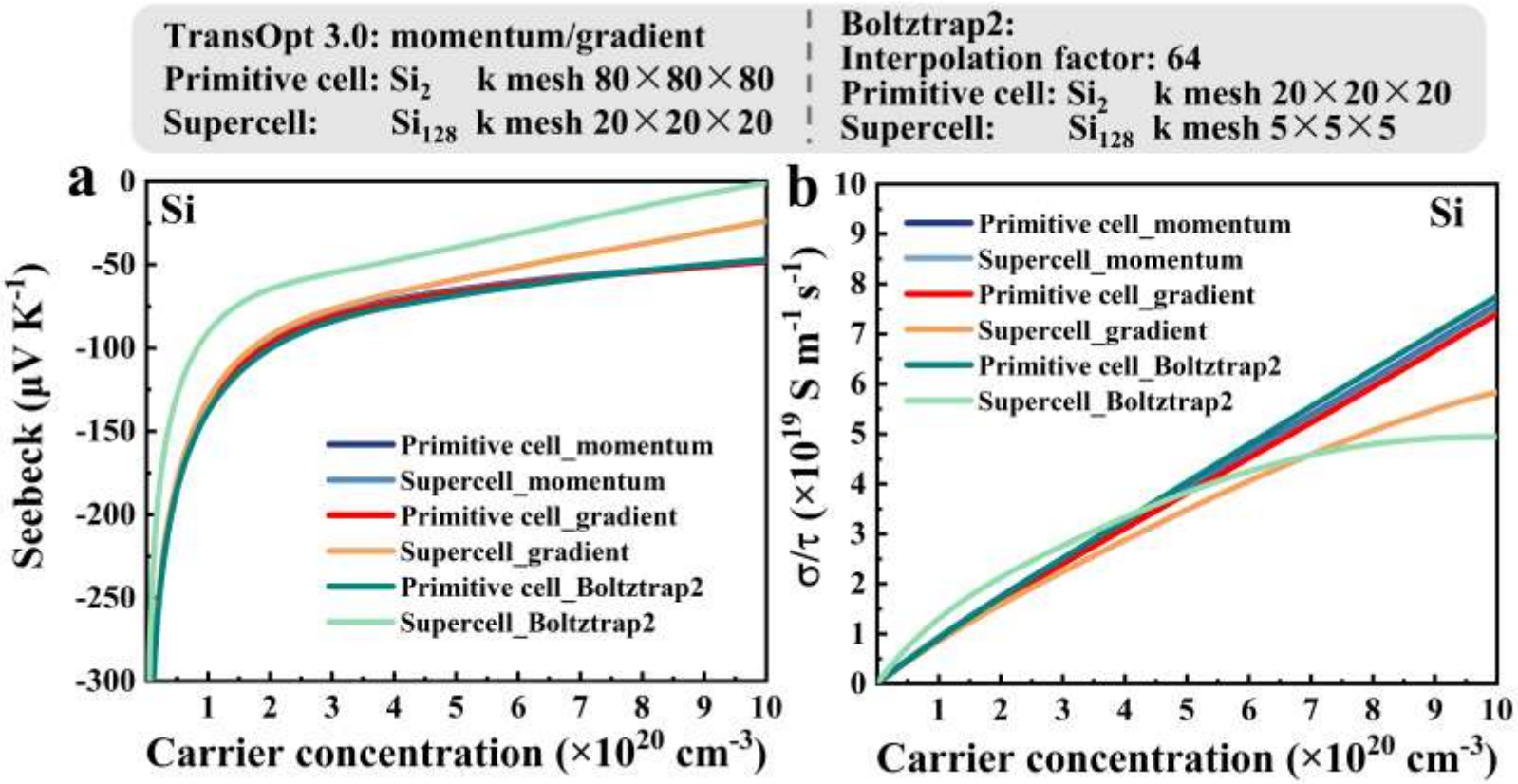

- Momentum matrix method provides better agreement between supercell and primitive cell results compared to gradient method or BoltzTraP2 interpolation.
- This scheme offers distinct advantages for systems involving doping or those with large primitive cells.
- Momentum matrix method for group velocity has been achieved in all the DFT codes compatible with TransOpt 3.0.

To be submitted

Calculated Results for Typical Thermoelectric Materials and Perovskites

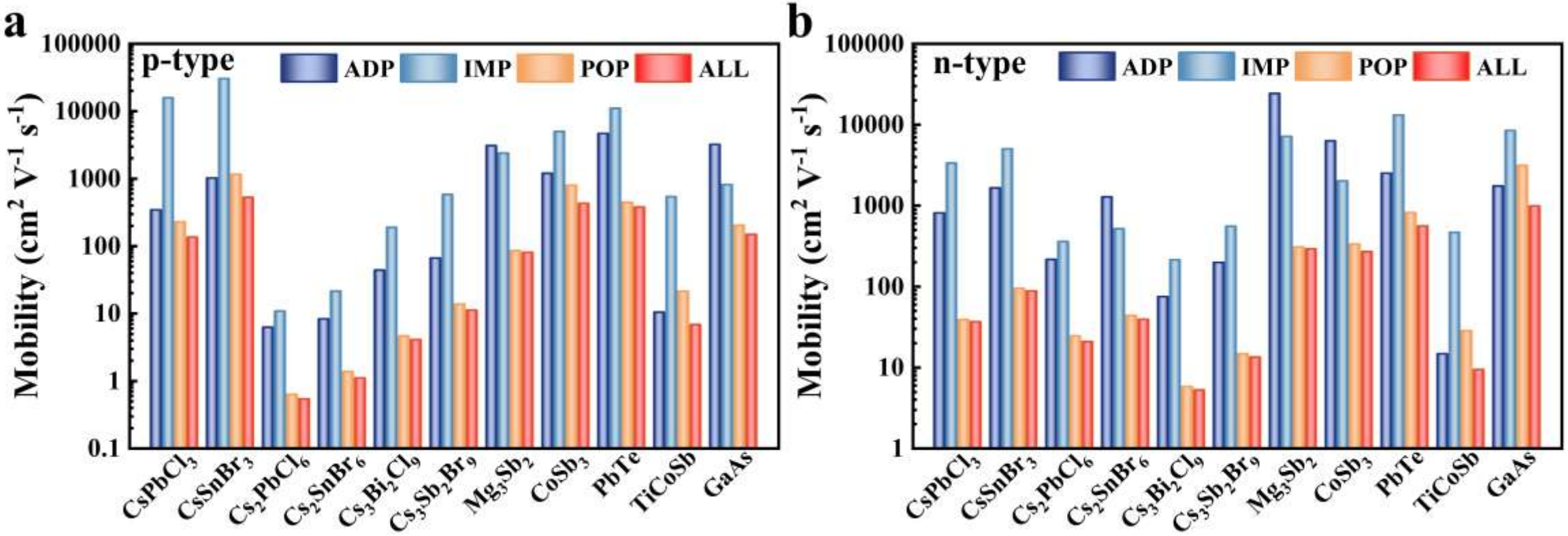

$n_0 = n_{imp} = 10^{18}$ cm^{-3}

- POP scattering dominates the total carrier mobility in majority of the investigated cases.

To be submitted

2.4 Something beyond

Jacob's ladder of the electrical transport calculation accuracy

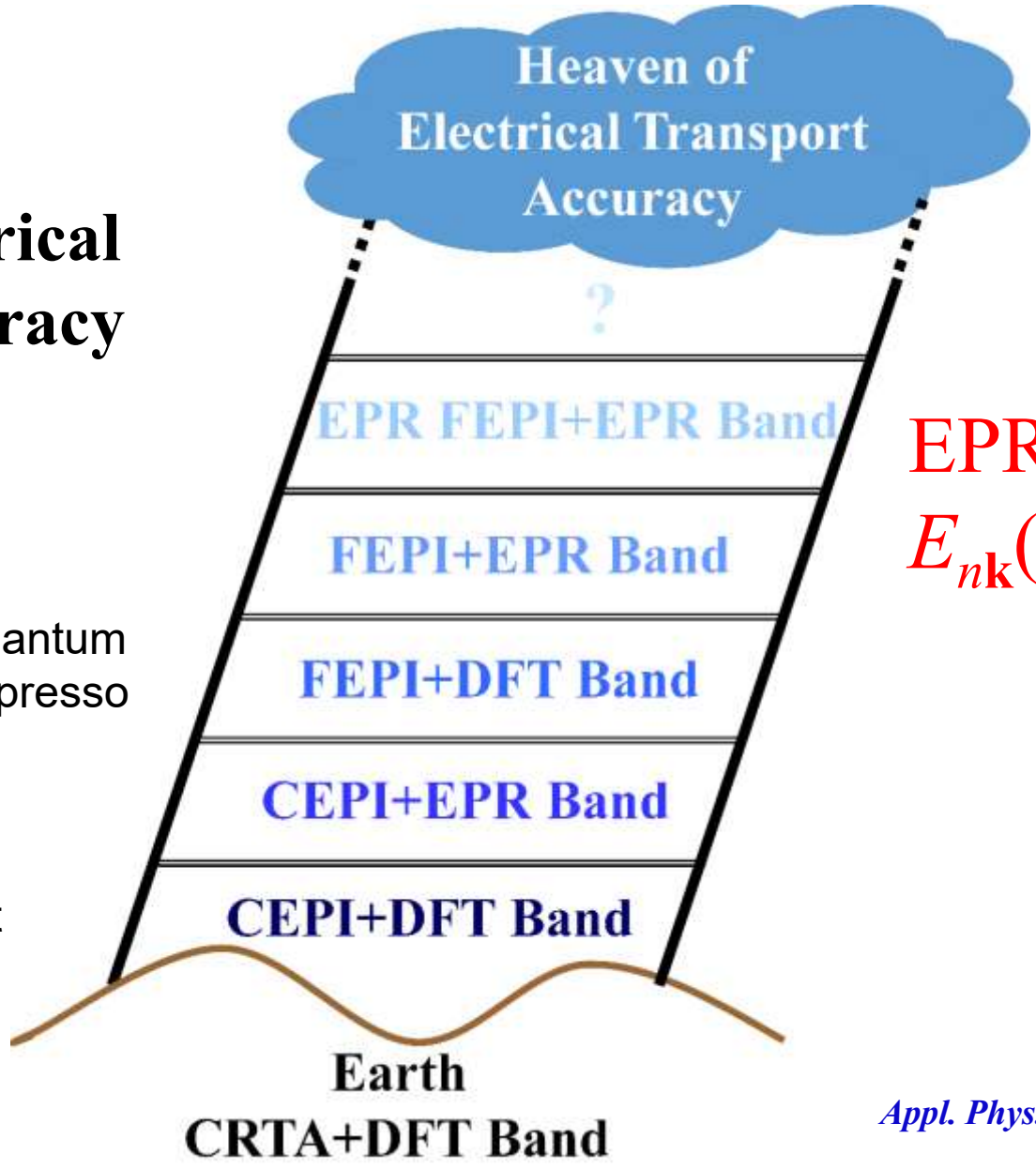

EPR Band

$E_{n\mathbf{k}}(T)$

Direct DFPT Sampling — Quantum Espresso

Leading Order Approximation — TransOpt

Constant Scattering Time — BoltzTrap

Appl. Phys. Lett. 120, 190503 (2022)

2.4 Something beyond **Temperature-induced band renormalization**

☐ Experiment

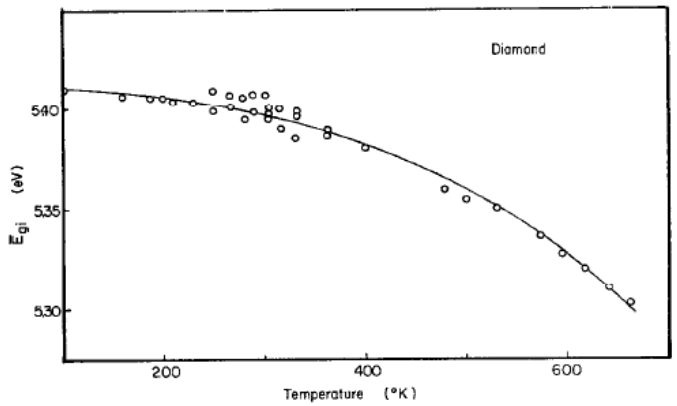

Diamond, Si, SiC, *Physica*, 34, 149 (1967);
J. Phys. Chem. Solids, 40, 791(1979)

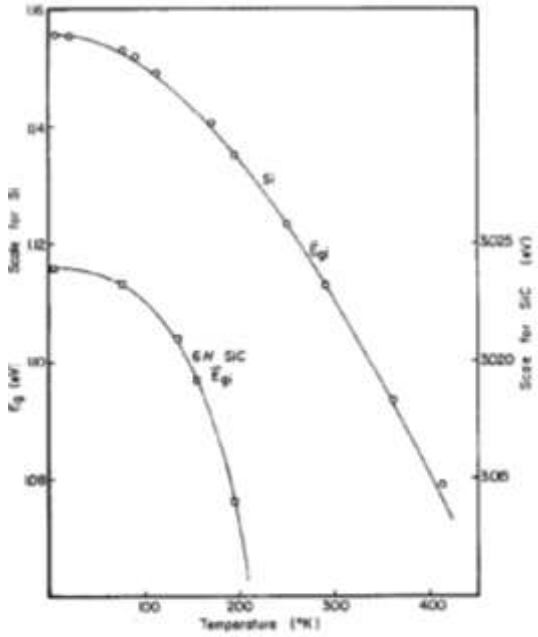

Fig. 2. Silicon and 6H SiC.

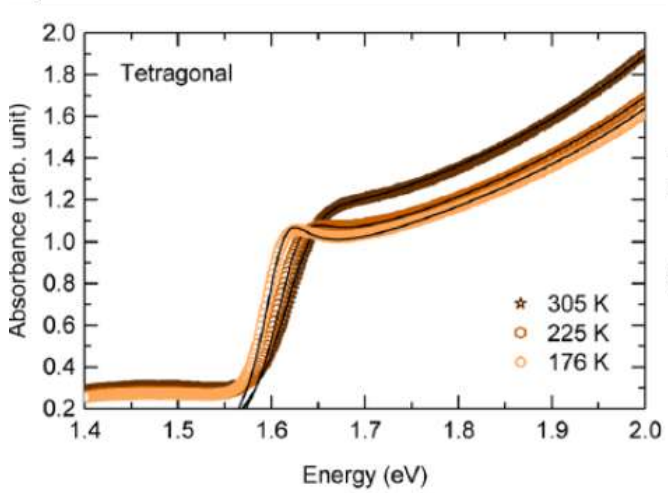

$MAPbI_3$, *J. Phys. Chem. Lett.*, 7, 3014 (2016)

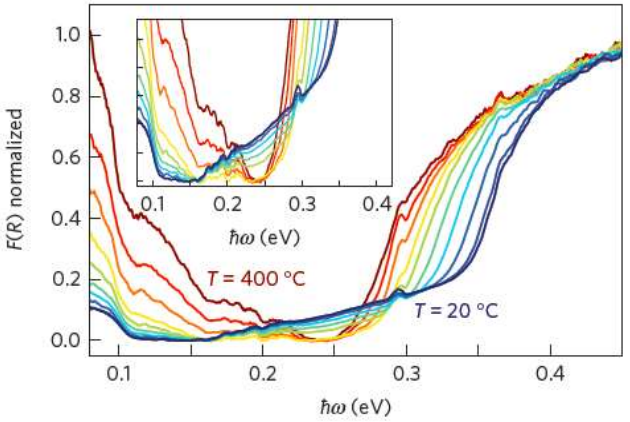

$CoSb_3$, *Nat. Mater.*, 14, 1223 (2015)

☐ Theory

Electron-Phonon Renormalization (EPR)

$$\Delta E_{n\mathbf{k}}(T) = \Delta E_{n\mathbf{k}}^{VIB}(0) + \Delta E_{n\mathbf{k}}^{VIB}(T) + \Delta E_{n\mathbf{k}}^{LE}(T)$$

Zero-point vibration at 0 K	Thermal vibration at T	Lattice expansion at T

2.4 Something beyond **Temperature-induced band renormalization**

☐ Electron energy at finite *T*:

◆ **Step1: Lattice expansion effect**
Method1: QHA by VASP and Phonopy
Method2: NPT AIMD by VASP

◆ **Step2: Vibration effect**
Method1: AHC theory in VASP6.5.1 or Abinit
- **Electron self-energy:** $\Sigma_{n\mathbf{k}}^{ep}(T) = \Sigma_{n\mathbf{k}}^{FM}(T) + \Sigma_{n\mathbf{k}}^{DW}(T)$
- **Electron energy at *T*:** $\tilde{\varepsilon}_{n\mathbf{k}} = \varepsilon_{n\mathbf{k}} + Re\Sigma_{n\mathbf{k}}^{ep}(T)$

◆ **Step2: Vibration effect**
Method 2: "one-shot" method by VASP and Phonopy
- **Atomic displacement at *T*:**

$$\Delta\tau_{\kappa\alpha} = \left(M_p/M_\kappa\right)^{1/2} \sum_\upsilon (-1)^{\upsilon-1} e_{\kappa\alpha,\upsilon} s_{\upsilon,T}$$
$$s_{\upsilon,T}^2 = \left(\hbar/2M_p\,\omega_\upsilon\right)\left(2n_{\upsilon,T}+1\right)$$

- **Electron energy at *T*** by using the effective structure under lattice expansion and thermal vibrations at *T*

◆ **Step2: Vibration effect**
Method 3: NVT AIMD by VASP
- **Electron energy at *T* :** time average of MD snapshots

☐ Electrical transport at finite *T*:

Method: Boltzmann transport theory by TransOpt
- **Electrical conductivity:**

$$\sigma_{\alpha\beta}(\varepsilon_F, T) = \sum_n \int \frac{d\mathbf{k}}{\Omega_{BZ}} \tilde{v}_{n\mathbf{k}\alpha} \tilde{v}_{n\mathbf{k}\beta} \tilde{\tau}_{n\mathbf{k}} \left[-\frac{\partial \tilde{f}_{n\mathbf{k}}(\varepsilon_F,T)}{\partial \tilde{\varepsilon}_{n\mathbf{k}}}\right]$$

- **Seebeck coefficient:**

$$S_{\alpha\beta}(\varepsilon_F, T) = \frac{1}{eT}\sigma_{\alpha\beta}(\varepsilon_F, T)^{-1}$$
$$\sum_n \int \frac{d\mathbf{k}}{\Omega_{BZ}} \tilde{v}_{n\mathbf{k}\alpha} \tilde{v}_{n\mathbf{k}\beta} \tilde{\tau}_{n\mathbf{k}} (\varepsilon_F - \tilde{\varepsilon}_{n\mathbf{k}}) \left[-\frac{\partial \tilde{f}_{n\mathbf{k}}(\varepsilon_F,T)}{\partial \tilde{\varepsilon}_{n\mathbf{k}}}\right]$$

- **Scattering rate:**

$$1)\ \frac{1}{\tilde{\tau}_{n\mathbf{k}}} = \frac{2\pi k_B T D_{def}^2}{\hbar C} \sum_m \int \frac{d\mathbf{k}'}{\Omega_{BZ}} \delta(\tilde{\varepsilon}_{n\mathbf{k}} - \tilde{\varepsilon}_{m\mathbf{k}'})$$
$$2)\ \frac{1}{\tau_{n\mathbf{k}}} = 2 \cdot Im\Sigma_{n\mathbf{k}}^{ep}(T)$$

Rev. Mod. Phys., 89, 015003 (2017)
J. Phys.: Condens. Matter, 32, 475503 (2020)

2.4 Something beyond **Temperature-induced band renormalization**

☐ Thermoelectric Half-Heusler compounds

Method1: AHC theory

- E_g of most systems gradually decreases with T. Median E_g change from 0 K to 1000 K is ~ -200 meV. Even at 0 K, the ZPR has some influences.

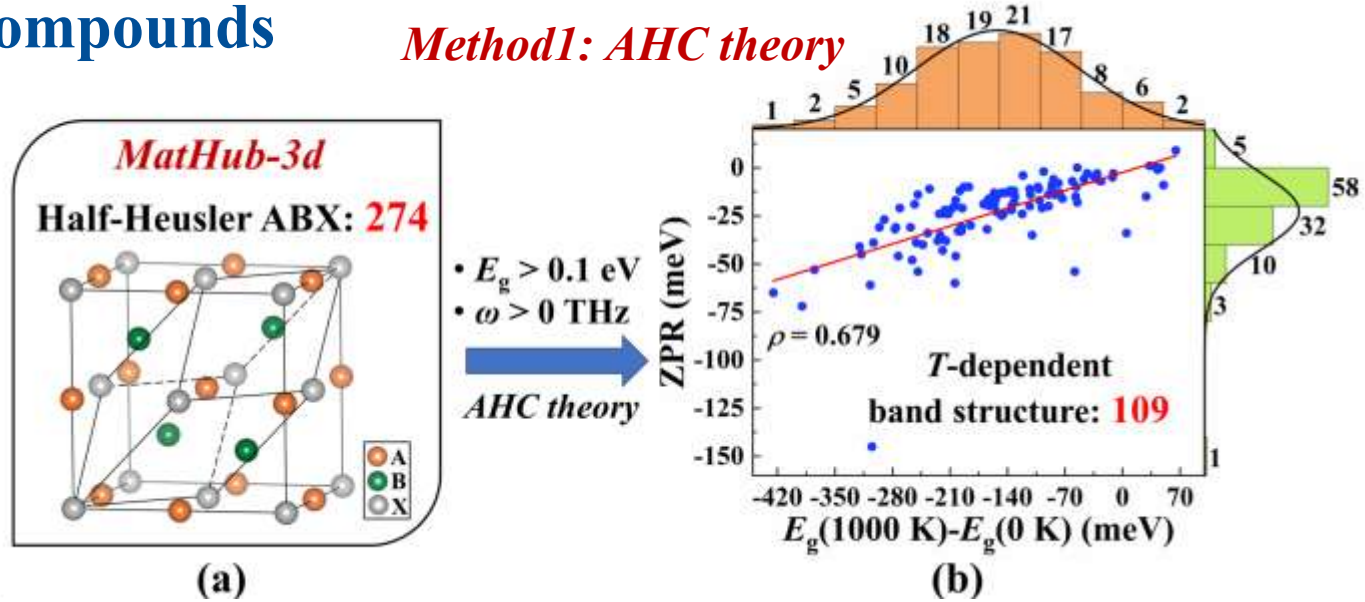

- The EPR band has been used in the calculations of Seebeck coefficients, for the first time.

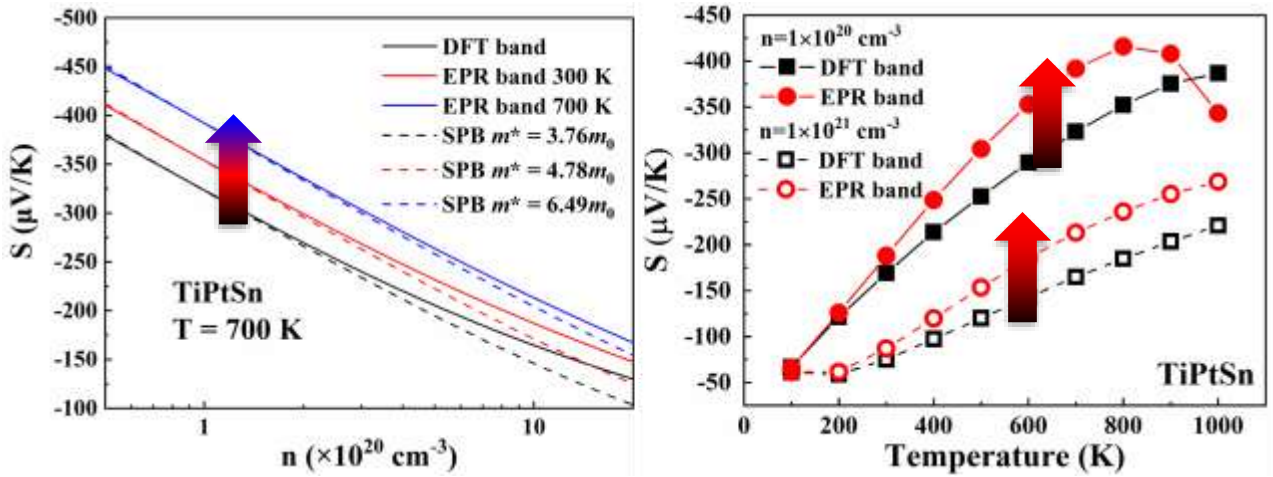

arXiv:2407.00433

2.4 Something beyond Temperature-induced band renormalization

Orthorhombic, tetragonal, and cubic $CsPbI_3$ (Method 2: "one-shot)

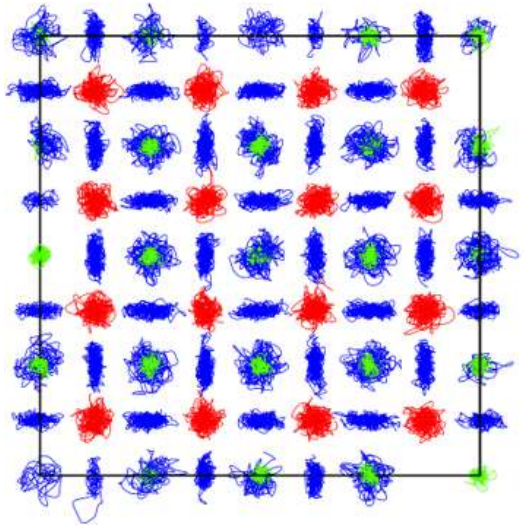

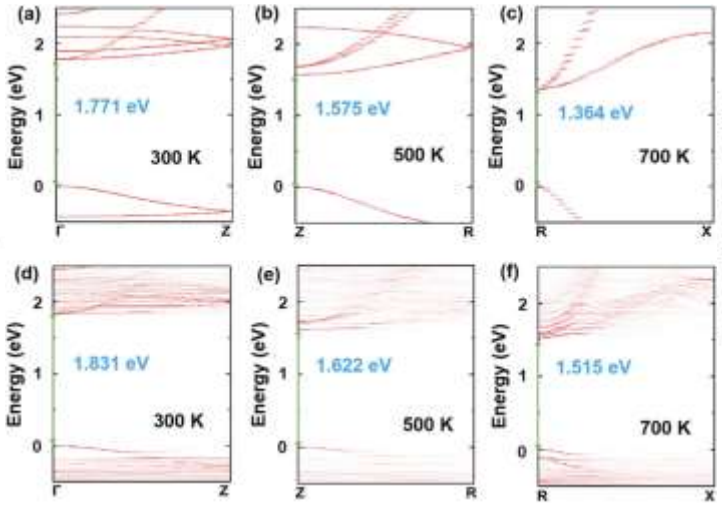

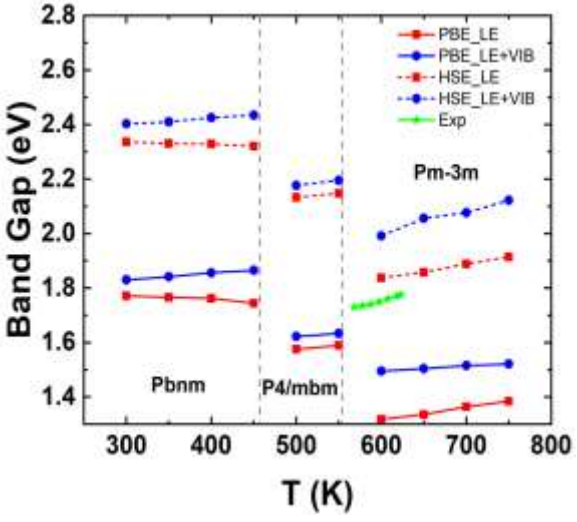

Strong structural fluctuation
Strong band gap renormalization
Strong suppression on transport

J. Comput. Chem., 42, 2213 (2021)
Phys. Chem. Chem. Phys., 24, 16003 (2022)

Optoelectronic Perovskites: Cubic $MAPbI_3$ (Method 3: AIMD)

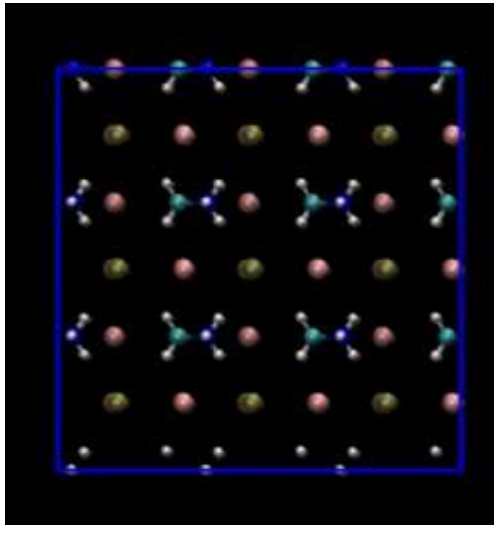

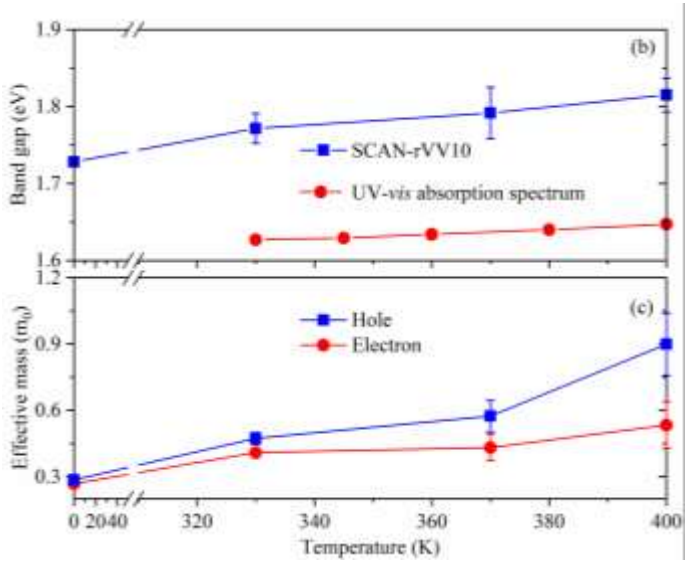

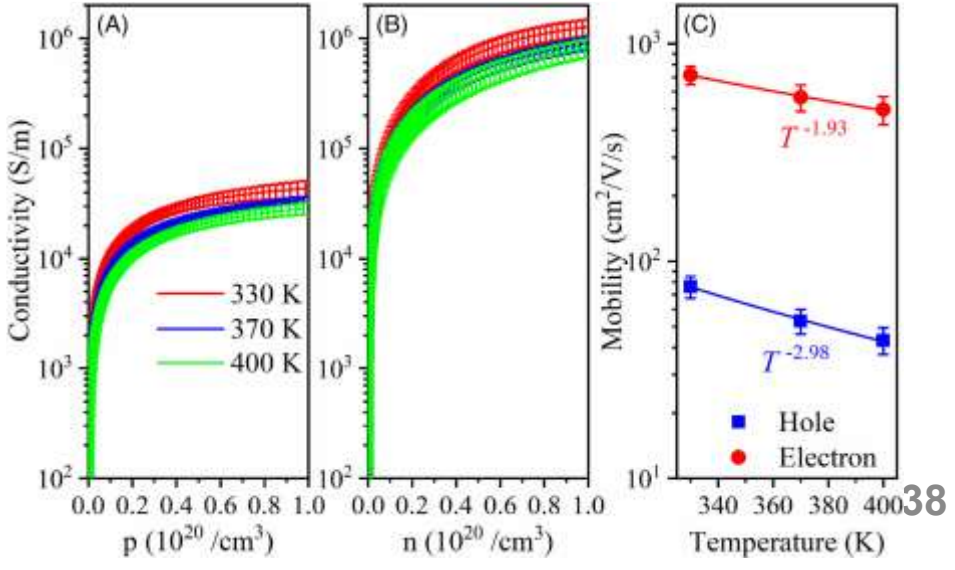

- Electrical transport properties within the framework of linear response theory

$$\sigma(\omega) = \frac{2\pi q^2 \hbar^2}{m^2 V \omega} \sum_{m,n,\mathbf{k}} \left(\langle \psi_{n\mathbf{k}} | \nabla_\alpha | \psi_{m\mathbf{k}} \rangle \langle \psi_{m\mathbf{k}} | \nabla_\alpha | \psi_{n\mathbf{k}} \rangle\right) \left(f^0_{n\mathbf{k}} - f^0_{m\mathbf{k}}\right) \delta(\varepsilon_{m\mathbf{k}} - \varepsilon_{n\mathbf{k}} - \hbar\omega)$$

- ✓ **Liquids & amorphous:** amorphous Cu-doped Ta_2O_5; liquid aluminum; liquid Zr; liquid and supercooled silicon…
- ✓ **Dense metals:** warm dense aluminum; dense silver plasma; warm dense helium-hydrogen mixtures…
- ✓ **Semiconductors:** monolayer and bilayer phosphorene; semiconducting fematinite-like structure (Cu_3SbS_4); perovskites…

3. Kubo framework

Kubo-Greenwood

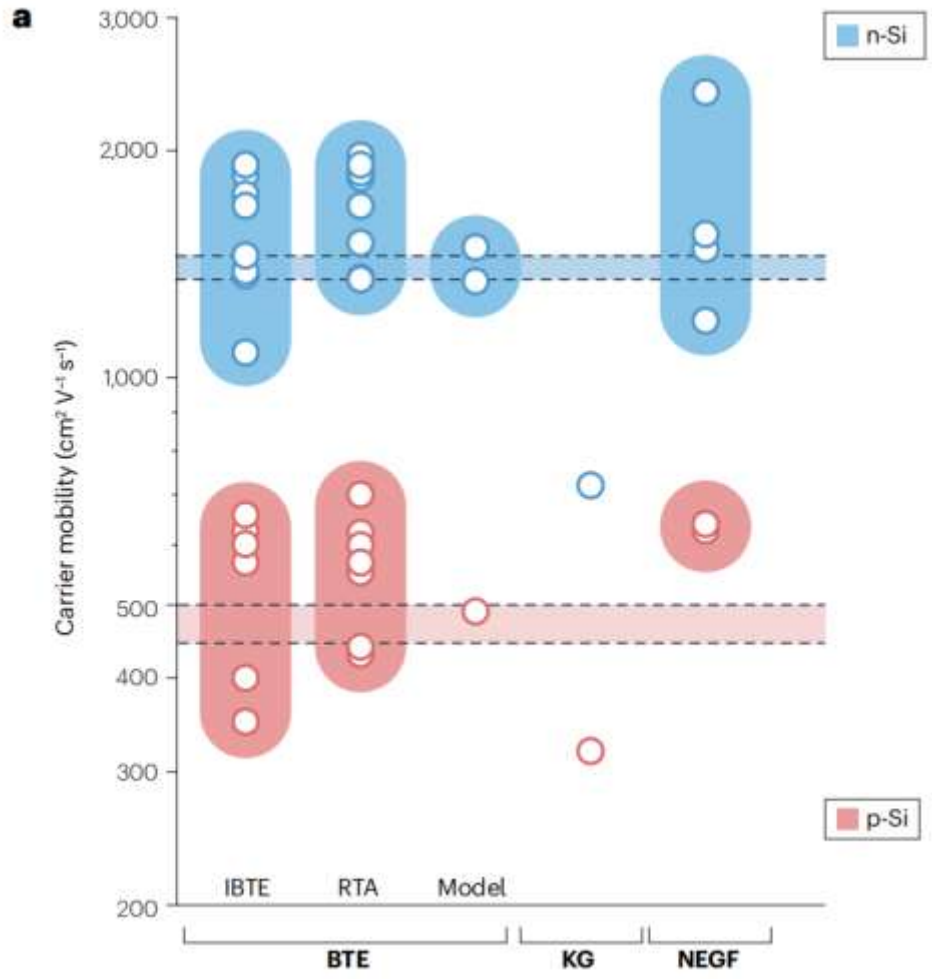

Calculated values of carrier mobility at room temperature using different frameworks and methods.

Nat. Rev. Phys., 7, 73–90 (2025)

Cubic Rb_3AuO antiperovskite

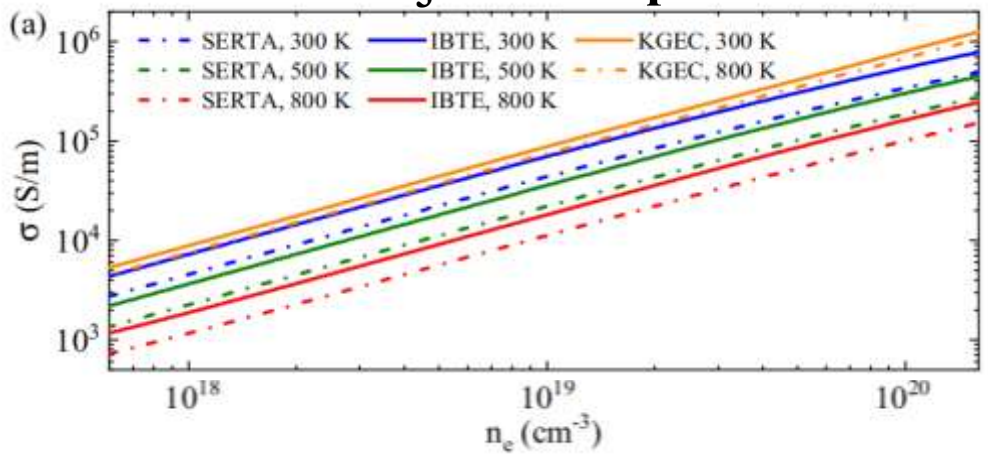

Phys. Rev. B, 102, 094314 (2020)

Cubic $SrTiO_3$

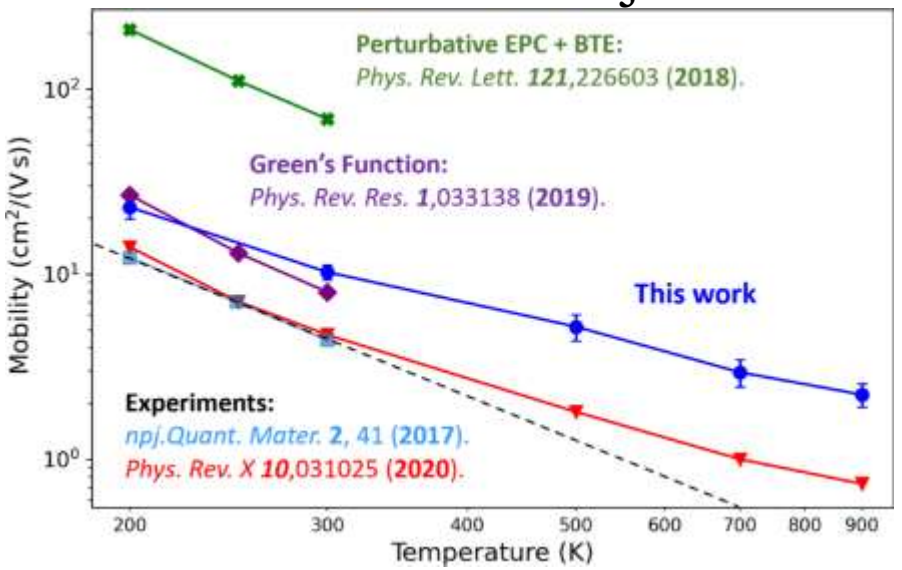

Phys. Rev. B, 110, 235202 (2024)

Summary on e-trans

☐ BTE level:

- ✓ **The calculation of full electron-phonon interaction is still demanding.**
- ✓ **Different softwares with different approximations on multiple scattering mechanisms are available.**

☐ Higher level:

- ✓ **Electron-phonon renormalization on band structures are considered in some materials.**
- ✓ **Kubo-Greenwood method is suitable for anharmonic materials.**

Overview

Background

Electrical transport

Lattice thermal conductivity

3.1 BTE in Lattice Thermal Transport

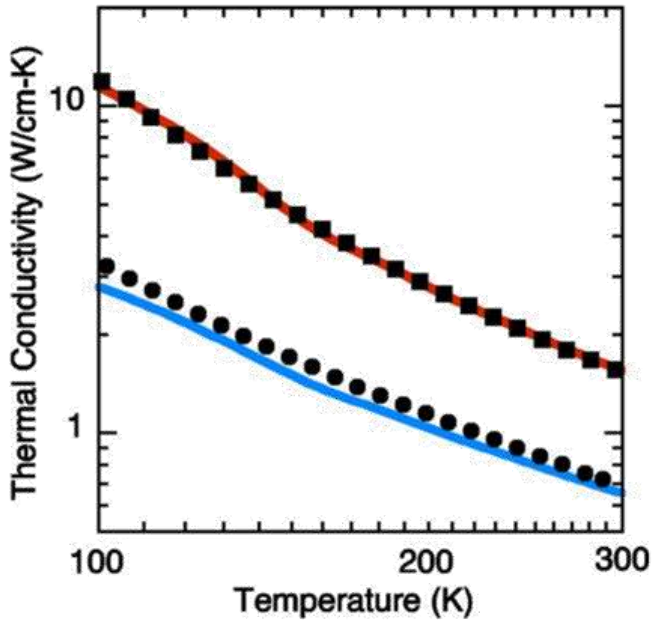

FIG. 1. (Color online) Lattice thermal conductivity $\kappa^{(i)}$ as a function of temperature. The red line and solid squares are the calculated and measured thermal conductivities of silicon, respectively, while the blue line and the solid circles are the corresponding quantities for germanium.

- Since **2007**, three-phonon calculations combined with **BTE** have become a standard approach for κ_L prediction, achieving high accuracy in conventional crystals.
- Phonon BTE is less demanding than full el-ph interaction.

Appl. Phys. Lett., 91, 231922 (2007)
Phys. Rev. B, 87, 165201 (2013)
Phys. Rev. B, 185, 1747 (2014)

3.1 BTE in Lattice Thermal Transport **Taylor Expansion of Potential Energy**

The potential energy is expressed using a Taylor expansion

$$E = E_0 + \frac{1}{2}\sum_{ij\alpha\beta} \boldsymbol{\Phi_{ij}^{\alpha\beta}} r_i^\alpha r_j^\beta + \frac{1}{3!}\sum_{ijk\alpha\beta\gamma} \boldsymbol{\Phi_{ijk}^{\alpha\beta\gamma}} r_i^\alpha r_j^\beta r_k^\gamma + \frac{1}{4!}\sum_{ijkl\alpha\beta\gamma\theta} \boldsymbol{\Phi_{ijkl}^{\alpha\beta\gamma\theta}} r_i^\alpha r_j^\beta r_k^\gamma r_l^\theta + \cdots$$

First-order

Atomic force

Structural properties

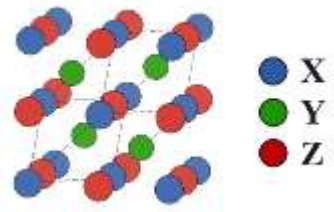

Second-order

Harmonic IFCs

Phonon dispersion

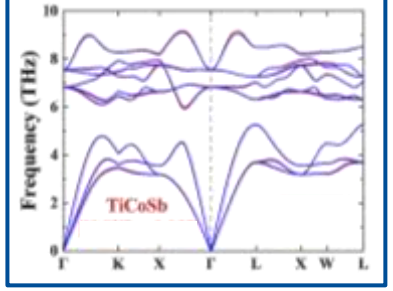

Higher-order

Anharmonic IFCs

Phonon scattering rate

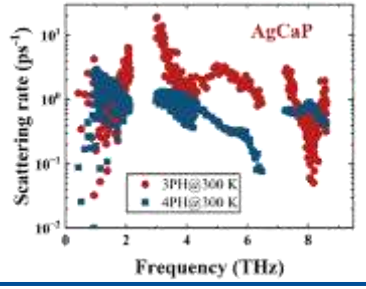

$$\kappa_L = \frac{1}{NV}\sum_\lambda C_V(\omega_\lambda) v_g^2(\omega_\lambda)\tau(\omega_\lambda)$$

Software: phonopy

$$D_{ij}^{\alpha\beta}(\mathbf{q}) = \sum_l \frac{\boldsymbol{\Phi_{i,jl}^{\alpha\beta}}}{\sqrt{m_i m_j}} exp[i\mathbf{q}\cdot(\mathbf{r}_i - \mathbf{r}_{jl})]$$

$$\sum D_{ij}^{\alpha\beta}(\mathbf{q})\,\mathbf{e}(\omega_\lambda) = [\omega_\lambda]^2\mathbf{e}(\omega_\lambda)$$

$$\mathbf{v}(\omega_\lambda) = \frac{1}{2\omega_\lambda}\langle\mathbf{e}(\omega_\lambda)|\frac{\partial D(\mathbf{q})}{\partial \mathbf{q}}|\mathbf{e}(\omega_\lambda)\rangle = \frac{\partial \omega_\mathbf{q}}{\partial \mathbf{q}}$$

Phonon Heat Capacity

- **Phonon heat capacity:** $C_V = \left(\frac{dU}{dT}\right) = \left(\frac{d\sum_{\mathbf{q}s} E_{\mathbf{q}s}}{dT}\right) = \sum_{\mathbf{q}s} \boldsymbol{c}_{\mathbf{q}s}$

- **Phonon energy:** $E_{\mathbf{q}s} = \left(n_{\mathbf{q}s} + \frac{1}{2}\right)\hbar\omega_{\mathbf{q}s}$

$$\kappa_L = \frac{1}{NV}\sum_{\lambda} C_V(\omega_\lambda) v_g^2(\omega_\lambda)\tau(\omega_\lambda)$$

- **Bose-Einstein distribution:** $n_{\mathbf{q}s} = \frac{1}{\exp\left(\frac{\hbar\omega_{\mathbf{q}s}}{k_B T}\right) - 1}$

- **Mode heat capacity:** $\boldsymbol{c}_{\mathbf{q}s} = k_B \left(\frac{\hbar\omega_{\mathbf{q}s}}{k_B T}\right)^2 \frac{\exp\left(\hbar\omega_{\mathbf{q}s}/k_B T\right)}{\left[\exp\left(\hbar\omega_{\mathbf{q}s}/k_B T\right) - 1\right]^2}$

High-temperature limit $\boldsymbol{c_{\mathbf{q}s} \sim k_B}$ $\boldsymbol{C_V \sim 3N_A k_B}$

Phonon Heat Capacity

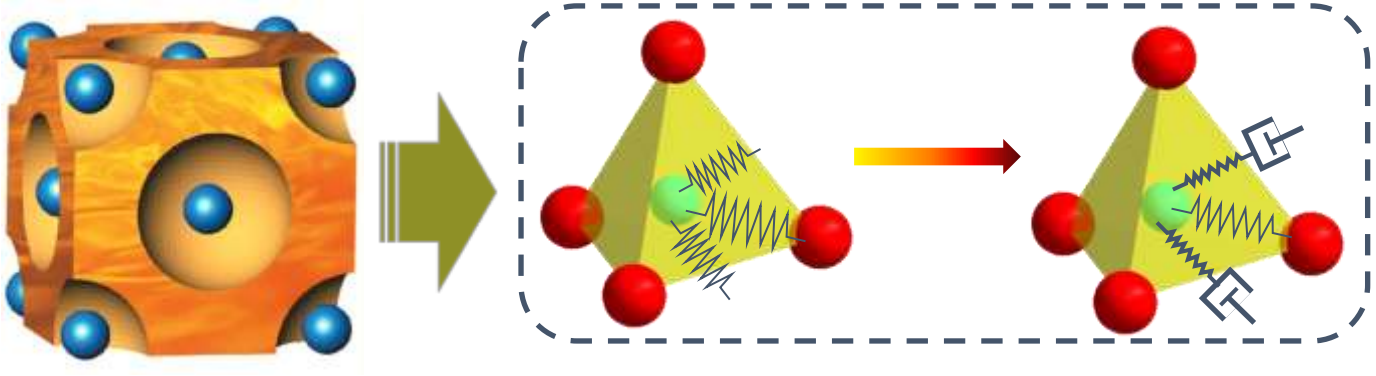

Crystal Structure of Cu_2S/Te (High-Temperature Phase)

- The number of heat-carrying modes is reduced, accompanied by the loss of some transverse modes.

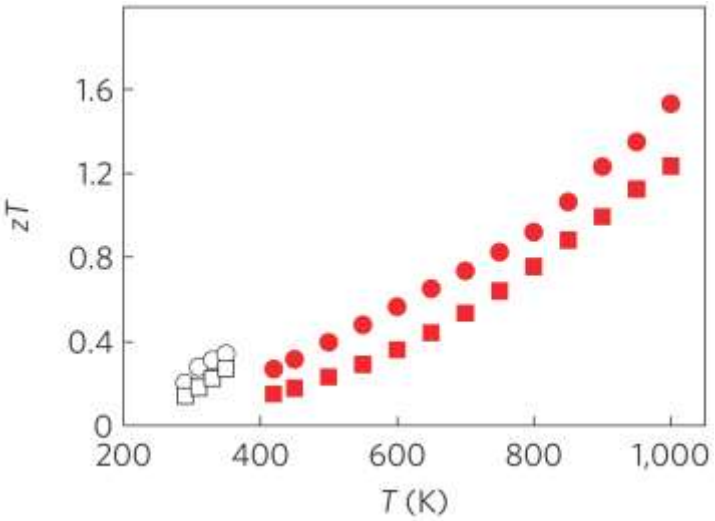

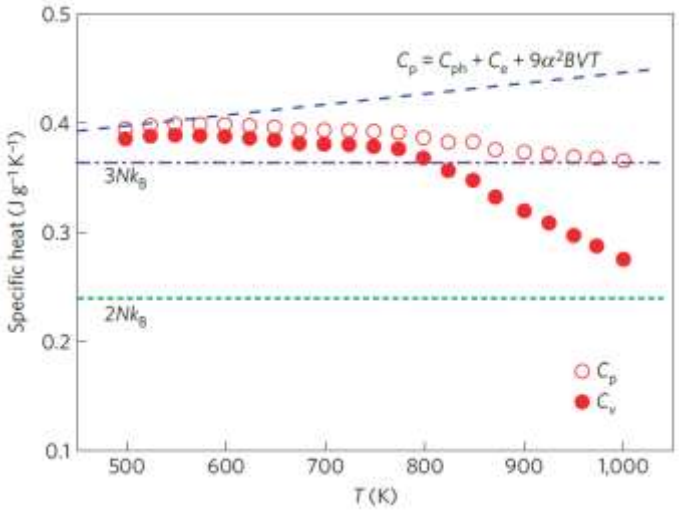

Nat. Mater., 11, 422 (2012)

☐ **Boson-peak-like feature**

Debye model at low T limit: $C_V \propto T^3$

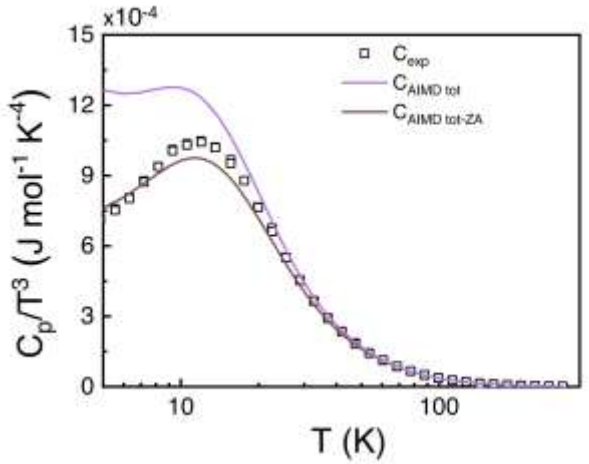

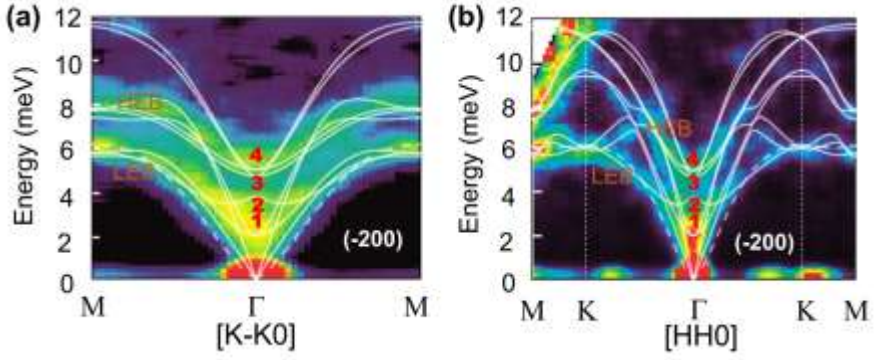

Nat. Commun., 15, 6248 (2024)

☐ **The potential energy is expressed using a Taylor expansion**

$$E = E_0 + \frac{1}{2}\sum_{ij\alpha\beta} \boldsymbol{\Phi}_{ij}^{\alpha\beta} r_i^{\alpha} r_j^{\beta} + \frac{1}{3!}\sum_{ijk\alpha\beta\gamma} \boldsymbol{\Phi}_{ijk}^{\alpha\beta\gamma} r_i^{\alpha} r_j^{\beta} r_k^{\gamma} + \frac{1}{4!}\sum_{ijkl\alpha\beta\gamma\theta} \boldsymbol{\Phi}_{ijkl}^{\alpha\beta\gamma\theta} r_i^{\alpha} r_j^{\beta} r_k^{\gamma} r_l^{\theta} + \cdots$$

Scattering strength $\Phi_{\lambda\lambda'\lambda''} = \sum_{ijk}\sum_{\alpha\beta\gamma} \frac{e^{\alpha}(i,\lambda)e^{\beta}(j,\lambda')e^{\gamma}(k,\lambda'')}{\sqrt{m_i m_j m_k}\sqrt{\omega_\lambda \omega_{\lambda'} \omega_{\lambda''}}} \boldsymbol{\Phi}_{ijk}^{\alpha\beta\gamma} e^{i(q\cdot r_i + q'\cdot r_j + q''\cdot r_k)}$

$$\tau_\lambda^{-1}(\omega) = \frac{\hbar\pi}{8}\sum_{\lambda'\lambda''} \left|\boldsymbol{\Phi}_{\lambda\lambda'\lambda''}\right|^2 \left[(n_{\lambda'} + n_{\lambda''} + 1)\delta(\omega - \omega_{\lambda'} - \omega_{\lambda''}) + 2(n_{\lambda'} - n_{\lambda''})\delta(\omega - \omega_{\lambda'} + \omega_{\lambda''})\right]\Delta_{\boldsymbol{qq'q''}}$$

Scattering phase space

$$\kappa_L = \frac{1}{NV}\sum_{\lambda} C_V(\omega_\lambda) v_g^2(\omega_\lambda) \tau(\omega_\lambda)$$

$$\frac{1}{\tau_{\mathbf{q}}} = \frac{1}{\tau_{3ph}} + \frac{1}{\tau_{4ph}} + \cdots\cdots$$

3.1 BTE in Lattice Thermal Transport **Softwares**

$$\frac{1}{\tau_{\mathbf{q}}} = \frac{1}{\tau_{3ph}} + \frac{1}{\tau_{e-p}} + \frac{1}{\tau_{4ph}} + \frac{1}{\tau_{GB}} + \frac{1}{\tau_{PD}?} \cdots$$

1. Linearized BTE solved without any empirical parameters

Phys. Rev. B, 86, 174307 (2012)

2. Applies the random displacement method to obtain higher-order IFCs.

J. Phys.: Condens. Matter, 26, 225402 (2014)

3. phono3py

Phys. Rev. B, 91, 094306 (2015)

……

Accurate electron–phonon interaction

$$g_{mn\lambda}(\mathbf{k},\mathbf{q}) = \sqrt{\frac{\hbar}{2M\omega_{\mathbf{q}\lambda}}}\langle \Psi_{m\mathbf{k}+\mathbf{q}} | \Delta V_{\mathbf{q}\lambda} | \Psi_{n\mathbf{k}} \rangle$$

Comput. Phys. Commun., 181, 2140 (2010)

Constant electron-phonon coupling approximation

$$\left| g^{\lambda}_{mn}(\mathbf{k},\mathbf{q}) \right|^2 = \frac{\hbar {D_A}^2 \omega_{\mathbf{q}\lambda}}{2VB}$$

Comput. Mater. Sci., 244, 113190 (2024)

Four-phonon Interactions

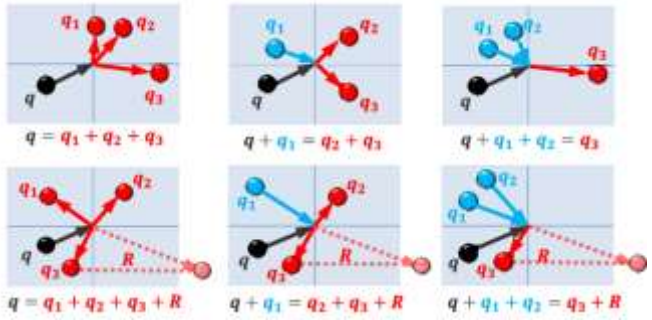

Phys. Rev. B, 96, 161201 (2017)

Also capable of treating grain boundary scattering

$$\frac{1}{\tau_B} = \frac{v}{L}$$

Scattering phase space

☐ **Filled skutterudites $Yb(Ba)Fe_4Sb_{12}$**

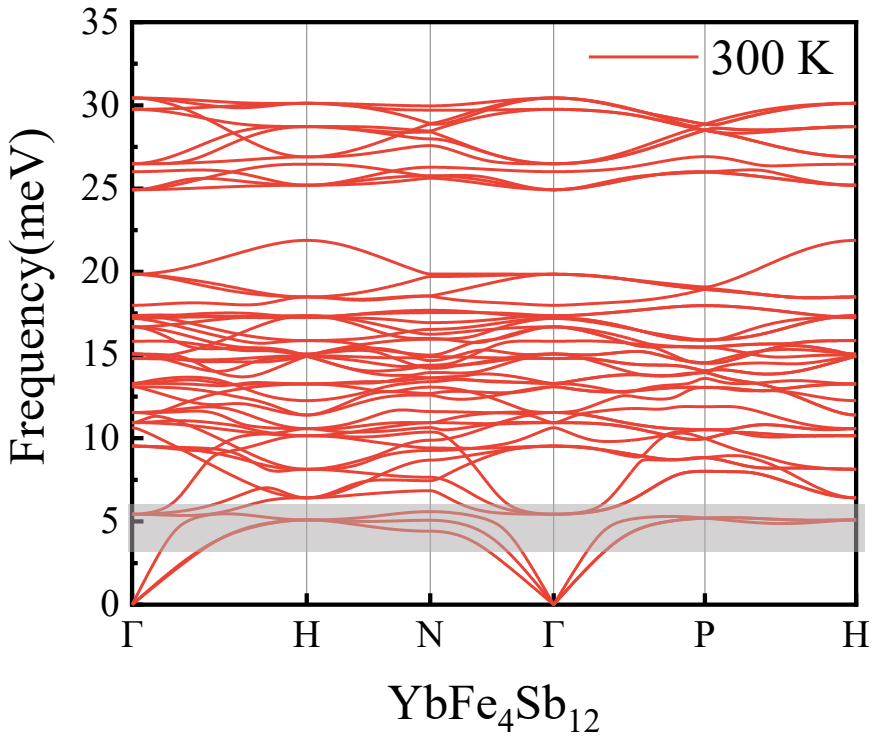

Weighted Scattering Phase Space (W)

$$W_\lambda^{\pm} = \frac{1}{2N}\sum_{\lambda' p''}\left\{\begin{matrix} 2(f_{\lambda'} - f_{\lambda''}) \\ f_{\lambda'} + f_{\lambda''} + 1 \end{matrix}\right\}\frac{\delta(\omega_\lambda \pm \omega_{\lambda'} - \omega_{\lambda''})}{\omega_\lambda \omega_{\lambda'} \omega_{\lambda''}}$$

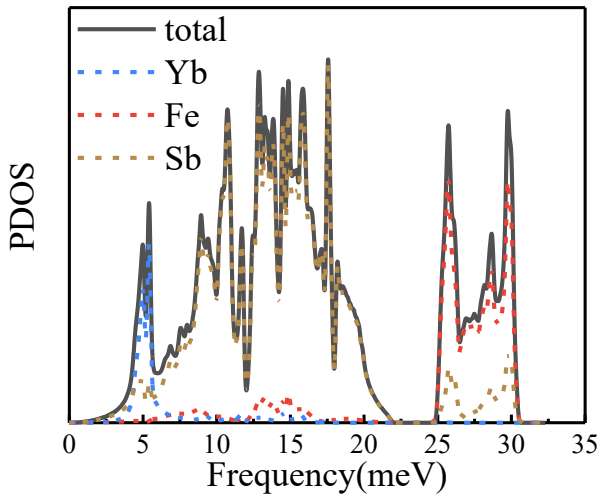

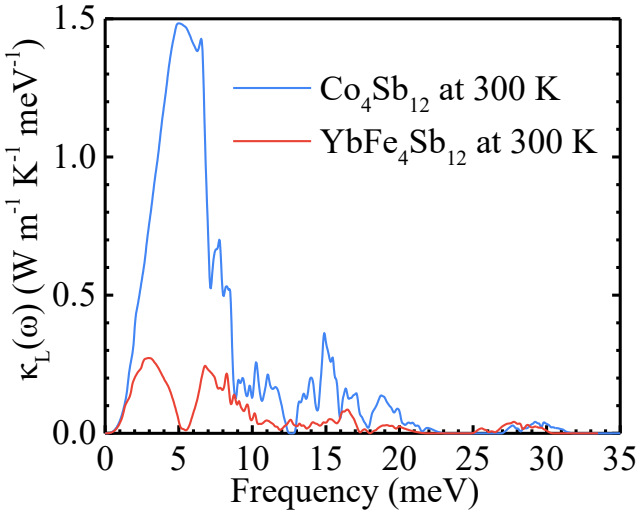

- The avoided-crossing filler modes greatly enhance the scattering phase space of $YbFe_4Sb_{12}$.
- The influence of low-frequency optical branches on phonon **scattering phase space** .vs. **Resonant scattering**.

***Phys. Rev. B*, 91, 144304 (2015)**

- **Pure *ab initio* force constant study.**
- **Dopants reduce the sound velocities and thus reduce the κ_L.**
- **Heavy-element doping induces avoided-crossing behavior in the phonon dispersion.**

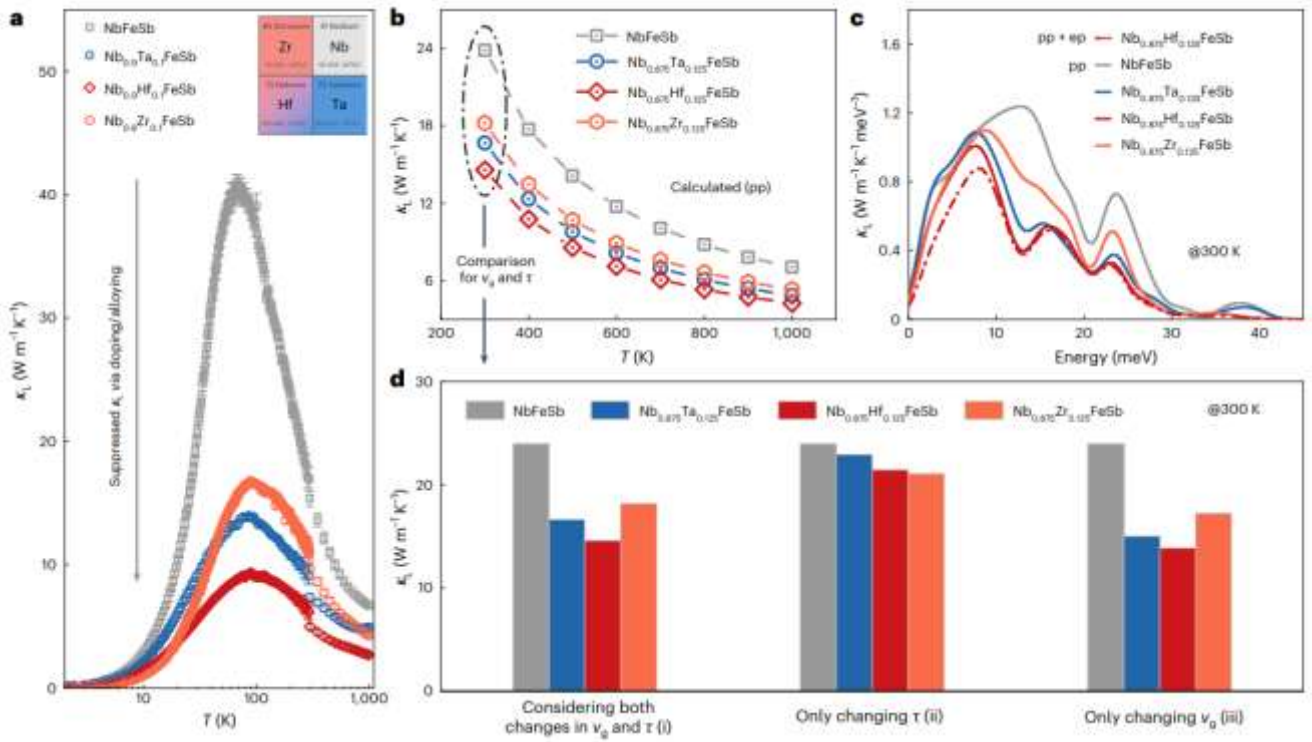

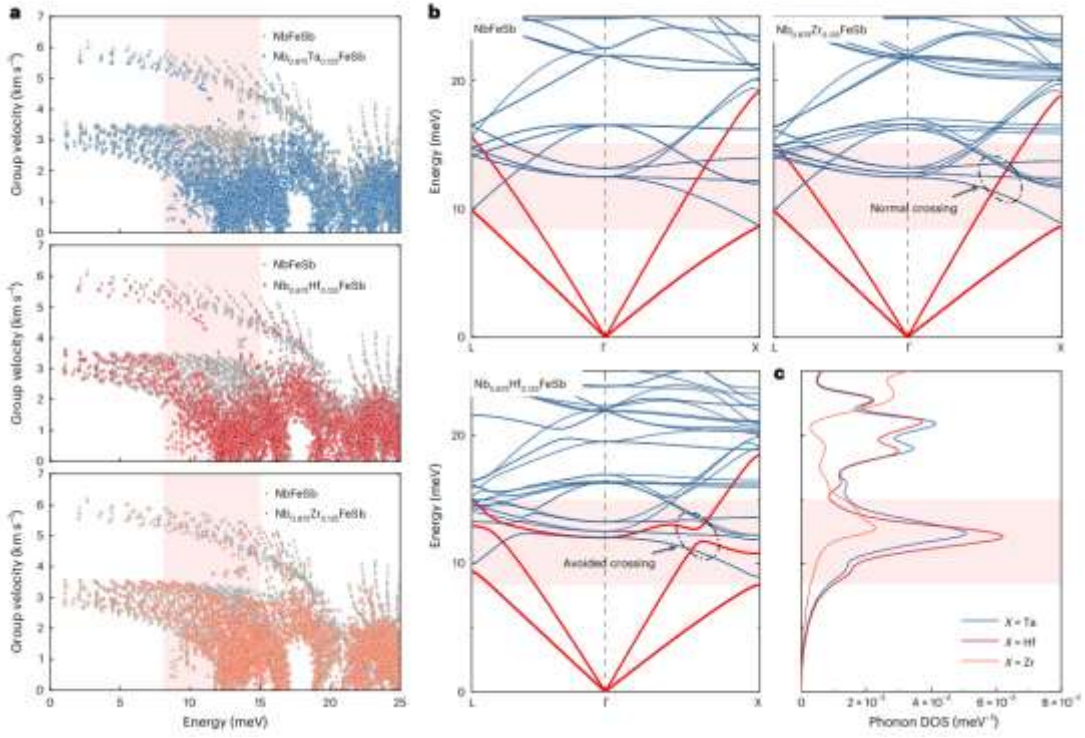

$Nb_{0.875}X_{0.125}FeSb$ (X= Zr; Nb; Hf; Ta)

Nat. Phys., 19, 1649-1657 (2023)

Effect of Ir/Co Doping on $FeSi_2$ κ_L

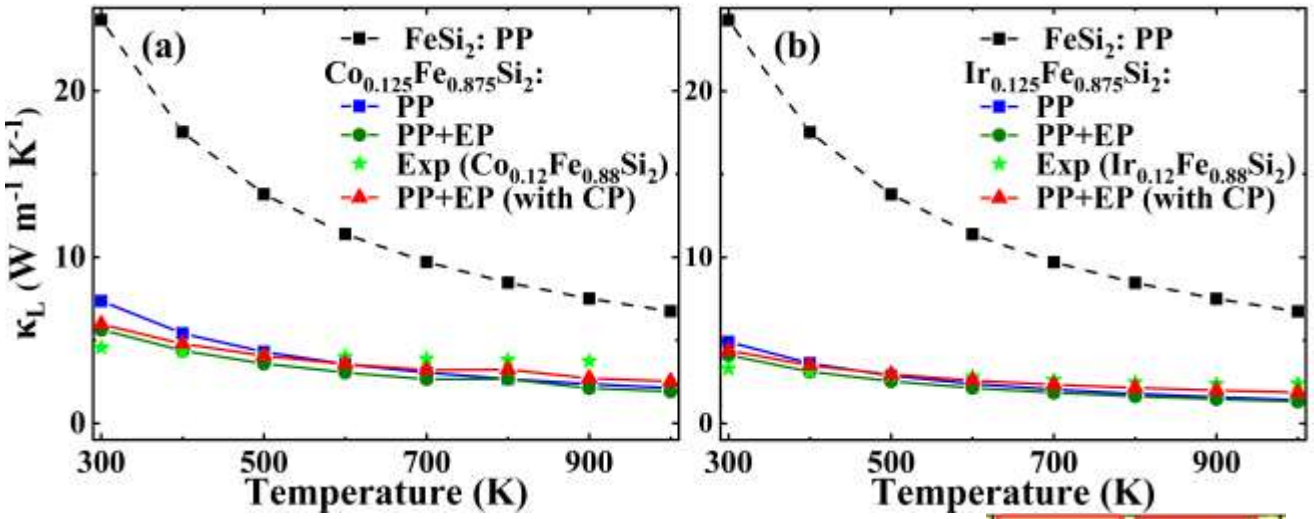

κ_L at **300 K(Experimental results):**

$Ir_{0.12}$: 82%, $Co_{0.12}$: 76%, $Co_{0.24}$: 65%

$$\eta = \frac{\kappa_L^{undoped} - \kappa_L^{doped}}{\kappa_L^{undoped}}$$

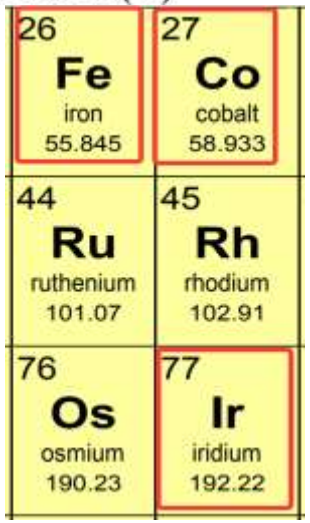

Calculated results

κ_L at **300 K(PP):**

$Ir_{0.125}$: 80%, $Co_{0.125}$: 70%, $Co_{0.25}$: 52%

κ_L at **300 K(PP+EP):**

$Ir_{0.125}$: 83%, $Co_{0.125}$: 77%, $Co_{0.25}$: 69%

- The modulation of force constants and EP coupling through adjacent-site doping can effectively reduce κ_L, not necessary to include the point defect scattering model.

J. Mater. Chem. A, 13, 33661 (2025)

3.2 Case Studies Using Phonon BTE Electron-Phonon Scattering

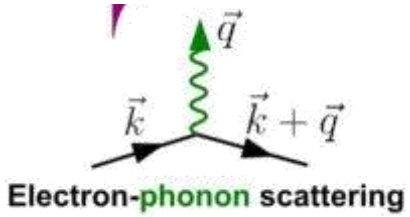

$$\frac{1}{\tau^{\mathrm{EP}}_{\mathbf{q}\lambda}} = \frac{2\pi}{\hbar}\sum_{mn,\mathbf{k}} |g_{mn\lambda}(\mathbf{k},\mathbf{q})|^2 \left(f_{n\mathbf{k}} - f_{m\mathbf{k+q}}\right)\delta\left(\varepsilon_{n\mathbf{k}} - \varepsilon_{m\mathbf{k+q}} - \hbar\omega_{\mathbf{q}\lambda}\right)$$

Skutterudite

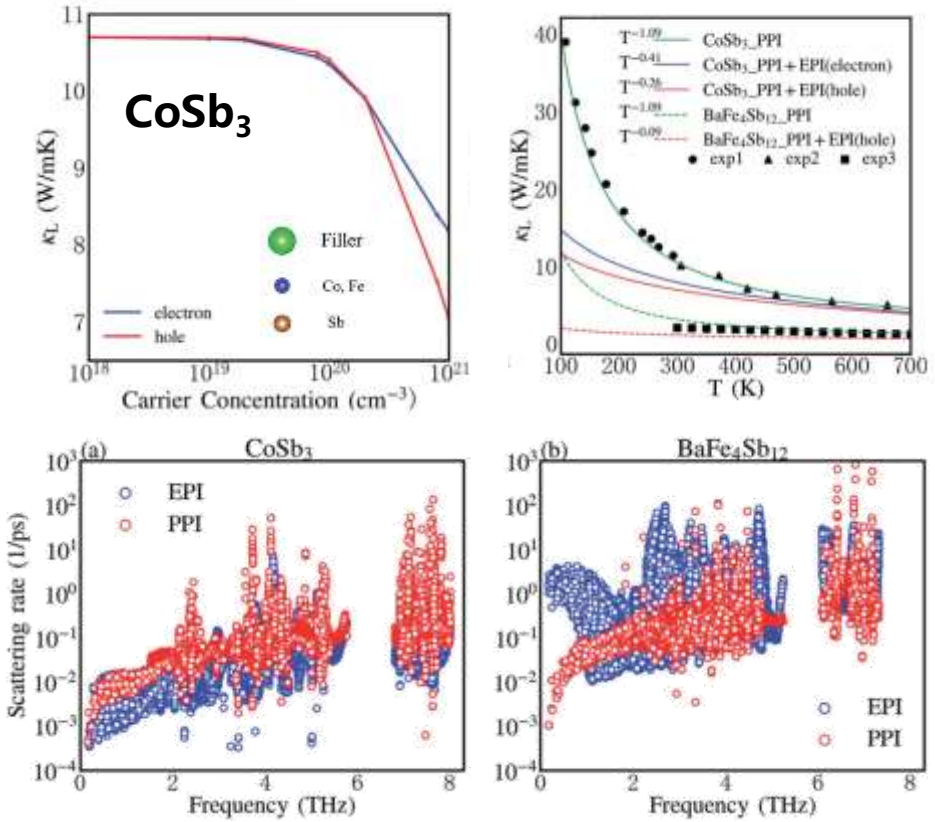

@300K-$BaFe_4Sb_{12}$ ↓64.8%

J. Mater. Chem. A, 10, 13484 (2022)

Half-Heusler

$$\eta = \frac{\kappa_{PP} - \kappa_{PP+EP}}{\kappa_{PP}}$$

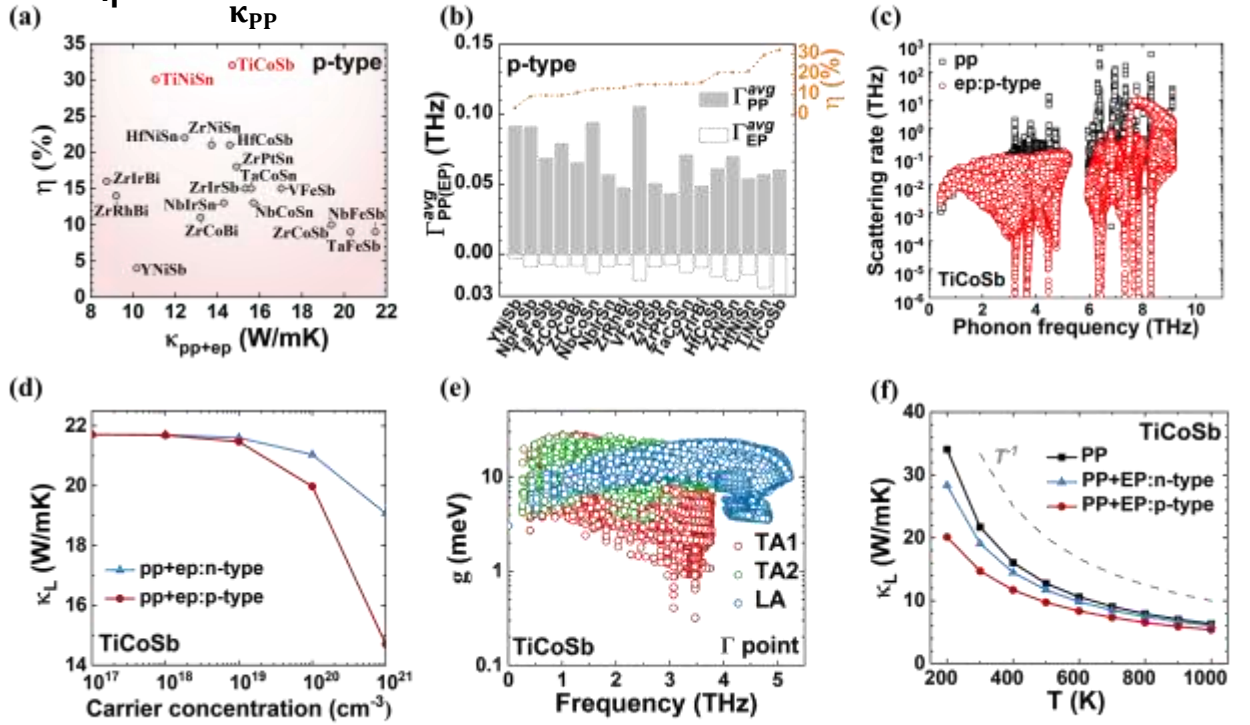

- At **300 K** with the carrier concentration of **10^{21} cm^{-3}**
- For the p-type doping, a more significant η for **TiCoSb (32%)**

Mater. Today Phys., 31, 100993 (2023)

3.2 Case Studies Using Phonon BTE **Efficient electron-phonon code: TTEP**

☐ Replace the expensive electron-phonon coupling

$$g^{\lambda}_{mn}(\mathbf{k},\mathbf{q}) = \sqrt{\frac{\hbar}{2M\omega_{\mathbf{q}\lambda}}}\langle\varphi_{m\mathbf{k}+\mathbf{q}}|\partial V_{\mathbf{q}\lambda}|\varphi_{n\mathbf{k}}\rangle \quad \text{---------} \ ①$$

by the acoustic phonon long-wavelength limit($|\mathbf{q}| \to 0$):

$$\langle\varphi_{m\mathbf{k}+\mathbf{q}}|\partial V_{\mathbf{q}\lambda}|\varphi_{n\mathbf{k}}\rangle \approx \mathrm{D}_A \cdot \mathbf{q} \quad \text{---------} \ ②$$

Efficient electron-phonon scattering rate for phonon transport:

$$\frac{1}{\tau^{EP}_{\mathbf{q}\lambda}} = \frac{\pi {D_A}^2}{VB}\sum_{mn,\mathbf{k}} \omega_{\mathbf{q}\lambda}\left(f_{m\mathbf{k}+\mathbf{q}} - f_{n\mathbf{k}}\right)\delta\left(\varepsilon_{n\mathbf{k}} - \varepsilon_{m\mathbf{k}+\mathbf{q}} - \hbar\omega_{\mathbf{q}\lambda}\right)$$

D_A: deformation potential $\omega_{\mathbf{q}\lambda}$: phonon frequency
V: Volume of unitcell B: Bulk modulus

Comput. Mater. Sci., 244, 113190 (2024)

Achieved a balance between accuracy and efficiency

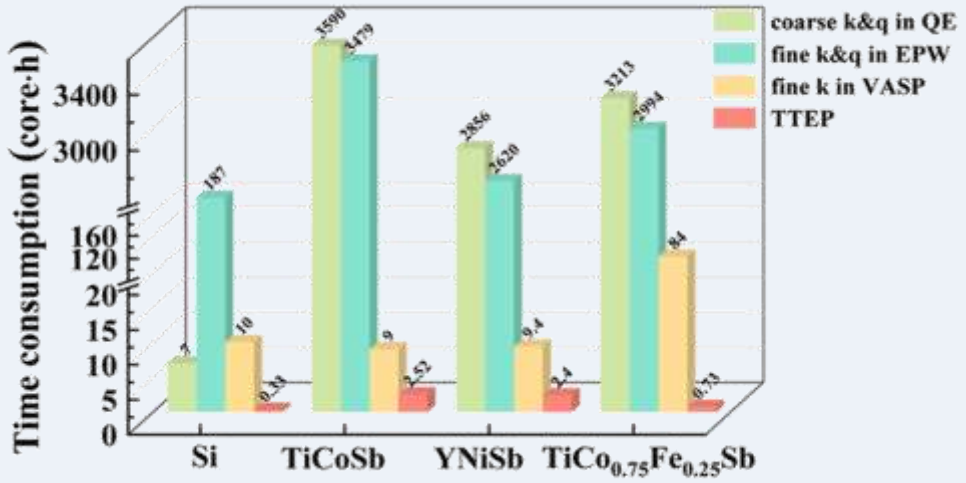

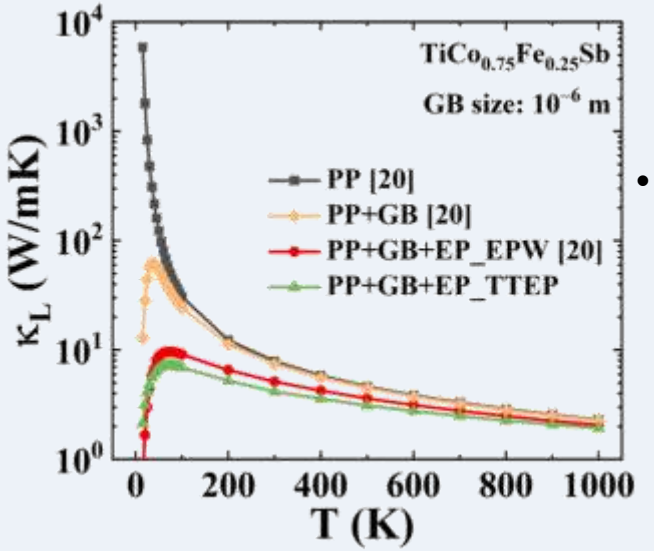

- The TTEP code can also handle **grain boundary scattering.**

Temperature-dependent force constants

$$E = E_0 + \frac{1}{2}\sum_{ij\alpha\beta} \boldsymbol{\Phi}_{ij}^{\alpha\beta} r_i^{\alpha} r_j^{\beta} + \frac{1}{3!}\sum_{ijk\alpha\beta\gamma} \boldsymbol{\Phi}_{ijk}^{\alpha\beta\gamma} r_i^{\alpha} r_j^{\beta} r_k^{\gamma} + \frac{1}{4!}\sum_{ijkl\alpha\beta\gamma\theta} \boldsymbol{\Phi}_{ijkl}^{\alpha\beta\gamma\theta} r_i^{\alpha} r_j^{\beta} r_k^{\gamma} r_l^{\theta} + \cdots$$

$\boldsymbol{\Phi}^{\alpha\beta}(T)$ $\boldsymbol{\Phi}^{\alpha\beta\gamma}(T)$

☐ Temperature-Dependent κ_L of Mg_3Sb_2

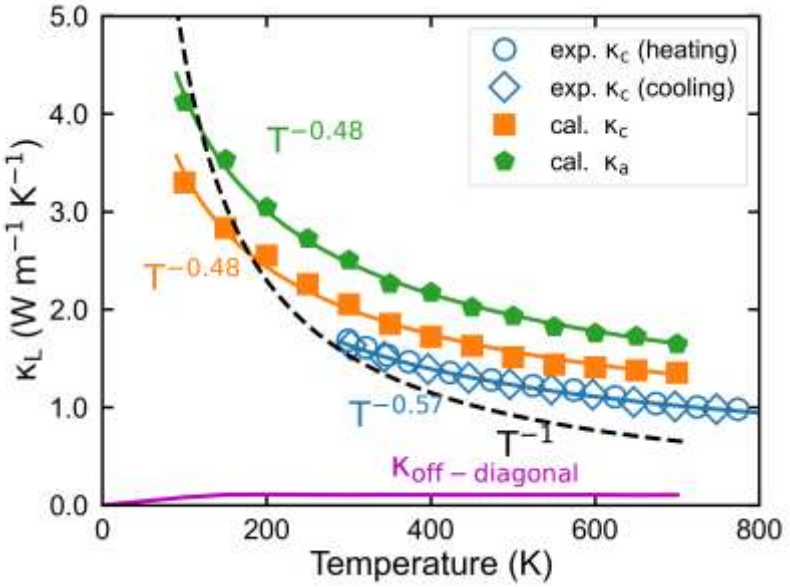

- Weak κ_L T-dependence in Mg_3Sb_2 (theory: $T^{-0.48}$; experiment: $T^{-0.57}$), deviating from the classical T^{-1} law.

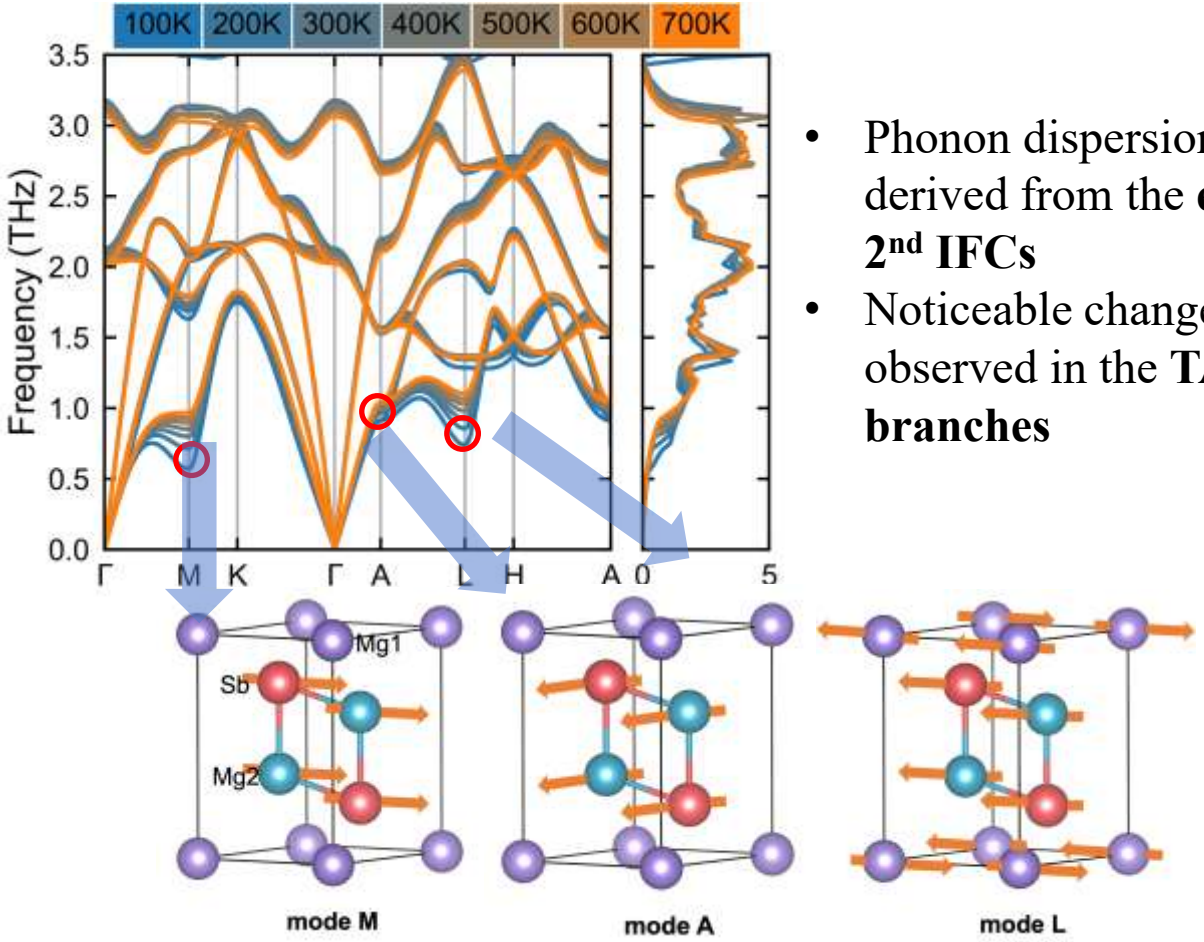

- Phonon dispersion is derived from the **effective 2nd IFCs**
- Noticeable changes are observed in the **TA branches**

- TA phonon hardening at high T → **weak κ_L–T dependence**, common in low κ_L materials.

Research, 2020, 4589786 (2020)

3.3 Something Beyond coherence κ_L

- $\kappa_L^{\alpha\beta} = \kappa_p^{\alpha\beta} + \kappa_c^{\alpha\beta}$

$$\kappa_C = \frac{\hbar^2}{k_B T^2 V N} \sum_{\mathbf{q}} \sum_{s \neq s'} \frac{\omega_{\mathbf{q}\lambda}^s + \omega_{\mathbf{q}\lambda}^{s'}}{2} v_{\mathbf{q}\lambda}^{s,s'}$$

- $$\otimes v_{\mathbf{q}\lambda}^{s',s} \times \frac{\omega_{\mathbf{q}\lambda}^s n_{\mathbf{q}\lambda}^s \left(n_{\mathbf{q}\lambda}^s + 1\right) + \omega_{\mathbf{q}\lambda}^{s'} n_{\mathbf{q}\lambda}^{s'} \left(n_{\mathbf{q}\lambda}^{s'} + 1\right)}{4\left(\omega_{\mathbf{q}\lambda}^{s'} - \omega_{\mathbf{q}\lambda}^s\right)^2 + \left(\Gamma_{\mathbf{q}\lambda}^s + \Gamma_{\mathbf{q}\lambda}^{s'}\right)^2} \left(\Gamma_{\mathbf{q}\lambda}^s + \Gamma_{\mathbf{q}\lambda}^{s'}\right)$$

- $$v_{\mathbf{q}\lambda}^{s',s} = \frac{\left\langle e_{\mathbf{q}\lambda}^s \left| \frac{\partial D(\mathbf{q})}{\partial \mathbf{q}} \right| e_{\mathbf{q}\lambda}^{s'} \right\rangle}{\omega_{\mathbf{q}\lambda}^s + \omega_{\mathbf{q}\lambda}^{s'}}$$

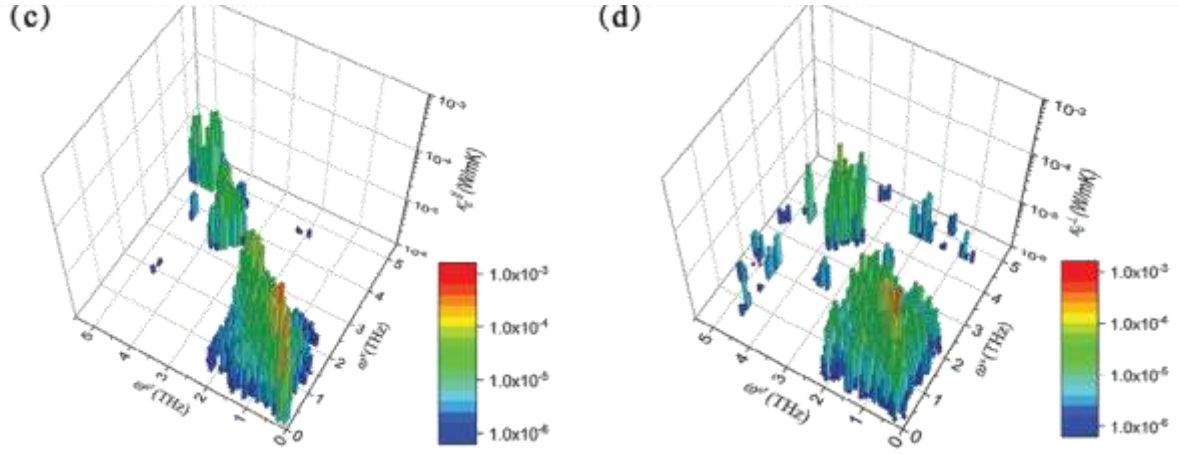

Adv. Sci., 11, 2406380 (2024)

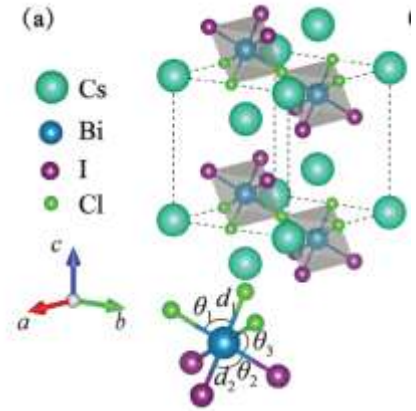

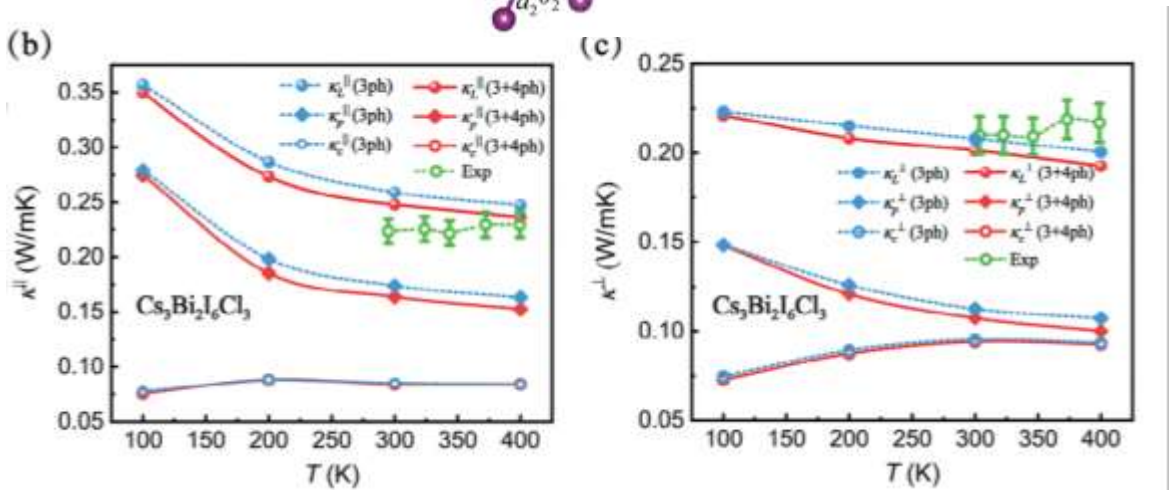

- Large coherence κ_L stems from large scattering rate (strong anharmonicity) and small frequency difference.
- The coherence κ_L is very common in ultralow κ_L materials.

Green-Kubo vs NEMD

GK-EMD method

$$\kappa_{\alpha\beta} = \frac{1}{k_B T^2 V}\int_0^{\infty} < J_\alpha(0) J_\beta(t) > dt$$

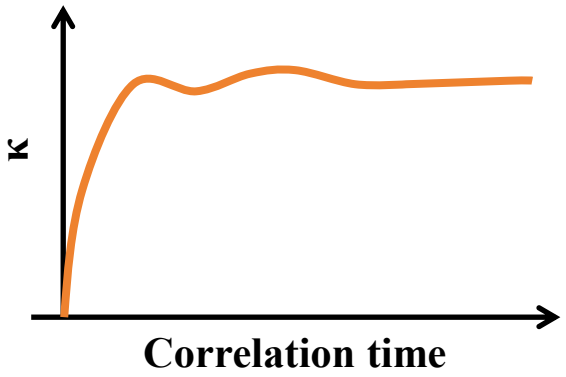

Convection term: $\mathbf{J}_{\text{conv}} = \sum_i \mathbf{v}_i \left(\frac{1}{2} m_i \mathbf{v}_i^2 + U_i\right)$

Conduction term:

$$\mathbf{J}_{\text{cond}} = \sum_i \mathbf{r}_i \frac{d}{dt}\left(\frac{1}{2} m_i \mathbf{v}_i^2 + U_i\right) = \sum_i \mathbf{r}_i (\mathbf{v}_i \cdot \mathbf{F}_i) + \sum_i \mathbf{r}_i \frac{dU_i}{dt}$$

NEMD method

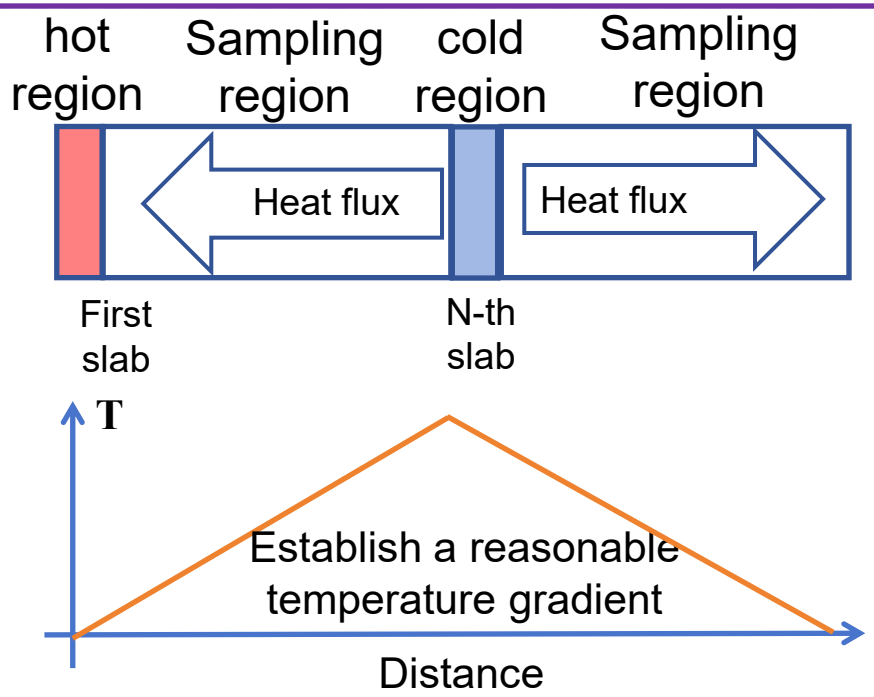

Fourier's Law:

$$\kappa = \frac{J}{-\nabla T}$$

Size Extrapolation:

$$\frac{1}{\kappa} = \frac{1}{\kappa_\infty} + \frac{\beta}{L_{ss}}$$

J. Chem. Phys., 22, 398-413 (1954)
J. Phys. Soc. Jpn., 12, 570-586 (1957)
J. Chem. Phys., 106, 6082-6085 (1997)

Green-Kubo method

BAs with 4phScattering

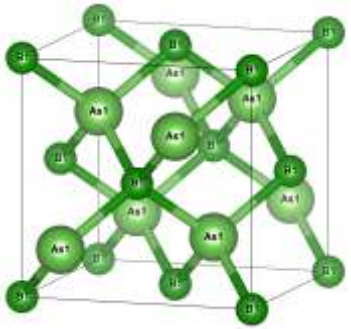

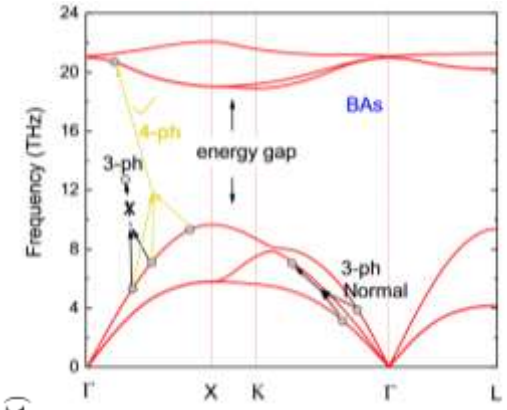

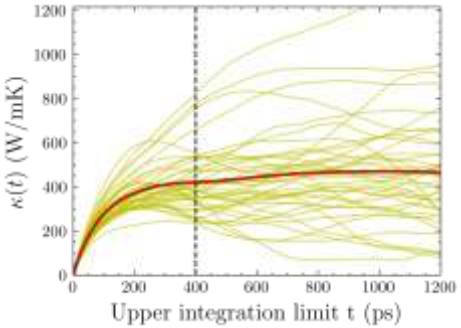

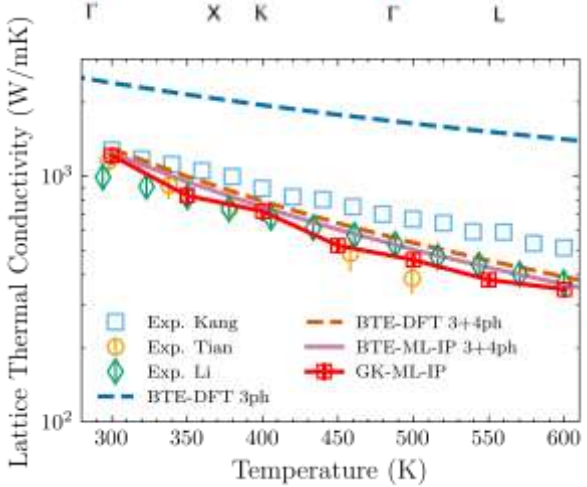

$$\kappa_{\alpha\beta} = \frac{1}{k_B T^2 V} \int_0^\infty \langle J_\alpha(0) J_\beta(t) \rangle \, dt$$

- Green–Kubo accurately predicts κ_L of BAs with four-phonon scattering.

Machine-Learning Potential MD

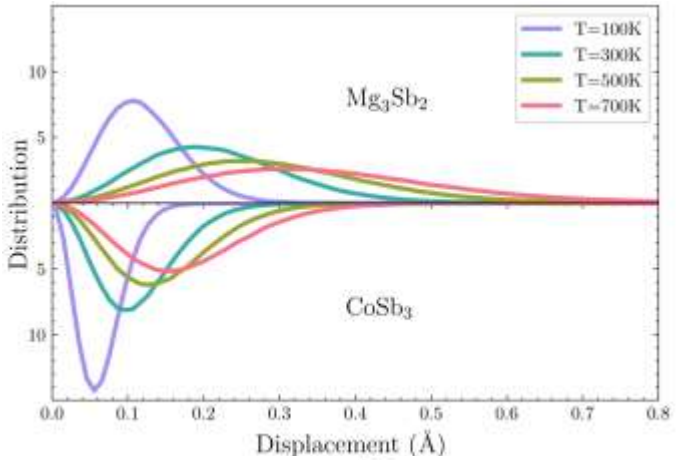

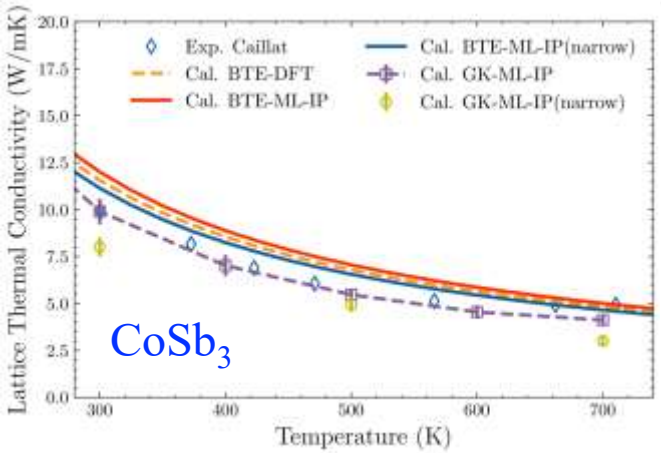

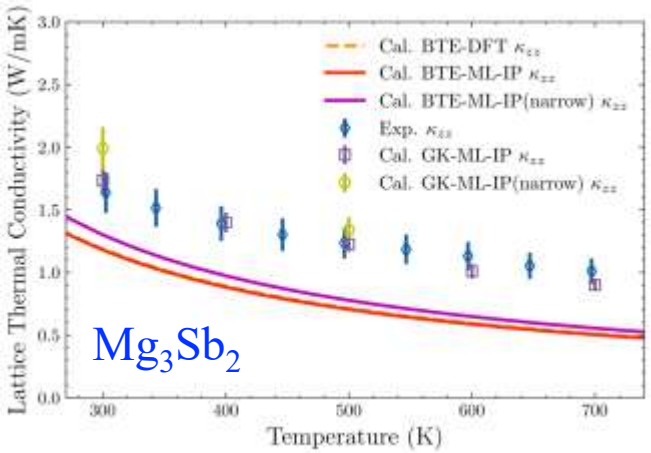

- GK naturally captures high-order interactions and temperature-dependent IFCs, yielding κ_L in good agreement with exp.

Phys. Rev. B, 104, 094310 (2021)

The failure of GK-MLIP in $Cu_{2-x}Se$

$$\begin{cases} J_{conv.} = \sum_i v_i \left(\frac{1}{2} m_i v_i^2 + U_i \right) \\ J_{cond.} = \sum_i r_i [(F_i \cdot v_i) + \frac{dU_i}{dt}] \end{cases}$$

- GK-MLIP method failed in materials with atomic diffusion due to the strong influence from the uncertainty of atomic potential energy U_i in GK.

Ambiguous Projection

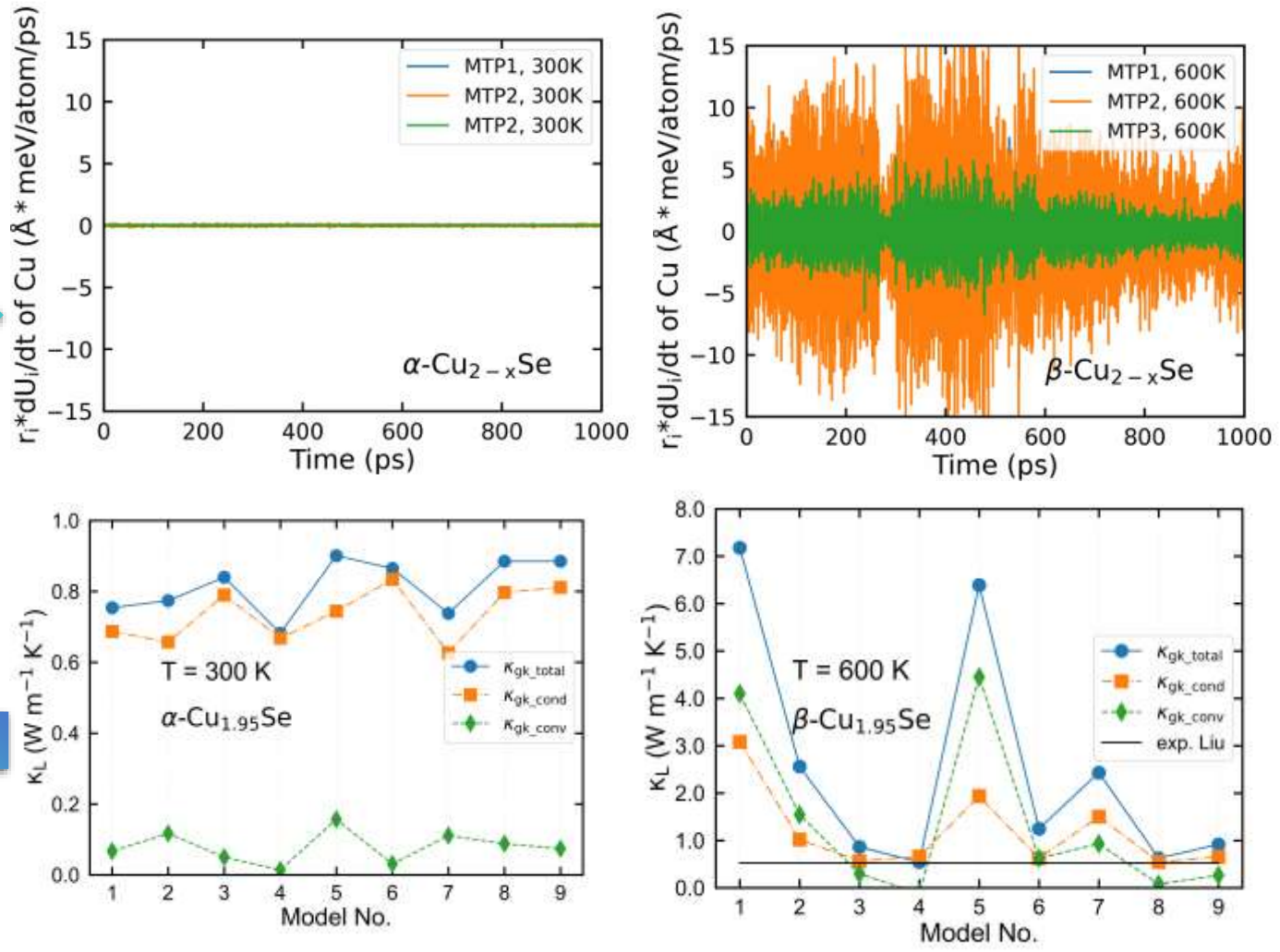

Phys. Rev. B, 108, 014108 (2023)

3.3 Something Beyond NEMD method

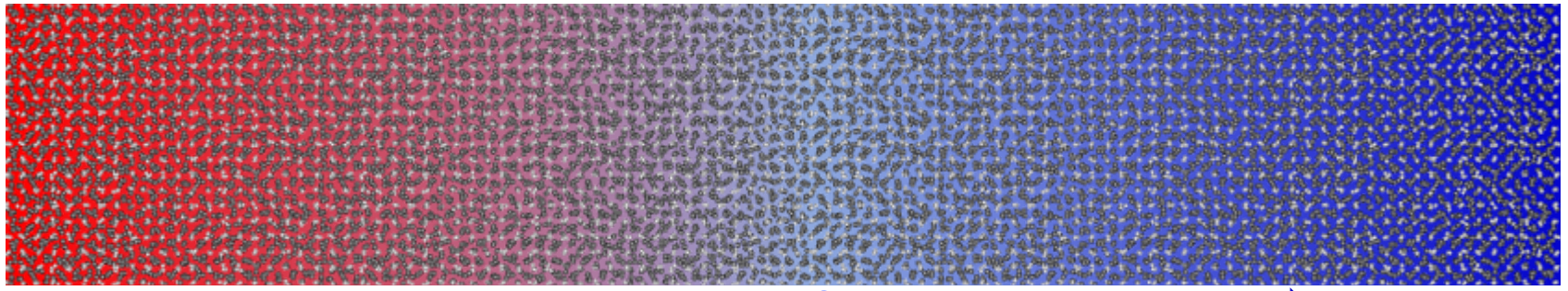

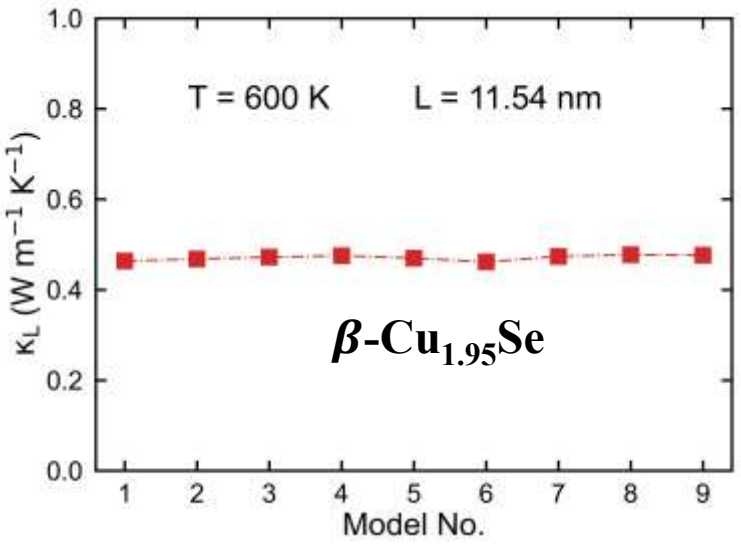

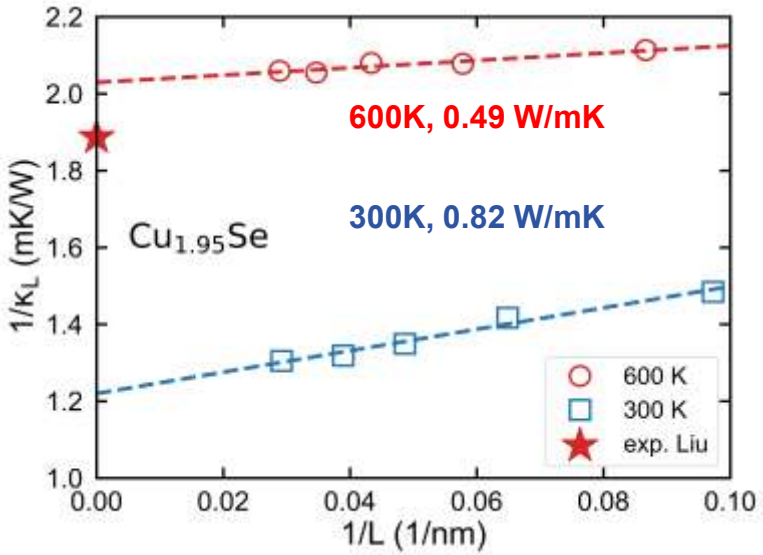

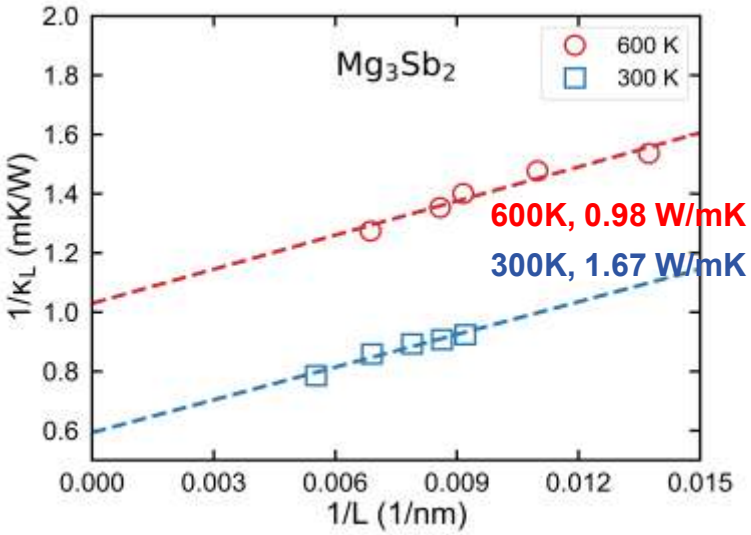

- Direct NEMD accurately predicts κ_L of β-$Cu_{1.95}Se$ and other crystalline materials.
- No noticeable fluctuations are observed among different ML models.

Phys. Rev. B, 108, 014108 (2023)

Atomic Energy Regularization

$$Loss = Loss_{label} + Loss_{dist.}$$

$$\begin{cases} Loss_{label} = \sum (y^{DFT} - y^{ML})^2 \\ Loss_{dist.} = \sum_t \sum_{i \in t} \dfrac{(U_i^{ML} - \bar{U}_t^{ML})^2}{2\sigma_i{}^2} \end{cases}$$

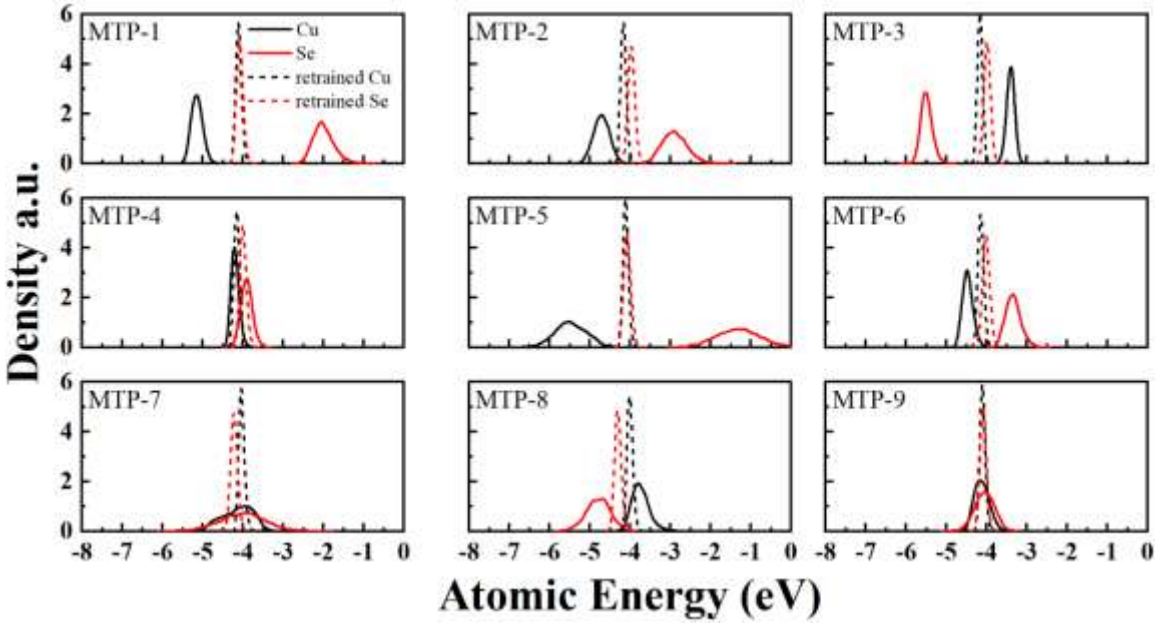

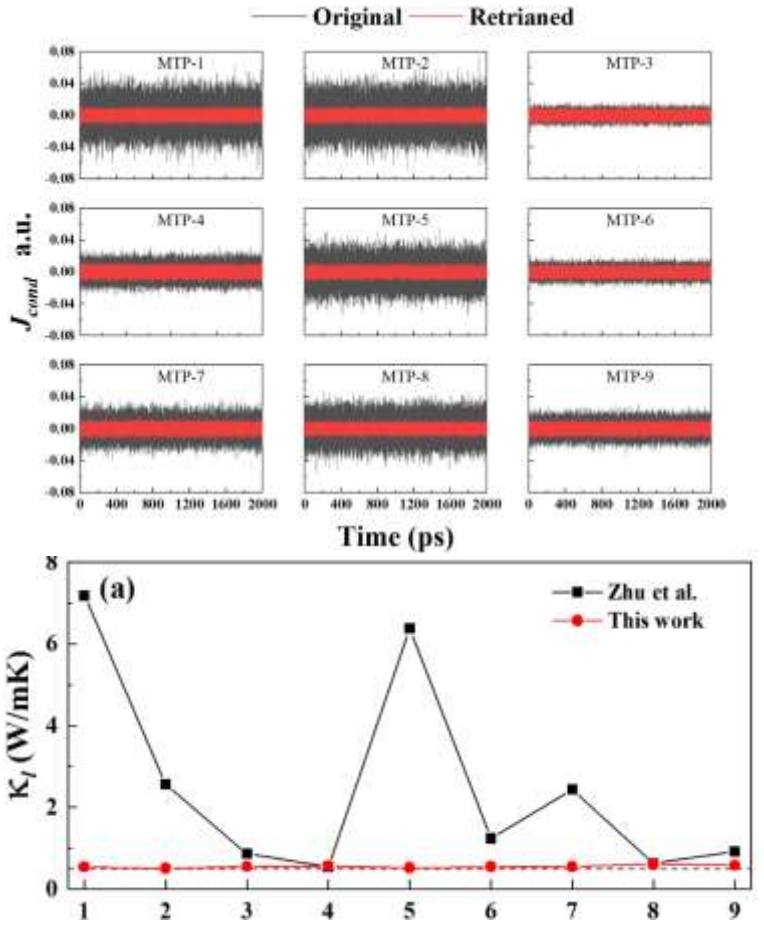

- Introduce the constraint on the distribution and absolute energy position of the atomic energy in the loss function.
- κ_Ls for $Cu_{2-x}Se$ predicted by each model exhibit high consistency in GK calculations, and agree well with experiments.

Phy. Rev. B, 112, 064306 (2025)

Summary on ph-trans

☐ BTE level:

- ✓ **The calculation of three-phonon interaction is less demanding than el-ph interaction, which make it more available in practice.**
- ✓ **The thermal transports based on three-phonon interaction for defective systems reshape the understanding on the influence of point defect.**

☐ Higher level:

- ✓ **Renormalization on force constants and coherence κ_L, are the hot topics for materials with strong anharmonicity.**
- ✓ **EMD and NEMD methods can solve the problems beyond the phonon picture.**

Summary

- The theories, softwares, and case studies for electrical and thermal transport based on BTE methods are summarized.
- The knowledges of basic transport are essential for advancing the overall comprehension in the thermoelectric transport, and uncovering new anomalies.


Yasong Wu


Yuyan Yang


Dr. Shengnan Dai


Prof. Jinyang Xi

Thank you for your attention!

- **ZA (out-of-plane acoustic) phonon in TMD monolayers**

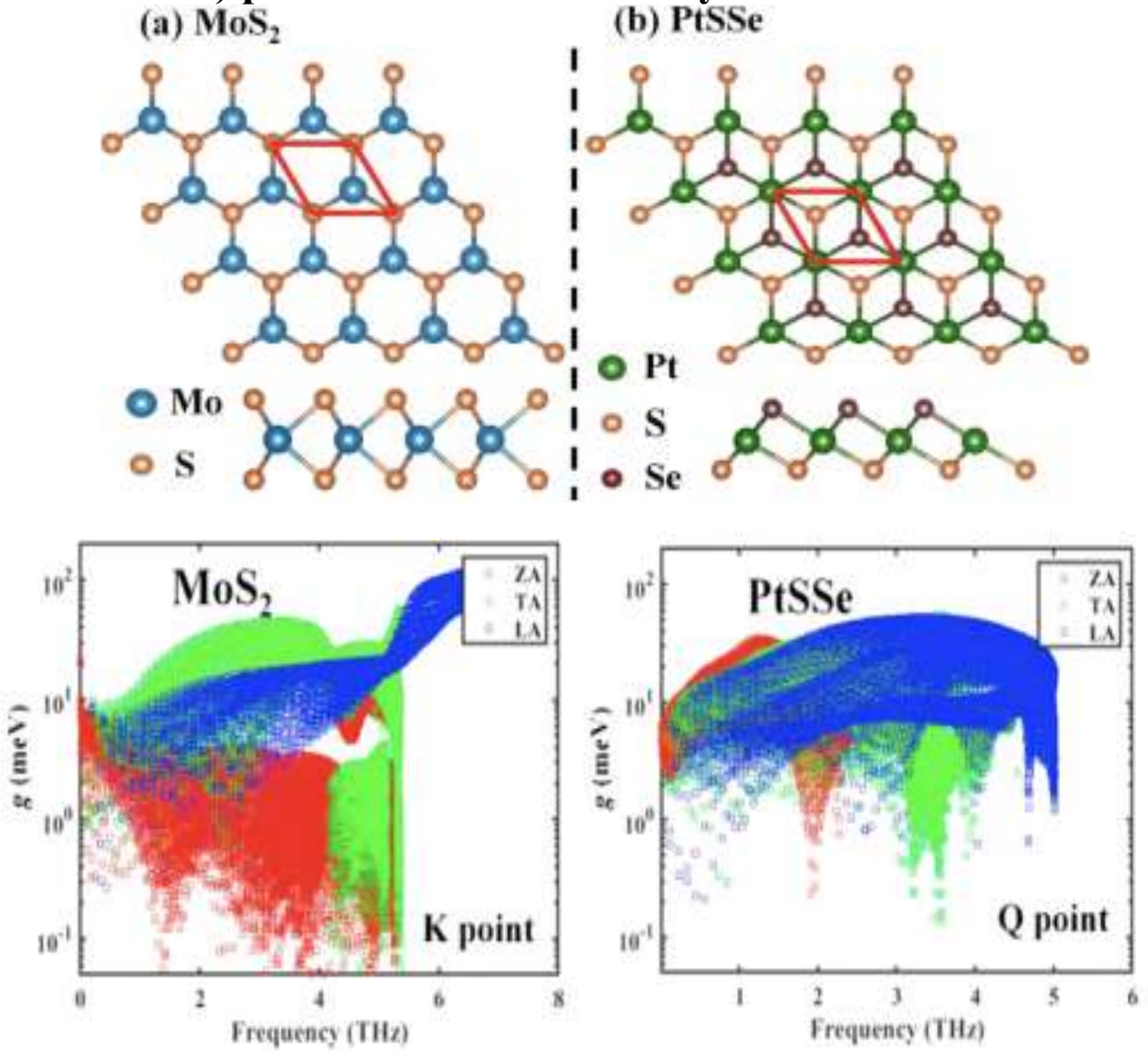

Lack of horizontal mirror symmetry in PtSSe enables a strong el-ZA ph coupling

Mater. Today Phys., 15, 100277 (2020)

3.1 BTE in Lattice Thermal Transport

- **Under a temperature gradient ∇T, the heat flux *J* is defined as:** $J = \sum_p \int f_\lambda \hbar\omega_\lambda \mathbf{v}_\lambda \frac{d\mathbf{q}}{(2\pi)^3}$

- Phonon distribution deviation arises from the temperature-gradient-induced **diffusion** and **scattering**:

$$\frac{df_\lambda}{dt} = \left.\frac{\partial f_\lambda}{\partial t}\right|_{\text{diffusion}} + \left.\frac{\partial f_\lambda}{\partial t}\right|_{\text{scattering}} = 0$$

- **Linearized Boltzmann Transport Equation (BTE):** $\mathbf{F}_\lambda = \tau_\lambda^0(\mathbf{v}_\lambda + \Delta_\lambda)$

$$\frac{1}{\tau_\lambda^0} = \frac{1}{\mathrm{N}}\left(\sum_{\lambda'\lambda''}^{+} \Gamma^{+}_{\lambda\lambda'\lambda''} + \sum_{\lambda'\lambda''}^{-} \frac{1}{2}\Gamma^{-}_{\lambda\lambda'\lambda''} + \sum_{\lambda'} \Gamma_{\lambda\lambda'}\right)$$

$$\Delta_\lambda = \frac{1}{\mathrm{N}}\sum_{\lambda'\lambda''}^{+} \Gamma^{+}_{\lambda\lambda'\lambda''}\left(\xi_{\lambda\lambda''}\mathbf{F}_{\lambda''} - \xi_{\lambda\lambda'}\mathbf{F}_{\lambda'}\right) + \frac{1}{\mathrm{N}}\sum_{\lambda'\lambda''}^{-} \frac{1}{2}\Gamma^{-}_{\lambda\lambda'\lambda''}\left(\xi_{\lambda\lambda''}\mathbf{F}_{\lambda''} + \xi_{\lambda\lambda'}\mathbf{F}_{\lambda'}\right) + \frac{1}{\mathrm{N}}\sum_{\lambda'} \Gamma_{\lambda\lambda'}\xi_{\lambda\lambda'}\mathbf{F}_{\lambda'}$$

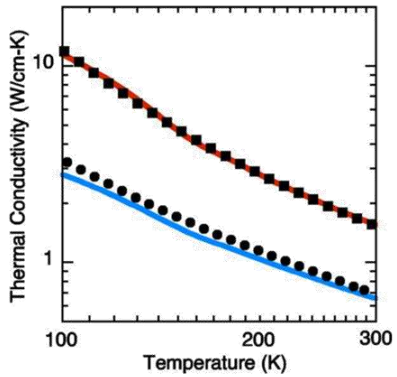

FIG. 1. (Color online) Lattice thermal conductivity $\kappa^{(i)}$ as a function of temperature. The red line and solid squares are the calculated and measured thermal conductivities of silicon, respectively, while the blue line and the solid circles are the corresponding quantities for germanium.

- Since **2007**, three-phonon calculations combined with **BTE** have become a standard approach for κ_L prediction, achieving high accuracy in conventional crystals.

Appl. Phys. Lett., 91, 231922 (2007)
Phys. Rev. B, 87, 165201 (2013)
Phys. Rev. B, 185, 1747 (2014)

3.3 Something Beyond **Temperature-dependent force constants**

Grüneisen parameter–projected phonon dispersion

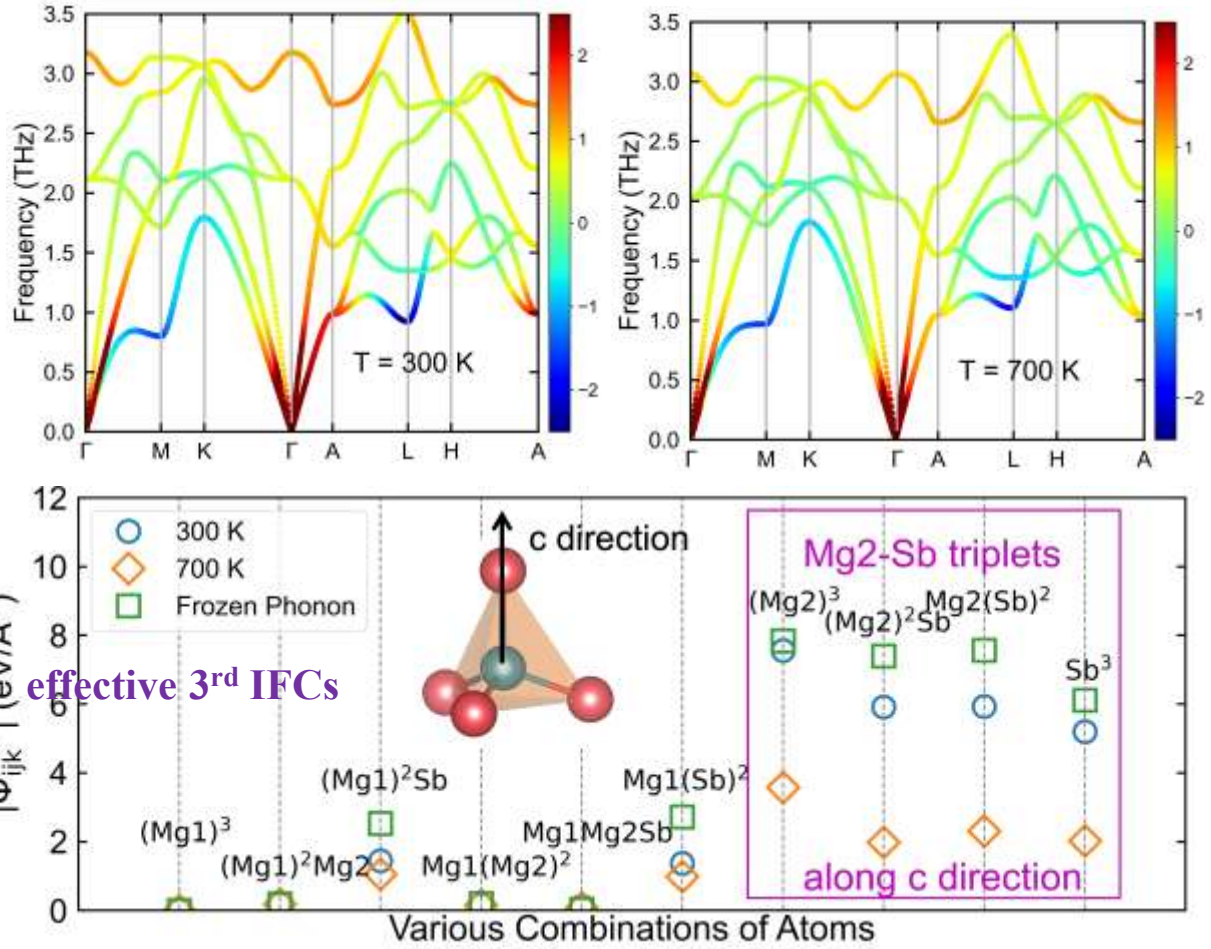

effective 3rd IFCs

- The reduction in the absolute Grüneisen parameter with T confirms that anharmonicity weakens in Mg_3Sb_2.
- Temperature-induced reduction of Mg–Mg and Sb–Sb 3rd IFCs leads to the weak κ_L–T dependence in Mg_3Sb_2.

Asymmetric energy/force–displacement curve

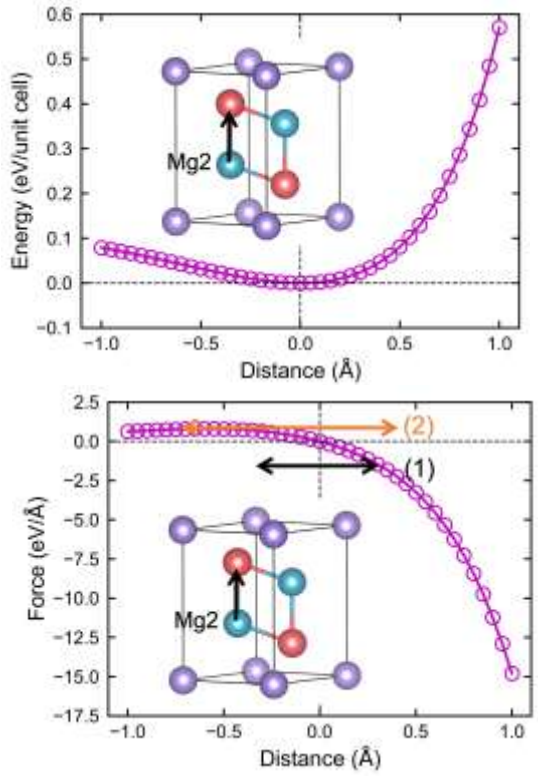

- The curve of the Mg2 atoms is asymmetric, and this asymmetry increases with temperature.

Research, 2020, 4589786 (2020)